Technical University of Denmark

DTU

Methods for planning and operating decentralized combined heat and power plants

Pálsson, Hálldór; Bøhm, Benny

Publication date:
2000

Document Version
Publisher's PDF, also known as Version of record

Link back to DTU Orbit

DTU Library
Technical Information Center of Denmark

RISØ   MASTER

Methods for Planning and Operating Decentralized Combined Heat and Power Plants

Halldór Pálsson

DTU

DISCLAIMER

Portions of this document may be illegible in electronic image products. Images are produced from the best available original document.

Methods for Planning and Operating Decentralized Combined Heat and Power Plants

Halldór Pálsson

Abstract   In recent years, the number of decentralized combined heat and power (DCHP) plants, which are typically located in small communities, has grown rapidly. These relatively small plants are based on Danish energy resources, mainly natural gas, and constitute an increasing part of the total energy production in Denmark.

The topic of this thesis is the analysis of DCHP plants, with the purpose to optimize the operation of such plants. This involves the modeling of district heating systems, which are frequently connected to DCHP plants, as well as the use of heat storage for balancing between heat and power production. Furthermore, the accumulated effect from increasing number of DCHP plants on the total power production is considered.

Methods for calculating dynamic temperature response in district heating (DH) pipes have been reviewed and analyzed numerically. Furthermore, it has been shown that a tree-structured DH network consisting of about one thousand pipes can be reduced to a simple chain structure of ten equivalent pipes without loosing much accuracy when temperature dynamics are calculated.

A computationally efficient optimization method based on stochastic dynamic programming has been designed to find an optimum start-stop strategy for a DCHP plant with a heat storage. The method focuses on how to utilize heat storage in connection with CHP production.

A model for the total power production in Eastern Denmark has been applied to the accumulated DCHP production. Probability production simulations have been extended from the traditional power-only analysis to include one or several heat supply areas.

Preface

This thesis is a part of the requirements of obtaining a Ph.D. degree in engineering at the Technical University of Denmark (DTU). The work has been carried out at the Systems Analysis Department at Risø National Laboratory, as well as the Department of Energy Engineering at DTU.

The work was financed mainly by the Nordic Energy Research Programme, but also by Risø and DTU. The Energy Research Programme is carried out in co-operation between the five Nordic countries, with the purpose of initiating and supporting collaboration between Nordic energy researchers.

The topic of the thesis is the analysis of decentralized combined heat and power plants (DCHP), with the purpose to optimize the operation of such plants. This involves the modeling of district heating systems, which are frequently connected to DCHP plants, as well as the use of heat storage for balancing between heat and power production. Furthermore, the accumulated effect from increasing number of DCHP plants on the total power production is considered.

The thesis consists of six research papers, published or planned to be published elsewhere, preceded by a synthesis report. Most of the results from the study are reported in the papers, but some results are presented in the synthesis. Furthermore, part of the work has been published in a technical report as a result of another research project.

Acknowledgements

4

Furthermore, I wish to thank the staff at the Systems Analysis Department for providing an excellent working environment, both with respect to research and social contact. Also, thanks to the staff at the Department of Energy Engineering (DTU) and Elkraft System for contact and assistance during the study.

Also I would like to thank Helge V. Larsen (Risø) for many fruitful discussions and co-authoring of papers, Gísli Tryggvason and Jijun Zhou (DTU) for discussions on various issues of DH systems, and fellow students and researchers in the Energy Research Programme for constructive critics during our annual Programme Meetings.

Special thanks to Tom Bilgrav, the plant operator at Hvalsø CHP plant, for providing the necessary data used in the project as well as for giving valuable insight into DCHP plant operation. Also thanks to Vestegnens Kraftvarmeselskab (VEKS) for providing data used for verifying simulation models.

Last but not least, many thanks to my wife and children, as well as friends and family, for supporting me during the study.

Lyngby, February 29, 2000,

Halldór Pálsson.

Summary

This thesis consists of six research papers and a synthesis report. The synthesis mainly describes and links the topics of the papers, but also includes some work not found in the papers. Four of the papers are previously published in conference proceedings, one is published in an international journal and one is unpublished.

These papers, contained in appendices A–F, are:

A H. Pálsson, Analysis of Numerical Methods for Simulating Temperature Dynamics in District Heating Pipes, 6. International symposium on district heating and cooling simulation, Reykjavik, 28-30 Aug 1997.

B Larsen, H.V.; Pálsson, H.; Bøhm, B.; Ravn, H.F., Equivalent models for district heating systems, 7. International symposium on district heating and cooling, Lund, 18-20 May 1999.

C Larsen, H.V.; Pálsson, H.; Bøhm, B.; Ravn, H.F., An aggregated dynamic simulation model of district heating networks, unpublished.

D H. Pálsson, Optimizing the use of heat storage in an engine-based CHP plant, 7. International symposium on district heating and cooling, Lund, 18-20 May 1999.

E Larsen, H.V.; Pálsson, H.; Ravn, H.F., Simulation tool for expansion planning of combined heat and power, 6. International symposium on district heating and cooling simulation, Reykjavik, 28-30 Aug 1997.

F Larsen, H.V.; Pálsson, H.; Ravn, H.F., Probabilistic production simulation including combined heat and power plants, Electric Power Systems Research (1998) vol. 48, pp. 45-56.

In recent years, the number of decentralized combined heat and power (DCHP) plants, which are typically located in small communities, has grown rapidly. These relatively small plants are based on Danish energy resources,

mainly natural gas, and constitute an increasing part of the total energy production in Denmark.

DCHP plants are characterized by the connection between a local district heating (DH) system and a regional power grid. The plants produce heat to the local DH consumers, as well as power to the grid, sold at a price that varies over time.

The thesis treats three main topics.

1. Modeling of a DH network, where the time dependent dynamics and time delays of the network are considered. A computer program for dynamic simulation of DH networks has been developed in the project, with the purpose of describing the behaviour of flows and temperature changes in a DH network in general. Furthermore, theoretical aspects of dynamic simulation methods have been analyzed, resulting in proofs of some vital numerical properties of one of the methods. Finally, there has been participation in work related to simplifying dynamic network models, in order to reduce computational work in simulations.

2. Operational planning of production in a DCHP plant, with main emphasizes on the optimal utilization of heat storage. An optimization algorithm has been developed, based on the dynamic programming method. In the optimization, the stochastic varying heat-load from consumers is taken into account, as well as the time varying power prices. The algorithm is shown to be very efficient, computationally, when used on a typical small DCHP plant.

3. Analysis of the co-operation between the regional power grid and the DCHP plants as a whole. A model, previously used for describing the total power production in Eastern Denmark, has been used for the total DCHP production. It is shown that the model is applicable on DCHP plants, but results are not as good as for the total production. Finally, the author has participated in work related to a method to perform probabilistic production simulation. In this work, a method which is classically used for power-only areas has been extended to include one or more heat areas.

The main results of the work are summarized below.

Methods for calculating dynamic temperature response in DH pipes have been reviewed and analyzed numerically. The stability of one of the methods, the node method, have been proven, and analyses of its accuracy properties have been worked out. Furthermore, alternative methods have been proposed and tested, with the aim to avoid numerical dispersion in the solution.

It has been shown that a tree-structured DH network consisting of about one thousand pipes can be reduced to a simple chain structure of ten equivalent pipes (or 1% of the original number of pipes) without loosing much accuracy when temperature dynamics are calculated.

The complexity of different models necessary for simulating DH systems and making heat load forecasts have been tested by comparison of simulations and measurements from Hvalsø and VEKS DH systems.

A computationally efficient optimization method based on stochastic dynamic programming has been designed to find an optimum start-stop strategy for a DCHP plant with a heat storage. The method focuses on how to utilize heat storage in connection with CHP production.

A model for the total power production in Eastern Denmark has been applied to the accumulated DCHP production. Probability production simulations have been extended from the traditional power-only analysis to include one or several heat supply areas.

Sammenfatning (Summary in Danish)

Denne afhandling består af seks videnskabelige artikler og en sammenfattende rapport. Denne rapport beskriver hovedsageligt emnerne i artiklerne, men inkluderer også arbejde som ikke findes i artiklerne. Fire af disse artikler er publiceret som konferencebidrag, én er publiceret i et international tidsskrift og én er ikke publiceret.

For en oversigt over artiklerne i Appendix A–F, se det forrige afsnit *Summary*.

I de senere år er der sket en kraftig forøgelse i antallet af decentrale kraftvarmeværker, som typisk er placeret i mindre byer. Disse relativt små værker udnytter danske energiressourcer, hovedsageligt naturgas, og repræsenterer en voksende andel af landets totale energiproduktion.

Et decentralt kraftvarmeværk er karakteriseret ved koblingen mellem det lokale fjernvarmenet og et regionalt elnet. Værket producerer varme til lokale kunder samt el til det fælles elnetværk, afregnet til en pris som typisk kan variere over tiden.

Afhandlingen vedrører tre hovedemner:

1. Modellering af fjernvarmenetværk hvor der tages hensyn til fjernvarmesystemets dynamik og tidsforsinkelser. I projektet er der udviklet et edb program til dynamisk simulering af fjernarmenetværk, med henblik på at belyse forholdene mellem strømning og temperatur i et netværk. Der er også lavet teoretiske analyser af de numeriske metoder, som bruges til bestemmelse af dynamisk temperaturfordeling i fjernvarmerør. Endvidere er der bidraget til arbejdet med udvikling af en metode til simplificering af modeller for dynamik i fjernvarmenetværk.

2. Driftsoptimering af et decentralt kraftvarmeværk med fokus på optimal udnyttelse af varmelager. I projektet er der udviklet en optimeringsalgoritme baseret på dynamisk programmering. I optimeringen tages der hensyn til det stokastisk varierende varmebehov fra fjernvarmekunder,

9

samt de varierende elpriser. Algoritmen viser sig at være særdeles effektiv når den er anvendt på et typisk mindre decentralt værk.

3. Analyse af samspillet mellem elnettet og de decentrale kraftvarmeværker. Et model, som tidligere er blevet lavet til at beskrive den totale elproduktion i Østdanmark, er blevet brugt til at belyse den samlede decentrale kraftvarmeproduktion. Der er i projektet også medvirket til udarbejdelse af metoder hvor en analyse baseret på stokastisk simulering af et el-område er blevet udvidet til at inkludere et eller flere varmeområder.

Et sammendrag af projektets hovedresultater følger nedenfor.

Metoder for beregning af dynamiske temperaturforløb i fjernvarmeledninger er blevet analyseret på et teoretisk grundlag. Stabiliteten i en af metodene, knudemetoden, er blevet matematisk bevist, og analyse af dens nøjagtighed er udført. Alternative metoder er også blevet foreslået og afprøvet, med hensyn til at undgå numerisk dispersion i simuleringer.

Det er blevet vist, at fjernvarmenetværk med træ-struktur og over tusind rør kan reduceres til en simpel linie-struktur med ti rør (eller ca. 1% af det oprindelige antal) uden væsentlig reduktion af nøjagtighed når dynamiske temperaturer beregnes.

Kompleksiteten af diverse modeller til simulering af fjernvarmesystemer er blevet afprøvet ved sammenligning af simuleringsresultater og målinger. Målinger fra Vestegnens Kraftvarmeselskab og Hvalsø Kraftvarmeværk er blevet brugt tid dette formål.

En beregningsmæssig effektiv optimeringsmetode, baseret på stokastisk dynamisk programmering, er blevet implementeret med det formål at finde en optimal start-stop strategi for et decentralt kraftvarmeværk med en varmelager. Metoden fokuserer på hvordan et varmelager bedst kan udnyttes i forbindelse med kraftvarmeproduktion.

En eksisterende model for den samlede elproduktion i Østdanmark er blevet brugt til at belyse den samlede produktion fra decentrale kraftvarmeværker. Endvidere er en metode til stokastisk simulering af elproduktion i et område, under hensyntagen til forskellige anlægstyper og deres rådighed, blevet udvidet til at inkludere et eller flere varmeområder.

Contents

Chapter 1

Introduction

1.1 Background of the project

In recent years, a lot of attention has been turned towards improving the efficiency of Danish energy systems. One reason for this is that Danish produced heat and power is largely produced from fossil fuels such as coal, oil and natural gas. This use of fossil fuels results in emission levels which are quite high, when compared to energy forms like hydro power, wind energy and nuclear power. Therefore, much can be gained in terms of emission reduction if the total efficiency of the system can be improved.

The importance of combined heat and power production (CHP) in existing power systems has become more evident in recent years. The main reason for this is the high thermal efficiency of plants producing both heat and electric power, compared to the conventional power-only plants and the implied environmental benefits.

CHP production results in thermal efficiency of about 85–94%, whereas the efficiency of conventional power-plants is about 45%. In Denmark, a governmental policy has been towards small decentralized CHP (DCHP) plants for the last ten years or so, c.f. Section 4.1. These plants typically produce in the range 1–10 MW power and provide DH to local, and in most cases, relatively small communities. Such DCHP plants typically deliver heat to local DH networks in where heat is distributed to individual consumers. This is in most cases the main obligation of such a plant. Furthermore, the growing number of DCHP plants will have more effect on the existing power system in form of increased production, which in turn requires that these plants are taken into account in the general planning and regulation of electric power production.

At a DCHP plant, the price of electric power varies, depending on the

13

time of day and the current weekday, which poses a problem for the plant operator. The heat demand must be fulfilled, but at the same time the production should take place when the price for power is high. This dilemma can be partly avoided by using a heat storage. The storage is used to store excess heat when power production is profitable, and to supply heat to DH consumers when the power price is low. Therefore the operator faces an optimization problem, which is to determine when to operate the CHP plant, taking into account the storage contents and the uncertain future heat-load.

1.2   Project description

In this work, the DCHP system is seen as an intermediate between the heat load and the power system. Of these, the heat load is in the most typical form characterized by a heat demand profile, given as the heat load, measured in MW, for each of the 8760 hours of the year. The power system is similarly characterized by a power price profile, typically given at the price, DKK/MWh, for each of the 8760 hours of the year. The DCHP system consists of a production plant, possibly with associated heat storage, and a district heating network, in which the heat is transported to the individual consumers.

The purpose of planning the generation of DCHP is then to supply the demanded heat load, while selling the co-produced electrical power to the electrical system, at the given prices, in such way that the economy for one year's operation is as good as possible. This indicates a natural partition of the analysis as follows:

- Properties and behavior of the DH network. The network forms a link between the heat consumers and the DCHP plant, in which complex phenomena like time delays and heat losses take place.

- The DCHP plant itself. This includes CHP production units and boilers, as well as the very important heat storage. Also included here are revenues in form of electricity and heat sales, as well as fuel costs and losses.

- The effect of a large number of DCHP plants on the existing power system. Currently the DCHP plants are not centrally controlled, which means that they form a base load which can vary rapidly between operation hours. This poses a problem for the overall power system operator, which has to regulate the total power production to meet the demand.

The purpose of this work is to analyze the three parts above in order to gain knowledge of the special properties of DCHP plants. This involves the behavior of the DH network, optimal planning of operation of a DCHP plant, as well as the combined implications of DCHP production on the national power grid.

1.3 Structure of the thesis

The thesis consists of a short synthesis report followed by six technical papers in respective appendices. Also, part of the work has been published in the technical report "Equivalent Models of District Heating Systems, for On-line Minimization of Operational Costs of the Complete DH System", see Pálsson et al. (1999), which is a result of another research project.

According to the threefold partition described above, Chapter 2 deals with the DH network, as the linkage between the heat plant and the consumers. Physical and dynamic properties of a DH network are described and analyzed in Appendix A. A method for simplifying DH network models is presented in Appendix B, and evolved further in Appendix C, which also incorporates a larger case study in form of the Hvalsø DH network.

In Chapter 3 the focus is on the DCHP plant itself, and on how to optimize the operation of such a plant. The main results are given in Appendix D, where the stochastic heat storage problem is posed and solved, using a simple model of a DCHP plant at the town of Hvalsø in Denmark. An optimization is performed by using a stochastic discrete dynamic programming method, where the found solution represents decisions of whether to produce or not in a given hour of the day or week.

Chapter 4 considers the effects of increasing DCHP production on the power network. A model of the cumulative DCHP power production is presented, with the aim of providing some prior knowledge of future production to the power system operator.

Finally the main conclusions of the thesis are drawn, thus summarizing analysis and findings. The bibliography at the end of the synthesis summarizes publications which are referred to in the synthesis. Additionally, each of the papers have their individual lists of references.

Chapter 2

Dynamic models of district heating networks

An important aspect of CHP production in Denmark is the use of heat for district heating (DH). It is therefore vital to understand the behavior of both DH consumers and networks in order to analyze the effect of DH on CHP production. This forms a link between plants and consumers.

A typical DH distribution system consists of one or more production units, a pipe network, as well as consumer houses or substations, see Figure 2.1. The plant produces heat to a given demand which is then transported through the pipes to the heat consumers. There, the heat is extracted from the water, either directly in radiators or heat-exchangers, and the cooled water is returned to the plant. See e.g. Yang (1994) and Aronsson (1996) for a detailed description of the behavior of DH consumers. For a complete description of the technical aspects of DH systems, refer to Bøhm (1988) and Frederiksen and Werner (1996) among others.

The main elements of the analysis are:

- Speed of transport. This involves a delay between the consumers' heat load and the load which is experienced at the production plant. This delay is furthermore different for each consumer which adds to the complexity of the connection between a plant and the DH consumers.

- Dynamics, such as flow and temperature propagation in the DH pipes as well as heat accumulation in the pipes.

- Heat losses from the pipes, which are always present because of the temperature difference between the DH water and the surroundings.

Much work has been done regarding network models in recent years, which

17
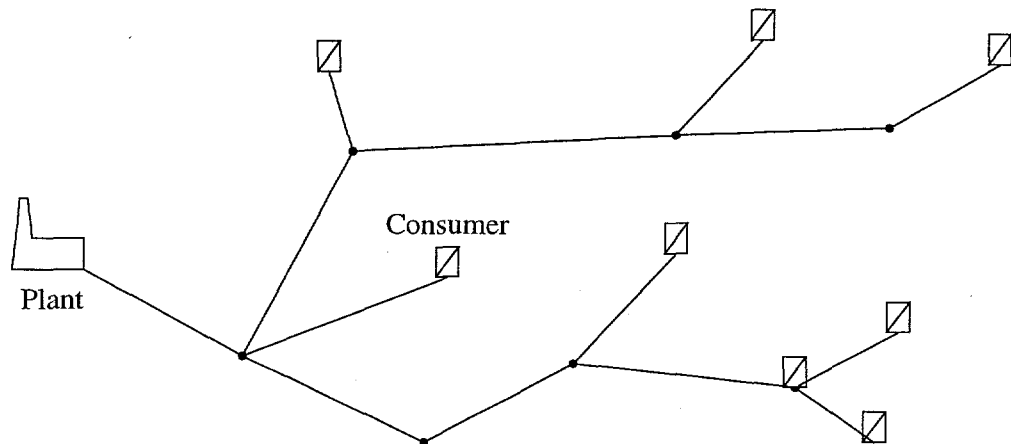
Figure 2.1: A typical structure of a DH network with heat-exchanger stations.

has mostly been applied to simulation and operational optimization. The methods used can generally be put into two classes:

- Physical models, where all the important components in a DH network are modeled explicitly and the whole structure of the network is taken into account.

- Black box models, where the physical composition of the network is disregarded and the modeling is in form of standard transfer function models (parametric or non–parametric) or neural networks.

In the first class, detailed models have been developed by considering the actual topology of the network as well as the physical layout and properties of the DH pipes. This involves using mathematical methods for computing the flow distribution, see e.g. Jeppson (1976) and Valdimarsson (1993), as well as the temperature distribution in the network, see Benonysson (1991) and Zhao (1995).

On the other hand, in the second class, the modeling is performed by using general and often simple modeling methods for the DH network. This typically involves classical time-series analysis, see Pálsson (1993), Sejling (1993), and neural networks, see e.g. Zhao (1995), and often results in simple and computationally efficient models. The main drawback of these methods is that they do not contain much physical information about the network, since the model parameters involved generally have little or no physical meaning. This means that the parameters have to be determined by using measurements of vital properties, in order to determine the model behavior.

In the present work, mathematical models of DH pipes have been analyzed in order to gain understanding of the numerical properties of the methods. Refer to Appendix A and Pálsson et al. (1999). A computer model for simulating DH networks has furthermore been developed which involves steady-state flow and temperature computations in a complete DH network on a time varying basis, taking into account the heat losses in the network. This model has been used further to analyze simplified network models, see Appendix B and Appendix C, in order to determine their usefulness.

The computer model has been tested and verified by using measurements from the DH company Vestegnens Kraftvarmeselskab (VEKS). They have provided data for a part of their distribution area, which has been used for getting a real problem perspective in testing the models, see Pálsson et al. (1999).

The four subsequent sections describe the most important aspects of DH networks, such as water flow, temperature dynamics (including heat losses), aggregated models, and finally some aspects regarding operational optimization of DH networks.

2.1 Computation of steady-state flows in large networks

In this first section the most basic thing regarding DH network simulation is considered, namely the computation of the flow distribution in the network.

This problem has been studied in depth, both specifically for DH systems and for electric circuit analysis, which is related to the DH flow problem. The discussion here is therefore based on previous studies. For information about flow computation specifically for DH network refer to Valdimarsson (1993) and for a more general discussion refer to Jeppson (1976) and Nielsen (1994).

Two properties are of concern when considering flow; water velocity (or mass flow) and pressure head. In general terms, the flow through a pipe is driven by the difference in pressure head between the two pipe ends. Thus, if the absolute pressure head is known in every pipe intersection, then the flow can also be found. This connection is described in the Darcy-Weisbach equation (see e.g. Valdimarsson (1993))

$$h = f \frac{8Lm^2}{D^5 \rho^2 \pi^2 g} \tag{2.1}$$

where h is the pressure head difference in meters, L is pipe length, D is pipe diameter, m is mass-flow, ρ is density and g is specific gravity.

The friction factor f given in (2.1) is generally dependent on the flow and is different in laminar and turbulent flow situations. For laminar flow the Hagen-Poiseuille equation is used which gives $f = 64/\text{Re}$, where Re is the Reynolds number, and for the more frequent turbulent flow an approximation to the Colebrook-White equation is used, namely

$$f = \frac{1.325}{\left(\ln\left(\frac{k}{3.7D} + 5.74\text{Re}^{0.9}\right)\right)^2} \tag{2.2}$$

2.1.1 Networks with a tree structure

In the case here, it is assumed that the flows at the heat consumer stations are determined explicitly. By demanding that mass is conserved in all pipes and pipe junctions, an unique flow value can be determined in every pipe in the system. Specifically, if the pipe system has no loops, then the flow can be computed without concerning pressure at all. In the case of loops, iterative procedures must be used to determine the flow, but only for the pipes in the loops. This is very important since a typical DH network contains very few or no loops, but many pipes and connection points (nodes).

A popular way of representing such a tree structure is to use a connectivity matrix. The procedure for this is as follows:

1. Assign numbers for all the nodes and pipes, counting from 1 for both classes. Each pipe will then have an unique number and be connected to two nodes, each with an unique number too.

2. Define a connection matrix A, which only consists of elements that are either 0, 1 or -1. For each pipe with index i connected to nodes with indices j and k, let $A_{i,j} = 1$ and $A_{i,k} = -1$.

3. Define a vector m, which represents the flows in the pipes such that m_i is the flow in pipe i from the first node defined to the second one.

4. Now, if Q_j is the discharge of flow from node j to an external sink, an equation for conservation of mass can be written as

$$A^T m = Q \tag{2.3}$$

It should be emphasized that these steps only describe the flow computations in the case where there are no loops in the system. For such simple case the flow can be determined simply by solving (2.3) for m, given Q. This can be done very efficiently since the matrix A is very sparse and only contains elements with 0, 1 or -1.

2.1.2 The case of network loops

In the case of loops in the system, a non-linear equation must be solved in order to find the flow in the loops. Note that only the actual pipes in each loop are concerned, which is in many cases only a fraction of the total number of pipes in the DH network. This is done by defining a balance equation for the pressure drop in a pipe from node i to node j, using the head loss due to flow given in (2.1)

$$\left(f \frac{8L|m|}{D^5 \rho^2 \pi^2 g} \right) m + h_i - h_j = 0 \tag{2.4}$$

If balance equations for all the pipes are assembled, then (2.4) can be written on a matrix form as

$$Cm + Ah = 0 \tag{2.5}$$

where C is a diagonal matrix containing a Darcy-Weisbach equation for each pipe. Note also that the matrix A is the same connectivity matrix as used in (2.3). It is now possible to combine (2.3) and (2.5) to form a complete balance equation for the network, which then becomes

$$\begin{bmatrix} C & A \\ A^T & 0 \end{bmatrix} \begin{bmatrix} m \\ h \end{bmatrix} = \begin{bmatrix} 0 \\ Q \end{bmatrix} \tag{2.6}$$

In order for this system to be solvable, at least one reference pressure must be determined, which will result in some additional values in the right hand side vector. Note also that C is in general a function of m, which means that the system is non-linear and must be solved by iteration. For further reference on this, see Nielsen (1994) and Valdimarsson (1993).

In the current section, aspects of flow computations have been presented. This includes formulas for calculating flows in a tree-like network, which is of main interest in the project, but it is also shown how to deal with loops in the network. The next step is to consider the temperature changes in the DH network, which is the topic of the following section.

2.2 Temperature dynamics

The primary interest in modeling DH networks in this study is to simulate the rate of energy transport through the system. This transport is mainly dependent on the water flow through the system, which was discussed in the preceding section, but also on the temperature levels in the DH network.

As mentioned before, the flow, which is driven by pressure differences along the pipes, is responsible for most of the energy transport. In fact, if all temperatures in the system were at one constant level, the flow would solely determine all the transport. So the question is how does the temperatures in the system change. There are mainly three things which impose changes in temperature in a DH system:

- Changes in supply temperature which are controlled by a system operator. These changes occur typically at production plants and can be both large and quickly varying.

- Return temperature changes due to cooling at the consumers houses or heat-exchanger stations. This should be relatively stable but quick changes can occur, especially for large and specific consumers such as public buildings.

- Heat losses in the DH pipes. Temperature drops due to cooling in pipes are very stable and can be described quite accurately by static models. However, the changes in supply and return temperatures affect the transient heat losses and the heat accumulation in the DH pipes. Heat losses are thus important, since they describe the main source of energy losses in DH systems. Refer to Bøhm (1999).

There is one important difference between flow and temperature dynamics. Changes is the flow are quickly transferred to the whole network in form of pressure waves, typically in matter of seconds. The temperature is on the other hand connected to the mass of water, which leads to the fact that effects from temperature changes in the DH network are transferred relatively slowly, in relation to changes in the flow. Thus, the response time from a production plant to a consumer station, with respect to temperature changes, can in some cases be up to several hours.

Two types of methods were considered in Benonysson (1991), which are referred to as *the element method* and *the node method.* The element method was found to be inferior to the node method, both with respect to accuracy and computational cost. The main reasons for the poorer performance of the element method were found to be problems regarding artificial diffusion of temperature profiles along the pipes, which could result in abnormal smoothing of sharp temperature profiles. On the other hand, the node method had no severe difficulties regarding artificial diffusion.

In Zhao (1995), an analytical solution to the case of dynamic temperature changes was introduced, assuming constant water velocity over time. A node method (similar to the one in Benonysson (1991)), based on the analytical

solution was presented in Zhao (1995) and found to be at least as good as the one in Benonysson (1991). It is though unclear if this leads to a better solution method when both accuracy and efficiency are taken into account.

The two methods for computing dynamic changes in water temperature, the element-model and the node-model, are based on somewhat different numerical and physical principles. This can be summarized as:

- The element method

    - Computations are based on a temperature profile along a pipe.

    - The method shows excessive artificial diffusion when the Courant number, see Appendix A, approaches zero (small time-step or low water velocity).

    - Heat losses in radial direction are computed by assuming a single uniform temperature in water and steel, and also uniform temperatures in insulation and surrounding ground (lumped approach).

    - In order to compensate for artificial diffusion, the method requires a number of floating point operations for each pipe, proportional to the size of the time-step used.

- The b–node method

    - Computations are based on a time history of temperatures and flows in one single point.

    - The method has some problems with artificial diffusion, especially for Courant numbers close to 0.75, but this problem vanishes if time-steps are smaller.

    - Heat losses are computed by assuming different water and steel temperatures. The heat capacity of the insulation and surrounding ground is not taken into account, thus no dynamic changes in insulation temperatures are considered.

    - When implemented correctly, the method requires a constant number of floating point operations for each pipe, independent of the time-step.

The difference of the two methods can be observed in Appendix A, where they were tested on a given temperature profile with three specific characteristics.

2.3   Simplified models of DH networks

In the preceding section, some of the parts of a DH network have been discussed, which are necessary to perform dynamic simulation of a DH system. This simulation can be performed to various degrees of accuracy, but the time needed for the computations may be excessive and it is therefore desirable to reduce this time.

The first obvious approach in simplifying a DH network is to reduce the number of pipe branches and consumers. In Hansson (1990) the problem of such network reductions was addressed and a simple model consisting of one pipe and one consumer was proposed. In Zhao and Holst (1997) an aggregated network model based on representative consumers was suggested and tested.

In Appendix B, as well as in Pálsson et al. (1999), a method is presented in which an original model of a DH network is replaced by a simplified one, with the purpose of reducing simulation time, but without loosing too much accuracy in the simulation. In Appendix C, the method is further enhanced and also tested on the Hvalsø DH network which involves over 1000 pipes.

The simplified model, referred to as an equivalent network, is generated by gradually reducing the topological complexity of the original network. During this reduction, the relevant model parameters of the network are transformed in such a way that the dynamic behavior of the equivalent network will resemble the original one.

Assume that a full description of a DH network exists, including data on the topology and the pipes (diameters, lengths, and heat conductivity). Moreover, assume that enough information exists for the consumers so that it is possible to compute representative constant mass flows for all branches. If, a representative constant common return temperature for all heat loads is identified, then an equivalent network can be found by repeatedly using the method described in appendices B and C.

The resulting equivalent network is then inspected to identify short branches, i.e. branches with lengths less than a few meters. Such branches are then removed by the method shown in Appendix C. This could be continued until there are only few branches remaining. The last branches removed in this procedure are not necessarily short, but the resulting network is still useful for some simulations.

In order to validate the reduction method, simulation tests were performed on real as well as on equivalent systems. Results show that a complex network with about 1000 pipes has a potential to be reduced to 10 pipes, as shown in Figure 2.2. For a description of the different models *B*, *C* and *D*, refer to Appendix C.
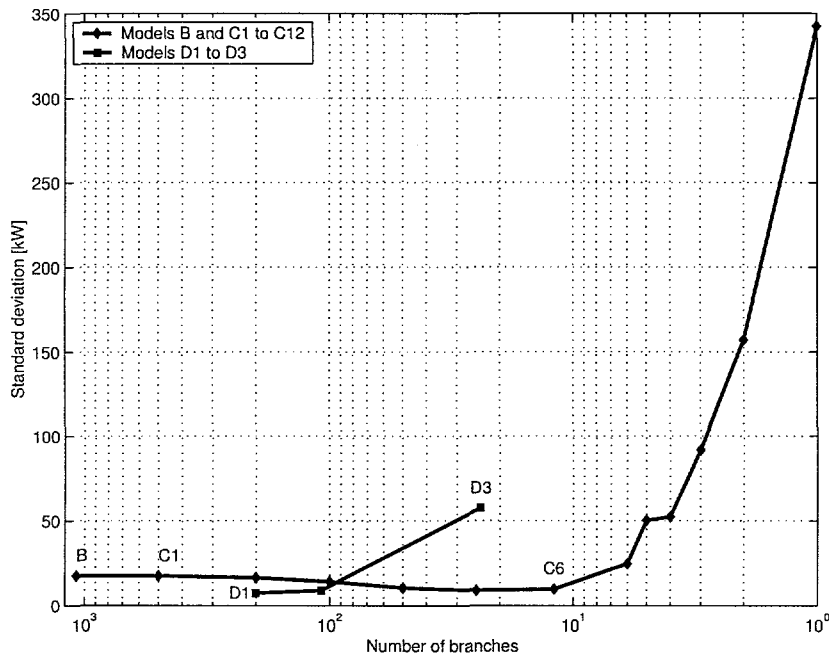
Figure 2.2: Standard deviation of error in energy flow at the plant, for various equivalent models representing different number of pipe branches

This simplification reduces computational time by approximately 99%, since this time is proportional to the number of nodes and branches. Furthermore, in order to verify the quality of the equivalent model parameters they were compared with parameters that are optimally estimated by using least-squares minimization. Results from this study are given in Appendix B

For a complete description of the simplifying process, refer to Pálsson et al. (1999).

2.4 Aspects of operational optimization

In the preceding sections, network aspects of a DH system have been discussed. This includes determination of flow and temperatures in a network as well as methods for simplifying network models. There are though some important things worth discussing, which include application and implementation of models as well as availability of necessary data.

Some of the most important aspects in relation to operations of a DH system include the following items:

- Availability of necessary model data, including:

- Network topology, such as spatial position of pipes as well as consumers and production plants. This information is typically available for some part or all of the relevant DH system.

- Descriptions of various types of pipes, which includes cross sectional description such as wall thickness of steel and insulation, as well as thermal properties.

- Parameters involving the behavior of the consumer side in different operational conditions. Also, individual consumers might behave differently with respect to other consumers

- What decisions can be made for system operation. The main decision element is the choice of supply temperature from production plants, but it typically depends on

  - Various prices, including fuel costs, production revenues (especially in CHP production) and pumping costs.

  - Conservation of energy, which is very much connected to the item above, but also includes heat losses from the DH network.

  - Emissions from the production. This can be an important factor if emission-taxes are high.

  - Various system constraints, such as minimum and maximum supply temperature to the consumers, as well as maximum flow which is related to the pumping capacity.

- Prediction of uncertain data, from one day up to one week ahead. Here the main issue is the consumer's heat load which is in general only known from measurements of yearly load. Since it is desirable to have an estimate of the future heat load, some forecasting methods have to be used.

The items above determine a basis for operational optimization, which forms a list of the most essential elements in performing such optimization. When optimizing the operation of DH systems in general, the scope of interest can be put into the following three classes.

- Operational optimization of production plants, such as boilers, CHP plants or heat-pumps.

- Operational optimization of a DH network, typically with respect to heat losses and pumping costs.

- Operational optimization for DH consumers, which can be either large heat-exchanger stations or single buildings.

It is possible to derive a mathematical representation of the operational costs by considering the relevant network components, such as electric consumption of pumps, fuel consumption and sold energy to the consumers, see e.g. Benonysson (1991). Given an operational strategy, the system behavior is taken into account and costs can be computed for this given strategy. The problem then consists of selecting the correct strategy which minimizes the costs.

2.5 Conclusions

In this current chapter some of the most important parts of DH systems have been discussed. This includes mathematical modeling, simplified networks and operational aspects.

Two methods have been under focus for computation of temperature dynamics. Of these two, the node method has been shown before to be computationally more efficient than the element method. Furthermore, it has been shown in Appendix A that the node method is unconditionally stable and its accuracy can be further improved on than in its original form.

The models for the pipes have been tested by using real cases and real measurements from a large transmission DH company, see Pálsson et al. (1999). This system, the Vestegnens Kraftvarmeselskab (VEKS), has provided data for a part of their distribution area, which has been used for getting a real problem perspective and to test the models.

When finding an equivalent network, the complexity of the DH network is reduced by gradually changing the tree structure into a chain structure with no branches. Correspondingly the various parameters which define the branches are transformed from the real network to equivalent parameters in the corresponding equivalent network.

The equivalent network is reduced further by observing that many nodes in this network are positioned close to each other, separated by short pipes. Such nearby nodes are collapsed to simplify the equivalent network. This procedure can be continued until there are only very few pipes remaining. The last pipes removed in the procedure are not necessarily short, but the resulting network could still be useful for some simulations.

Testing of such equivalent DH networks has been performed simulating two case studies, using the original network as well as the equivalent network. It has been shown that a relatively large network, consisting of more than

1000 pipes, can be simplified into an equivalent one consisting of only 10 pipes, without significant loss of accuracy.

Chapter 3

Operation of decentralized combined heat and power plants

This chapter concerns the central aspect of the thesis, namely the planning of production at a DCHP plant, in an optimal way. The most common type of DCHP production units in Denmark is considered, which is based on piston engines, burning natural gas. For a general description of technical and economical aspects of CHP production, refer to Horlock (1987) and Horlock (1992).

In general terms, a typical decentralized CHP plant is fitted with a heat storage in the form of a hot water tank. Furthermore, many of the production units are based on piston engines as mentioned above. In several of those cases, existing heat-only (boiler) plants have been converted to such CHP plants, but with the duty of delivering heat to DH consumers unaltered. Thus, the main concerns when operating CHP plants is do deliver enough heat, and sell power to the highest price possible.

The fact that the price of electric power varies, depending on the time of day and the current weekday, poses a problem for the plant operator. He must fulfill the heat demand, but at the same time try to produce when the price for power is high. Furthermore, the operator has to take into account that the future heat demand has a stochastic element involved and is therefore not explicitly known.

This dilemma can be partly avoided by using the heat storage to store excess heat when power production is profitable, and to supply heat to the DH customers when the power price is low. Therefore the operator faces an optimization problem, which is to determine when to operate the CHP plant, taking into account the storage contents and the uncertain future heat-load. This is often referred to as the stochastic heat storage problem.

Aspects of the heat storage problem have been studied and solved in many
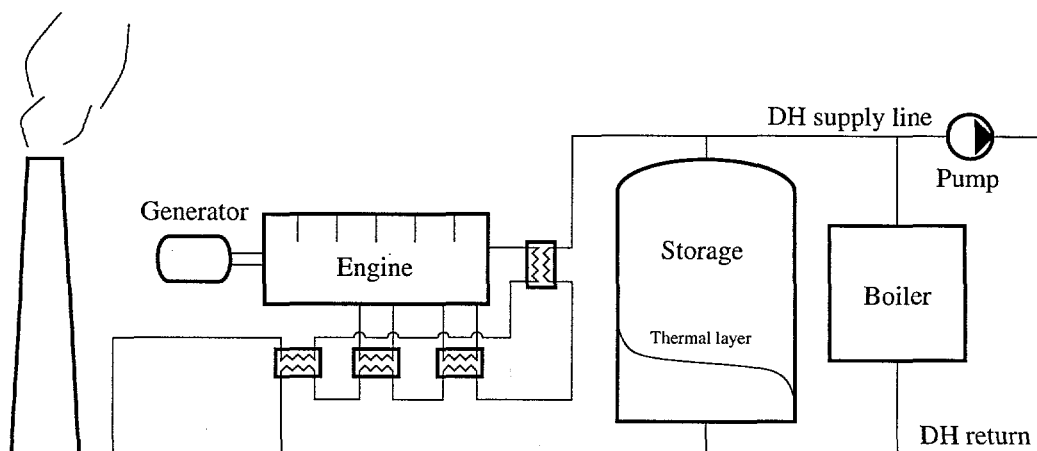
Figure 3.1: A plant with a thermal storage and one CHP unit

different ways. Most of the work has been done by using deterministic opti-
mization procedures, such as general nonlinear programming, mixed-integer
linear programming and dynamic programming, refer to e.g. Pálsson and
Ravn (1994), Eriksson (1994), Jørgensen and Ravn (1994), Ravn and Ry-
gaard (1994). When considering stochastic optimization, the problem has
been solved by using the so-called progressive hedging algorithm as well as
dynamic programming.

In Appendix D, a method is derived with the purpose of solving the
stochastic heat storage problem. The method is based on stochastic dy-
namic programming, and involves finding a decision for each hour of the day,
whether to produce or not.

3.1   Description of Hvalsø CHP plant

A DCHP plant in the town of Hvalsø has been used as a reference case
in the current study. The purpose has been to obtain a basis for various
measurements, e.g. heat load and DH temperatures, as well as a detailed
description of a DH network.

The plant is located in the center of Zealand in Denmark, and is connected
to a DH network serving over 600 heat consumers. These consumers are
mainly single family houses, but some larger consumers are also connected
to the network.

Figure 3.1 shows a schematic diagram of the plant, which is fitted with
heat storage. The production units at the plant consist of an engine, produc-
ing 3.5 MW heat and 2.9 MW electrical power. The engine is accompanied
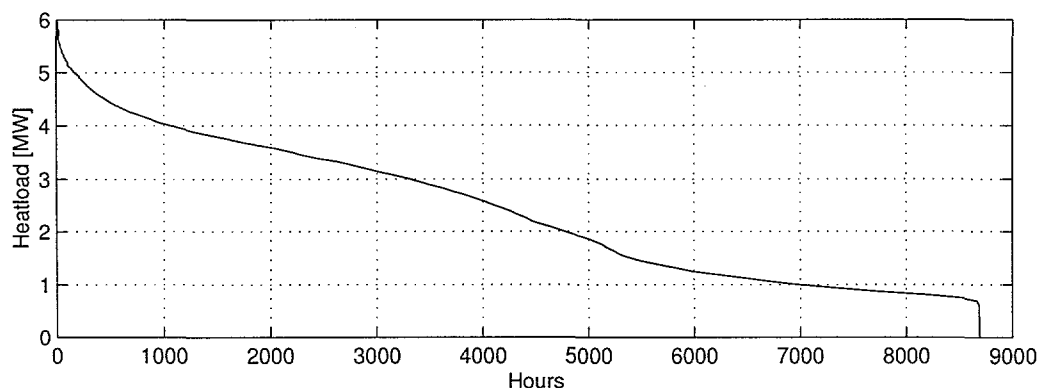
Figure 3.2: Load duration curve for yearly heat load at the Hvalsø DH plant in 1998.

by two heat-only boilers which produce 4 MW and 6 MW heat, respectively.

The annual load is distributed as shown in Figure 3.2. It is seen that the load is higher than the maximum output from the engine (3.5 WM) for about one fourth of the time, but the use of heat storage minimizes the need for using the boilers in such extreme conditions.

3.2 Modeling a decentralized CHP plant

In this section a simple mathematical model of a CHP plant is presented, which can consist of pure CHP units with fixed heat/power ratios, heat-only boilers, as well as a single heat storage unit. No attempt is made to model plant thermodynamics in detail, since the main focus on storage operation with respect to sold electric power. Refer to Horlock (1987) for a detailed theoretical discussion of both thermodynamics and economics CHP plants in general.

3.2.1 General remarks about production units

Large CHP units are often divided into two classes: (i) Extraction units and (ii) Back-pressure units. The extraction units possess the ability to adjust the ratio between heat and power production, whereas the back-pressure units must produce at a fixed ratio. Frequently, units in these classes are large and centralized with the obligation to fulfill the demand of power as well as heat.

When considering rather small decentralized CHP plants, some aspects of the production characteristics change. The small size implies that power production on a large-scale network can be considered *stiff*, which means

that an individual plant has no real effect on the power-network load and does not take part in regulating the total power production (However, the combined effect of many DCHP may be important, see Chapter 4). Another characteristic is that the main priority for the plant operator is to fulfill the heat demand, which literally makes power a secondary product in terms of production commitment.

The main advantages of using piston engines in CHP production are the high operational efficiency along with relatively low start-up costs. The engine is connected mechanically to a power generator, but the heat is extracted from the cooling water, lubrication oil and most importantly, the exhaust gas. The direct connection to a generator requires that the engine have a constant rotation speed in order to conform to the power-network frequency. Thus if startup costs are omitted, which are the result of warming the engine up to operational temperature, the most important decision is if to produce or not.

As mentioned before, decentralized CHP plants are often equipped with one or more heat-only boilers. The main function of these is to provide heat in case of a high heat-load for a long period of time, as well as in breakdown situations. If these units are kept warm, startup costs are generally low and are therefore disregarded in this study. Thus, the operation of a boiler is determined in the same manner as in the engine case, only with different cost structure.

3.2.2   The heat storage

A typical heat storage unit is in the form of a tank, filled with DH water, as shown in Figure 3.1. The supply/return water is loaded/unloaded respectively through the top and bottom of the storage, which in turns generates a thermal layer between the supply and return water. Active usage of the storage will keep the thermal layer thin, which is important since blending of the supply and return water reduce the usability of the water in terms of exchange of heat.

The effect of the thermal layer thickness is not considered in this study, which leads to the assumption of a sharp boundary between supply and return water. The heat losses from the storage can be estimated by calculating the heat flow through the wall, top and bottom, but in most cases the losses are very small and could be disregarded.

3.2.3   A plant operation model

In the current work, a simple plant consisting of production units and one storage tank is considered, as shown in Figure 3.1. When operated, the units

produce at full capacity with constant efficiency, thus the lower efficiency at partial load and start-up are disregarded.

The cost of operating the engine is mainly related to the gas usage, as well as the produced power and heat, which gives a negative cost. Running a boiler on the other hand results in positive cost, representing the gas usage, as well as negative cost because of the produced heat.

The dynamic changes in the heat storage during a given time interval are dependent on the production, the heat-load, as well as the heat losses from the storage. It is convenient to denote the storage contents as the relative stored energy with respect to the interval between empty and full storage. This denotes in particular the relative height of the thermal layer in the storage, as shown in Figure 3.1.

To summarize the description above, the following problem is stated. Minimize, by choice of production at each hour over the coming week, the expected cost (operating cost minus income from sold power), subject to operating constraints on the plant and storage, and given that heat demand in each time step is satisfied. In the next section the stochastic heat demand from DH customers is considered.

3.3 Modeling the stochastic heat load

A fundamental element in a complete dynamic model of a decentralized CHP plant is the heat-load in the DH-network connected to the plant. There are three main things affecting time dependent changes, or dynamics, of the heat-load:

- House heating, which depends on e.g. the outdoor temperature, solar radiation and wind speed.

- Hot tap water usage, which is dependent on the behavior of the local inhabitants connected to the DH-network.

- Time delays in the DH network, as well as heat losses from the pipes.

Figure 3.3 shows the heat load and measured outdoor temperature in Hvalsø during winter, spanning over a period of 15 days. It can be observed that the load is correlated with the temperature, which can be utilized in modeling and predicting heat load.

Stochastic modeling of heat-loads in DH systems has been studied extensively, see e.g. Sejling (1993). Most of the work has been focused on determining the heat-load with the aid of known outdoor temperature (or predictions of temperature). This has for example resulted in black box
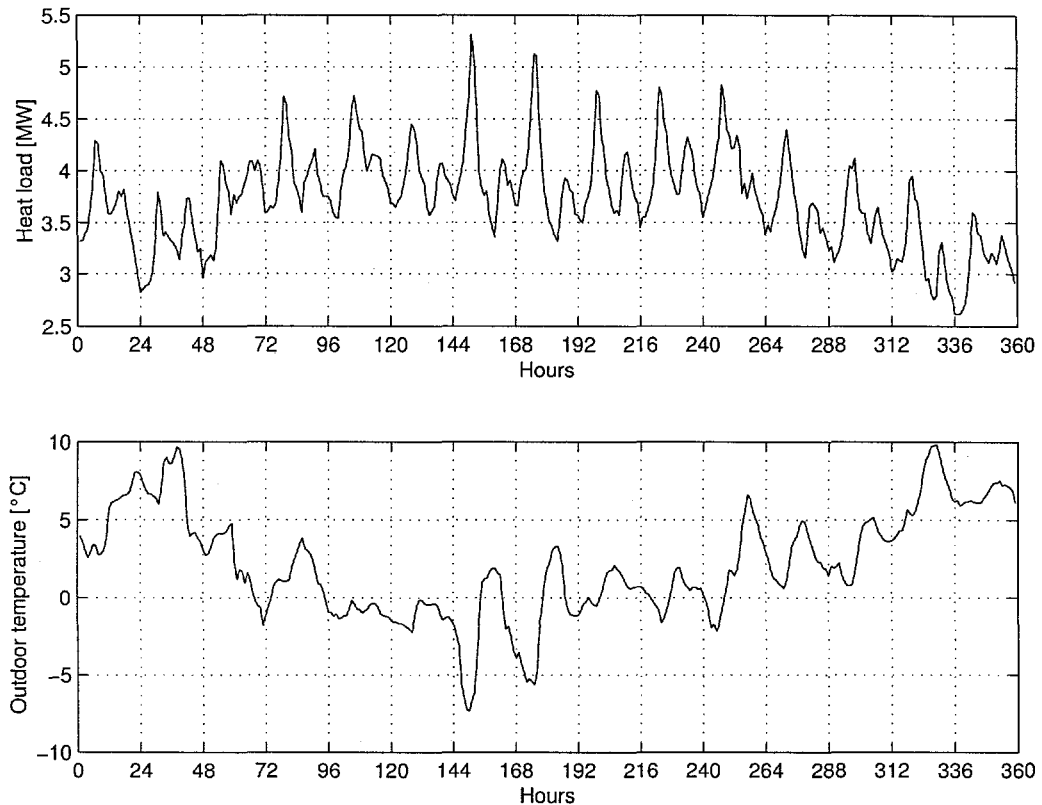
Figure 3.3: Heat-load and outdoor temperatures at Hvalsø. A selected period from the winter of 1998.

models of the type: Autoregressive Moving Average with extraneous input (ARMAX) (see e.g. Madsen (1995) and Bøhm et al. (1994) for reference), with time dependent model parameters.

In Madsen et al. (1990), a time series model was recommended for use with heat load prediction. This model has been modified here, to only include the outdoor temperature as an input variable. Figure 3.4 shows a comparison between measurements and respectively, 1 and 18 hours predictions.

Finally, Figure 3.5 shows how the standard deviation of the prediction errors changes with increasing prediction horizon. The errors are computed on one hand by considering the data used for estimation, and on the other hand by using a different data set (cross validation). As expected, use of the different data set results in larger deviation, since it has not been used for determining model parameters as in the first set.

The future heat-load must be considered and predicted with some reasonable accuracy, in order to choose an optimal operation strategy for a
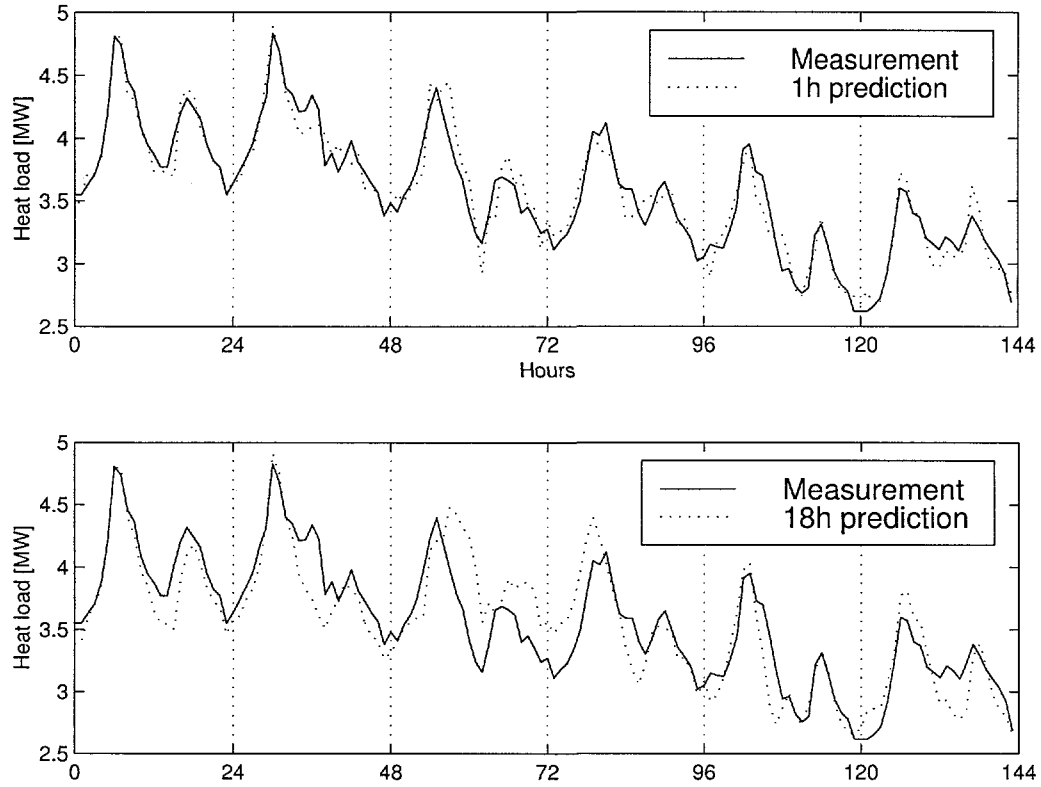
Figure 3.4: Difference between two prediction horizons and the true heat-load measurements for a 6 day period.
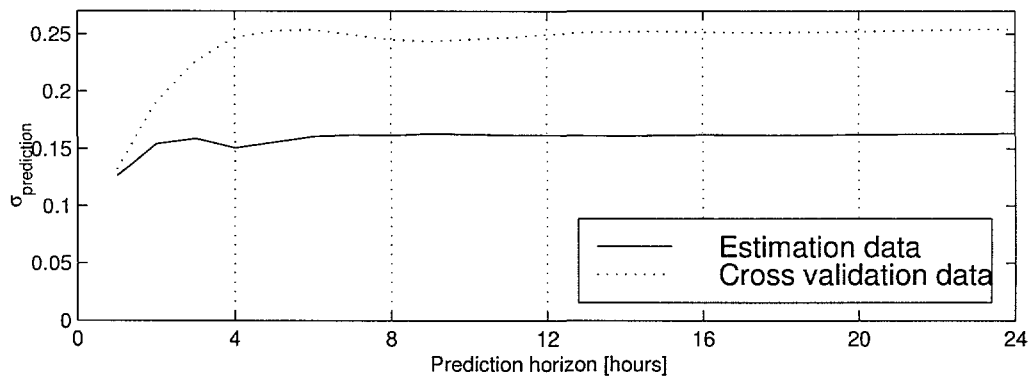
Figure 3.5: Average prediction errors for different prediction horizons.

DCHP plant. These predictions must extend over a suitable time-horizon, so that the operation can be planned with an optimal utilization of the plants' storage.

In Appendix D, the heat-load was modeled without taking the outdoor temperature into account. The following model was found sufficient to describe the heat-load Q as a stochastic process

$$Q(t) = a_1 Q(t-1) + b_1 Q(t-24) + b_2 Q(t-25)$$
$$+ f_0 + f_1 \cos(\tfrac{\pi t}{12}) + f_2 \sin(\tfrac{\pi t}{12}) + f_3 \cos(\tfrac{\pi t}{6}) + f_4 \sin(\tfrac{\pi t}{6}) + e(t) \quad (3.1)$$

where e is the error between actual and predicted output and a, b and f are parameters to be estimated.

Given measured data for Q, it is possible to estimate the parameters once and use them for prediction. Another approach, which is described in Bøhm et al. (1994), is to use recursive estimation of parameters. This approach ensures that if the dynamic properties of the heat-load change, the parameters will follow. In this study, only the former approach has been used.

3.4   Optimal control and dynamic programming

In this section, an optimization method is described which can be used to solve the problem posed in Section 3.2, taking the stochastic heat-load from section 3.3 into account. This is covered more thoroughly in Appendix D (Pálsson (1999)).

3.4.1   Dynamic programming

The so-called dynamic programming method is used here, which is described e.g. in Bellman (1964). A general definition of this method, when applied to the present problem, can be written as

$$\max_{\mathbf{u}} \left\{ \sum_{t=0}^{N-1} r_t(x_t, u_t) + r_N(x_N) \right\} \quad (3.2)$$

subject to,

$$x_{t+1} = d_t(x_t, u_t) \quad (3.3)$$
$$0 \leq x_t \leq 1 \quad (3.4)$$
$$u_t \in \{0, 1\} \quad (3.5)$$

Here, $\mathbf{u} = [u_0, u_1, \ldots, u_{N-1}]$, and the function $d_t(x_t, u_t)$ corresponds to the definition of model dynamics. Furthermore, x_t denotes the relative contents of the storage at the beginning of time t, N is the total number of periods, r_N is a given cost function which evaluates the final content of the storage, and r_t is the cost of production over period t.

The problem above can be rewritten such that instead of solving the whole optimization problem, small problem is solved at each time-step, which conforms to the Bellman optimality principle. The steps of this separation method are given as follows:

1. Define $F_N(x_N) = r_N(x_N)$

2. Then for $t = N - 1, N - 2, \ldots, 0$ let

$$F_t(x_t) = \max_{u_t}\{r_t(x_t, u_t) + F_{t+1}(d_t(x_t, u_t))\} \qquad (3.6)$$

$$\phi_t(x_t) = u_t^*(x_t) \qquad (3.7)$$

where the cost-to-go function $F_{t+1}(d_t(x_t, u_t))$ must be defined in each step and u_t^* is the optimum obtained from (3.6). The definition of the cost-to-go function is arbitrary, but is piecewise linear in the present case.

3. At this step, x_0 is typically supplied as present storage contents and then finally for $t = 0, 1, \ldots, N - 1$ let

$$u_t^* = \phi_t(x_t^*) \qquad (3.8)$$

$$x_{t+1}^* = d_t(x_t^*, u_t^*) \qquad (3.9)$$

Now u_t^* contains the optimum strategy at time t, which forms a total of $N - 1$ decision variables. The real strength of the dynamic programming method is that this solution can be obtained with computational complexity, proportional to the number of time-steps, N.

Another strength of the method is that if x_t changes at t, then information about u^* still exists since it is given in the strategy function $\phi_t(x_t)$. This is important in the present work, because the heat-load is stochastic and thus x^* is not known in advance.

Results from an optimization for a winter period and a summer period are shown in Appendix D. It is concluded that the stochastic dynamic programming method as implemented here, finds an optimum strategy for both cases, and is furthermore computationally efficient and robust.
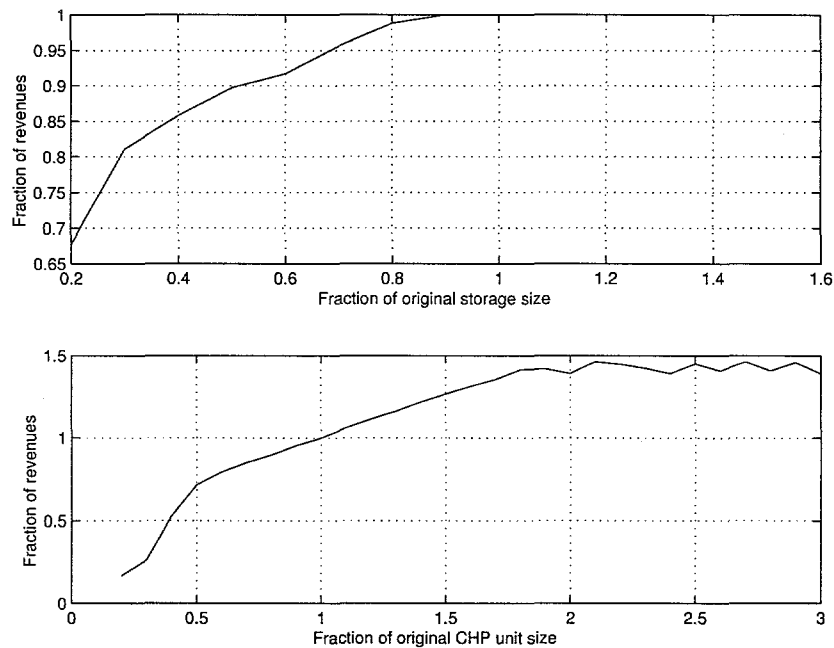
Figure 3.6: Sensitivity analyses of unit size and storage size, with respect to given heat load.

3.5   Sensitivity analyses of plant parameters

Results from the operational planning in Appendix D indicate that the plant can be operated optimally in the specific periods. But this only includes one specific plant, where the ratio between the storage size and the capacity of the CHP unit is fixed.

Figure 3.6 shows the result of operational planning when the storage size and the CHP production capacity is gradually changed. It should be noted that only one of the parameters has been changed at a time. It should also be noted that only generation costs are considered.

For changes in storage size, it is seen from the figure that a larger storage at Hvalsø would give no gains. The storage is apparently designed to precisely meet the needs of the current plant. As the storage becomes relatively smaller, its importance becomes visible. The revenues are reduced, since there is not enough storage capacity to fulfill the heat demand between high tariff periods.

In the case of changes in CHP unit capacity, it is seen that a larger unit would give higher revenues. There is though a saturation point where the unit is twice as large as in Hvalsø. The reason for the increase in revenues is that the larger unit has the opportunity to produce almost solely in the

higher tariff periods if the storage is large enough to provide the necessary heat in between those periods.

3.6 Conclusions

Due to high thermal efficiency when compared to traditional power-only plants, CHP plants have become more popular in recent years. In Denmark, a trend has been towards building relatively small CHP units in decentralized urban areas, in which heat is produced for use in DH and power is sold to a global power network. Varying prices of power pose a problem for the operation of the DCHP plants, which can be compensated for by installing heat storage, which is used as a buffer between heat production and heat demand.

In the current work an optimization method is proposed, especially designed to find an optimal boolean structured start-stop strategy for a simple DCHP plant, consisting of piston engines and boilers. For the optimization, stochastic dynamic programming is used, focusing on the storage and the stochastic nature of the heat-load. The resulting method solves an integer optimization problem with a computational complexity linearly connected to the number of boolean variables in the problem.

Results from case studies show that the method is computationally very efficient, solving a problem with 168 (every hour in one week) boolean variables in a few seconds on an ordinary PC computer. The results are also found to be optimal for a stochastic optimization, but with a slight suboptimality in a deterministic reference case, see Appendix D.

Finally, results from simple sensitivity analyses indicate the importance of a correct storage size, as well as how the revenues change with varying production capacity.

Chapter 4

The power system implication of decentralized combined heat and power plants

The number of decentralized combined heat and power (DCHP) plants in Denmark has increased considerably in recent years. These plants are operated individually and can furthermore sell electricity to the power network at will. This increasing number, and thus the increasing participation of DCHP production in the total power production, has put some strain on the power plants which are used to balance production with demand. It is therefore of interest for the power system operator, who is responsible for the power balance, to obtain a reasonably accurate model of the total power production in the DCHP plants.

Typically, a DCHP plant produces and delivers heat to a local district-heating system on demand. But the power is sold to a central power network, for a price which is dependent on time of day. These price changes are referred to as power tariffs. In order to ensure good economy, a DCHP operator has to produce power when the price for power is high.

Because of the independent nature of the many DCHP plants, it is quite difficult to predict or model the total power production from these plants. Nevertheless, it can be assumed that if the power tariffs are the same for all the plants, then they should operate in a similar way during the day.

4.1 Decentralized production in Denmark

The recent growth in the DCHP production in Denmark is illustrated in Figure 4.1, which also shows that this growth has taken place within ten
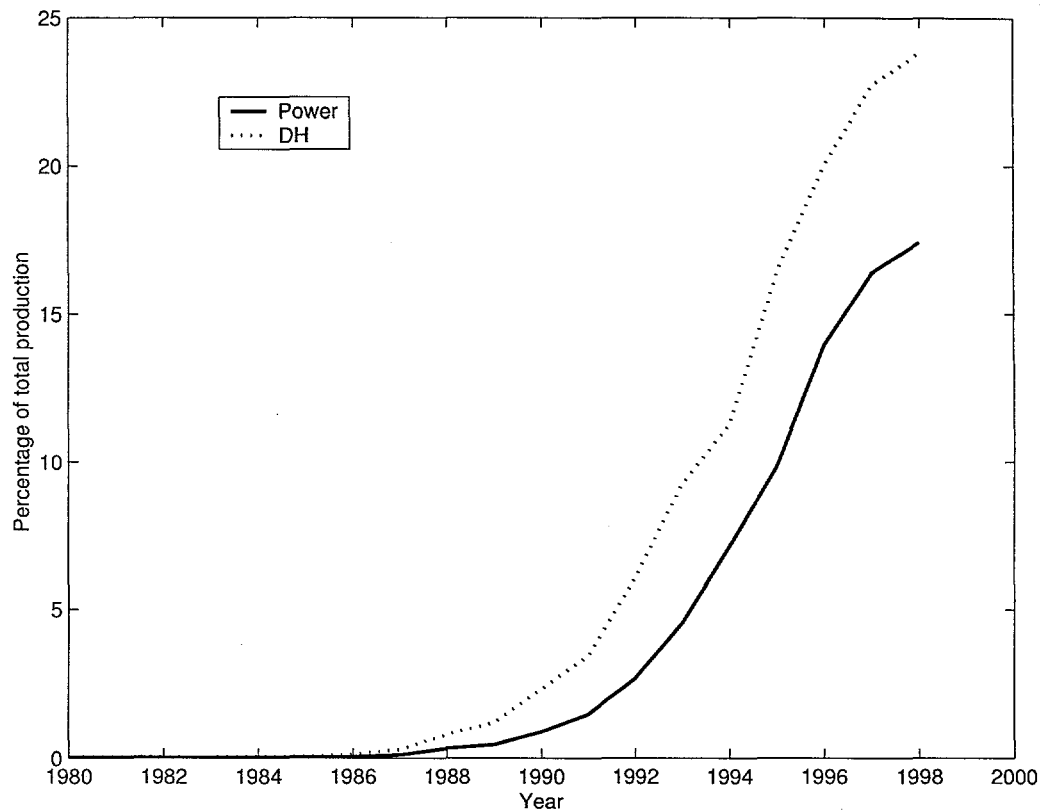
Figure 4.1: Percentage of DCHP power production in Denmark, with associated heat production to DH systems.

years or so. See Energistyrelsen (1998) for the source of data.

The figure shows a slow startup in 1985 followed by a rapid growth in the years 1991 to 1997. Furthermore, the growth begins to saturate after 1997, probably because the most feasible DH areas have been equipped with DCHP plants. The figure also shows the percentage of DH heating associated with DCHP, compared to the total DH production.

The typical case in Denmark for DCHP production is when the plants deliver heat to a local DH system in relatively small communities. Many such DH networks exist and have traditionally been operated by heat-only boilers. Furthermore, they are often isolated from larger transmission networks, which makes them ideal for conversion from boilers into DCHP.

One of the important driving forces behind the growth of DCHP plants is the economic feasibility of the production. Because of the environmental benefits of DCHP production, the Danish government decided to pay DCHP plants 0.1 DKK for each produced kWh, which corresponds to about 60% of
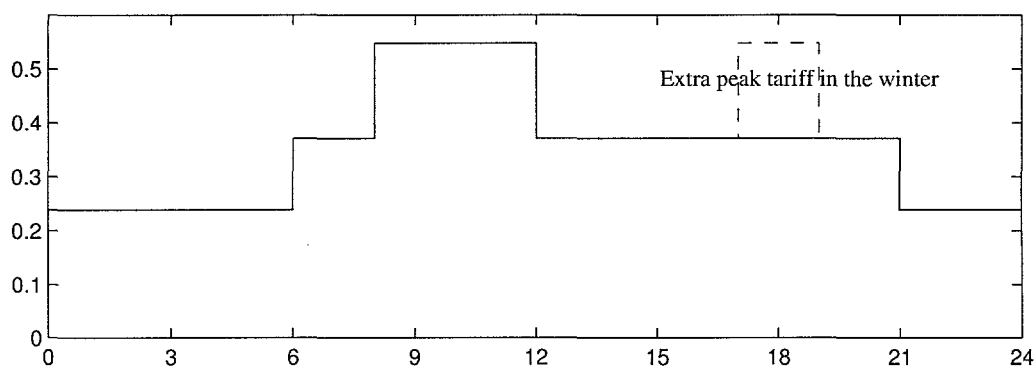
Figure 4.2: The power tariff at Hvalsø

the lowest power tariff. This has since been reduced to 0.07 DKK per kWh for larger plants.

The DCHP plants are of various types and use different fuel. These include piston engines burning natural gas, which is the most common equipment in the smaller plants, as well as gas turbines and combined cycle plants, also burning natural gas. The choice of fuel is typically natural gas from the North Sea, but can also be in the form of bio-gas, straw, wood chips and oil.

In the current situation, the power tariff is fixed in Eastern Denmark. Figure 4.2 shows the tariff for sold electricity in DKK, during the 24 hours of the day. Note that the figure includes the extra revenue of 0.1 DKK per kWh, which was mentioned above.

4.2 Models of the time varying power production

In this section, an attempt is made to model the sum of power production from the DCHP plants in Eastern Denmark (Zealand).

An existing model of the total power consumption in Zealand, refer to Nielsen et al. (1998), is used as a basis in the modeling work. When this existing model was applied on the specific problem for DCHP, it turned out that it was very difficult to obtain a convergent solution for the model parameters. The reason for this is probably the special behavior of the independent DCHP plants, which have a total freedom of choosing to produce or not.

4.2.1   Reference model

Here follows a description of the original model which was used in Nielsen et al. (1998) for modeling the total power production in Zealand.

The model is assumed to be used for specifying the power production P_t on an hourly basis t. The definition of P_t is then given as

$$P_t = \mu + Y_t + D_t + f_1(T_t) + f_2(W_t) + f_3(R_t) + e_t \qquad (4.1)$$

where Y_t denotes a yearly variation, D_t denotes diurnal variations, μ is a constant and e_t is a stochastic error term. Furthermore, f_1, f_2 and f_3 describe the dependence to the outdoor temperature T_t, wind speed W_t and solar radiation R_t, respectively.

The yearly variation Y_t is modeled as a cubic spline, and thus μ can be discarded since it can be included in the spline. There is a total of 29 spline points specified over one year, with a larger concentration of points around Christmas and the summer holidays.

The diurnal variation D_t is described in the original model with trigonometric functions, or Fourier series. Different types of days are also taken into account and classified as: (a) working days, (b) Saturdays and other half-holidays and (c) Sundays and other holidays. The model description for D_t is given in Nielsen et al. (1998) as

$$D_t = \sum_{i=1}^{3} I_i(t) \left(\mu_i(t) + \sum_{j=1}^{5} \left(c_{i,j}(t) \cos \frac{2\pi j h_d(t)}{24} + s_{i,j}(t) \sin \frac{2\pi j h_d(t)}{24} \right) \right)$$
$$(4.2)$$

where $I_i(t)$ is an indicator for the different types of days ($I_0(t) = 1$ then a working day is considered, etc.), $\mu_i(t)$ is a constant term dependent on the type of day and $h_d(t)$ is the time of day in hours. In order to ensure an unique solution, $\mu_i(t)$ must be restricted such that

$$\mu_1(t) + \mu_2(t) + \mu_3(t) = 0 \qquad (4.3)$$

The constants, μ_i, and the Fourier coefficients, $c_{i,j}(t)$ and $s_{i,j}(t)$, are specified for each combination of $i = 1, 2, 3$ and $j = 1, 2, 3, 4, 5$ as

$$\alpha(t) = \gamma_0 + \sum_{i=1}^{5} \left(\gamma_i^c \cos \frac{2\pi i h_y(t)}{24 N_d} + \gamma_i^s \sin \frac{2\pi i h_y(t)}{24 N_d} \right) \qquad (4.4)$$

where $\alpha(t)$ is one of $\mu_i(t)$, $c_{i,j}$ or $s_{i,j}$, $h_y(t)$ is the time of year in hours and N_d is the number of days in the year.

Finally, the functions $f_1(T_t)$, $f_2(W_t)$ and $f_3(R_t)$ in (4.1) are defined as

$$f_1(T_t) = \frac{a_{T_2}}{1 + \exp\left(a_{T_1}(T_t - a_{T_0})\right)} \qquad (4.5)$$

$$f_2(W_t) = a_W W_t \qquad (4.6)$$

$$f_3(R_t) = a_{G_2} \exp(-a_{G_1} R_t) \qquad (4.7)$$

where a are unknown parameters. Note that $f_1(T_t)$ and $f_3(R_t)$ are the only non-linear contributions to the model in (4.1).

Now the problem can be stated as follows: Given a time period $t = 0, \ldots, n_t$ as well as data values for P_t, T_t, W_t and R_t, find the parameters γ in (4.4), a in (4.5–4.7) and the cubic spline for Y_t, such that the sum of squares for e_t is minimal.

4.2.2 Parameter estimation

The model described in the preceding subsection was fitted with DCHP production data, which was provided by Elkraft. A general nonlinear data fitting algorithm was used to find the parameters.

Figure 4.3 shows the accumulated DCHP production for three years. The values shown in the figure are normalized, so that the average production is the same for all the years. The real average production is 20.2 MW, 30.4 MW and 39.1 MW respectively for the years 1995, 1996 and 1997. It is apparent that 1995 is somewhat different in structure than the other two. Therefore the modeling here is based on 1996, in order to be able to cross validate the model with 1997 data, as shown in the next section.

Results for the model estimation include a climatic part, shown in Figure 4.4, and both diurnal and yearly variation as shown in Figure 4.5. It is seen that the effect of outdoor temperature is quite high; about 80% of the load in cold weather is described by the temperature. Furthermore, the diurnal variations are at maximum during the summer, which can be explained by the fact that in spite of reduced heat load, the plants still produce at full capacity in the peak tariff periods.

The model describes DCHP production to a slight lesser degree than when it is used to describe the total power production in Eastern Denmark The average absolute error for the model is 9.85% with a goodness of fit (R^2) equal to 0.946, compared to 5% and $R^2 = 0.98$ for the original model, reported in Nielsen et al. (1998).

In the next subsection, the current model is applied to predict the DCHP production in 1997.
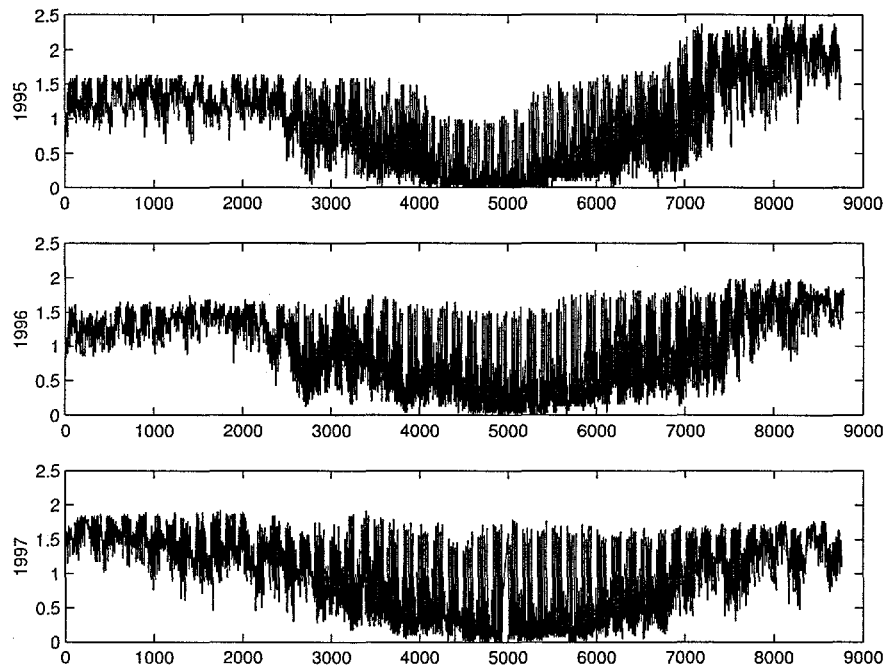
Figure 4.3: DCHP production in the NESA district 1995–1997
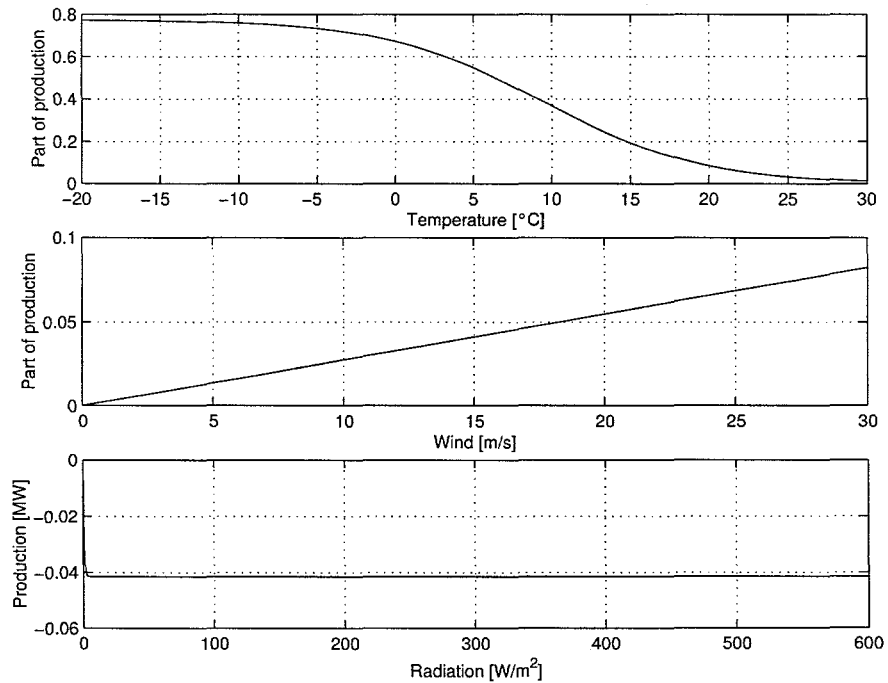
Figure 4.4: Climate effect on the power production
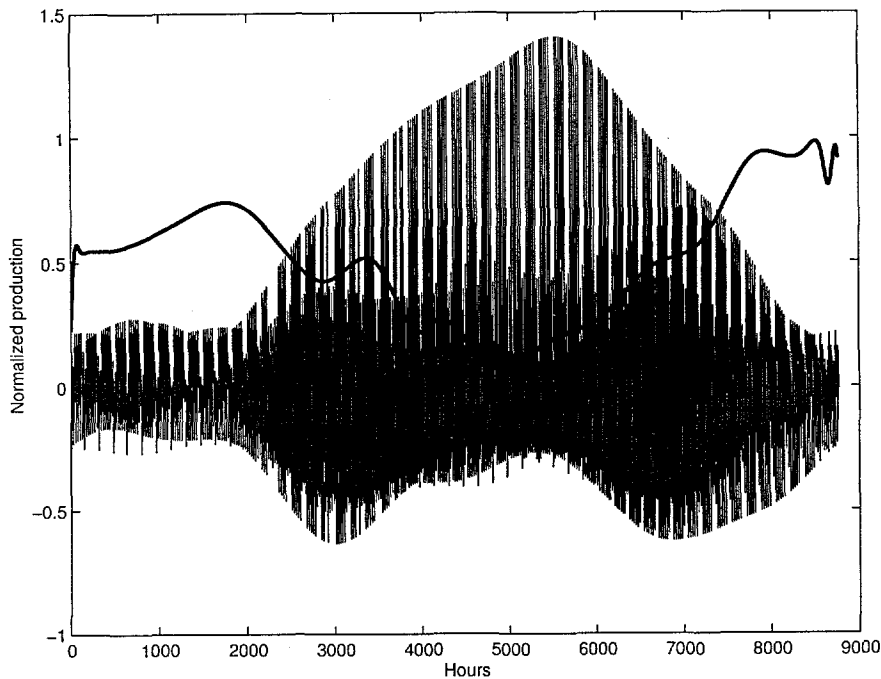
Figure 4.5: Yearly (slowly varying) and diurnal effects

4.2.3   Prediction of production

Here prediction of the accumulated power production from DCHP plants is performed, by using a model based on one year old production data from 1996. It is assumed that the climate variations are known, and thus climate data from 1997 is used to predict the production in 1997.

Figure 4.6 shows a comparison between real production data from 1997 and a model result, in a time window where the fit is good. The figure also shows the model errors for the whole year, which indicate that the first month or so has serious errors in form of a persistent negative value, which becomes lesser when approaching the autumn of 1997.

The goodness of fit for this cross validation is 0.848, which is considerably worse than in the model validation in the preceding section. The mean absolute error is found to be 17.8%, also quite higher than before. The main reason is that the changes in the production structure between years are quite visible, as seen in Figure 4.3, so it is diffucult to model one year which is based on another one.
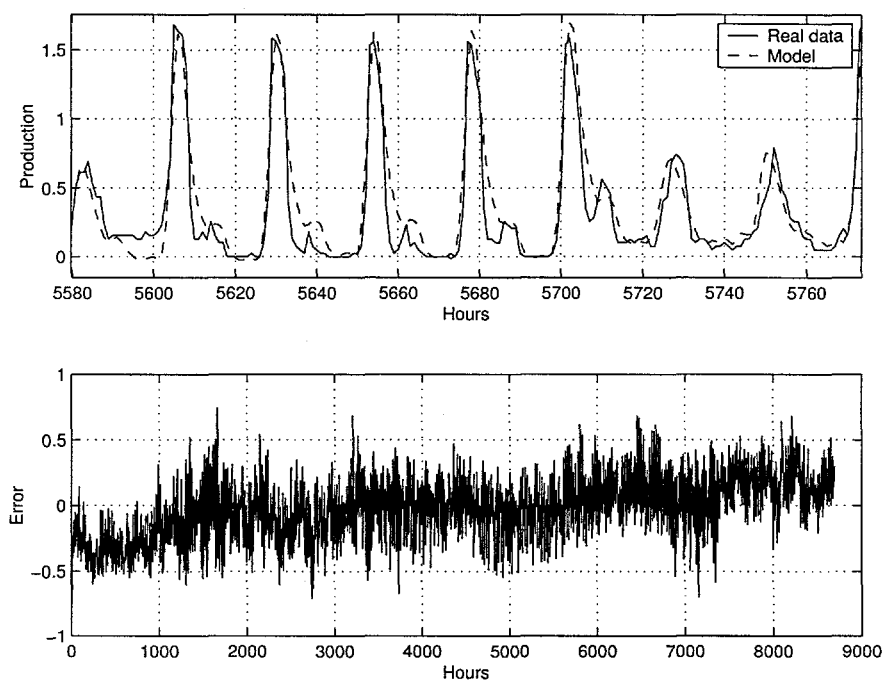
Figure 4.6: Selected model results and the errors during the whole 1997

4.3 Probabilistic production simulation

In this section a method to perform probabilistic production simulation of CHP systems is discussed. The method is based on similar power-only studies but was extended to include heat areas, as described in Søndergren and Ravn (1996). In the current work, the method is fully described in Appendix E and Appendix F, see also Larsen et al. (1997).

An important element in the planning of future heat and power production systems is the dimensioning of the system, that is finding the appropriate types and capacities of production plants. This involves the assessment of possible plant failures, referred to as forced outages, which could result in lack of available production capacity. Then the planning problem consists of obtaining a balance between reliability of supply and a seldom used reserve capacity.

Traditionally, the dimensioning problem for power-only systems has been analyzed by using probabilistic production simulation. In this method the power demand is represented by a probability distribution, and each power plant is represented by its capacity and forced outage rate, i.e. the probability of not being able to produce. This information is combined in the simulation, which gives results regarding the expected production of each power plant

and the expected power demand that cannot be met because of failures in the production system.

However, due to the large extent of combined heat and power production (CHP) in Denmark, also the heat demand has to be considered when planning the Danish power system. Therefore, work has been done to extend the classical method by incorporating the heat, see Larsen et al. (1997). The combined demand is represented by a two-dimensional probability distribution, where the two dimensions are power demand and heat demand, respectively. The CHP plants are represented by their power and heat capacities and forced outage rates.

For power-only systems there is a probability of unsatisfied power demand, due to forced outages. Similarly for CHP systems, there is a probability of unsatisfied heat demand. In addendum, an overflow power production may occur, assuming that the heat production has priority over the power production. This is due to the problem of simultaneously satisfying both heat and power demands from the same plants. To study the problem, simulation models have been developed in appendices E and F, which can represent condensing and back-pressure plants, heat-only boilers and also extraction plants, which are special in that there is no fixed relationship between heat and power production.

In the models both discrete and continuous representations of the two-dimensional probability distribution for the demand have been introduced, using Fourier series for the continuous distribution.

An example of a probability distribution for heat and power demand for a period of one year is shown in Figure 4.7. By introducing one production unit at a time, taking into account production capacity and probability of failure, the unsatisfied demand is gradually reduced. In this way the final probability distribution for the residual unsatisfied demand is found. This distribution is used to estimate the expected unserved heat and power demands and overflow power production.

Furthermore, by performing simulations for various scenarios with different production plants, it is possible to obtain a reasonable balance between security of supply and total installed capacity.

4.4 Central control of DCHP plants

An important aspect of decentralized CHP production is the total effect of such power plants on a national power system. First, it should be mentioned that the produced heat is generally used in isolated heat areas, which means that control decisions with respect to heat are independent in each area. This
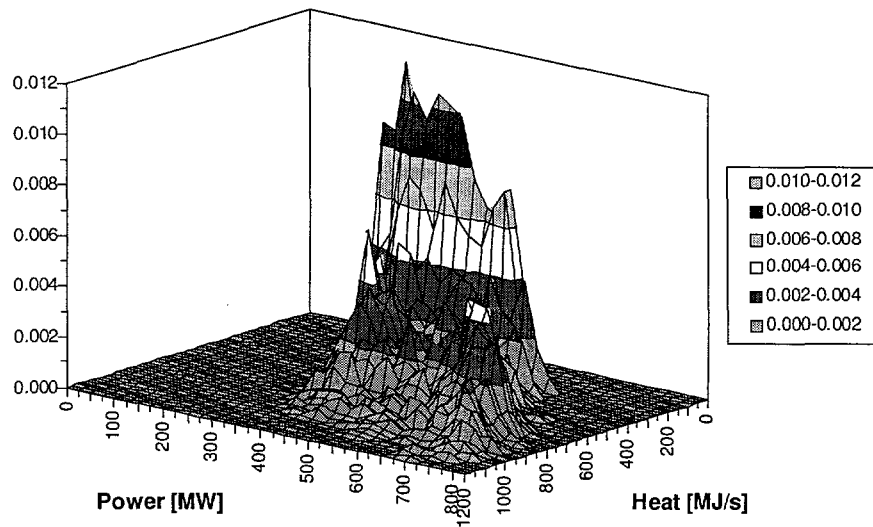
Figure 4.7: Probability density function after simulation with one heat area and one power area

is not the case for the power production, since every plant delivers power to the Eastern Denmark power grid.

The decentralized plants are currently not centrally controlled (as their name indicates) by other means than the varying price for power. While large centralized plants are responsible for regulating the total production to the power demand, the decentralized plants can produce at will. Thus, when the power price rises suddenly (as seen for the sixth hour in Figure 4.2 then many (if not all) the decentralized plants will begin to produce, which results in a high demand for regulating the total power production down to the demand level. One way of solving this is to impose some central control on the small plants, more specifically in form of changing the power price on short notice or handing different price structures to different plants.

Possible ways of controlling the total DCHP production can include the following ones:

- Individual plants operate with different tariff structures. This would typically be in form of different hours for changes from e.g. low tariff to high tariff. The result would be a smoothened rise in production when looking at the system as a whole.

- Changes in the tariff structure on a short notice for all the plants. This is more difficult to implement than the option above, but would give the

central authorities more flexible control over DCHP production, since plant operators would adjust the production schedule with regard to the power price.

- Direct control. The plants are contacted and ordered (asked) to start or stop production. Plants would get compensation for obeying to such orders, if it includes costs. This communication could be done via the telephone, the Internet, or the power grid.

Another way of dealing with large changes in decentralized production is to estimate these changes in the near future and plan centralized production accordingly. This has been done in Section 4.2 to a reasonably accuracy, taking into account climate predictions (mainly outdoor temperature) as well as various types of days (work days, holidays).

4.5 Conclusions

In this chapter, some aspects of the effect of DCHP production on the Eastern Denmark power grid have been discussed. This includes a short description of the DCHP situation in Denmark, followed by a model for the cumulative production from many DCHP plant in the Eastern part of Denmark.

Results show that an existing model for the total power production in Eastern Denmark can be applied to DCHP systems, but a lesser degree of fit goodness as well as increase in errors is observed. Furthermore, the model is especially erroneous when used for predictions, that is when data from the year 1996 is used to generate model parameters, and then the parameters are used for modelling DCHP production in the year 1997.

With large and even increasing shares of co-production of heat and power, it is important to be able to analyze system behavior when planning the expansion of CHP systems. This implies among other things evaluation of imbalances between demand and supply of heat and power. In the papers in Appendices E and F, the traditional method of power-only analyses has been extended to CHP systems with multiple heat areas, containing the main CHP-type production units of back-pressure and condensing types. Based on this, it has been shown how probabilistic production values may actually be calculated, and a simple synthetic case has illustrated the various concepts.

Chapter 5

Final conclusions

Here the main topics and results of the thesis are summarized and final conclusions are drawn.

In Chapter 2 some of the important parts of DH networks have been considered. This includes flow computations, dynamic temperature computations as well as methods for simplifying DH network models.

Two methods have been under focus for computation of temperature dynamics in Appendix A. The node model has been shown before to be computationally more efficient than the element model. Further analyses in this work of the node model result in a proof of its stability, as well as in an estimate of its accuracy. Also, alternative methods for increasing the accuracy of both the node model and the element model are proposed.

The models for the pipes are tested by using real cases and real measurements from a large transmission DH company, see Pálsson et al. (1999). This system, the Vestegnens Kraftvarmeselskab (VEKS), has provided data for a part of their distribution area, which is used for getting a real problem perspective and to test the models.

It is shown that a tree-structured DH network consisting of about one thousand pipes can be reduced to a simple chain structure of ten equivalent pipes (or 1% of the original number of pipes) without loosing much accuracy when temperature dynamics are calculated.

The equivalent DH network has been tested by simulating two case studies, using the original network as well as the equivalent network. It is shown that the results calculated for the equivalent network are very close to the results from simulations of the original network.

Due to high efficiency of CHP plants when compared to power-only plants, they have become more widespread in recent years. In Denmark, a trend has been towards building relatively small CHP units in decentralized areas or communities, in which heat is produced for use in DH and power is sold to

53

a global power-network. Time dependent prices of power pose a problem for the operation of the CHP plants, which can be compensated for by installing a heat storage, which is used as a buffer between heat production and heat demand.

Thus, in Chapter 3, an optimization method is proposed, especially designed to find an optimal boolean structured start-stop strategy for a simple CHP plant, consisting of piston engines and boilers. For the optimization, the stochastic dynamic programming method is used, focusing on the storage and the stochastic nature of the heat-load. The resulting method solves an integer optimization problem with a computational complexity which is linearly connected to the number of boolean variables in the problem, which indicates that the method is very efficient.

Finally, Chapter 4 considers the effects of increasing DCHP production on the total power system. The capacity of DCHP plants has grown rapidly in recent years, and since these plants are generally free to produce power at will, problems can arise in terms of increased regulation needs.

An existing model for the total power production in Eastern Denmark has been applied to the accumulated DCHP production. The model can be adjusted to a given dataset with good results, but when applied in long term prediction (typically a year long horizon), the results are considerably worse. The reason seems to be the rapidly changing capacity and form of DCHP production between years.

With large and even increasing shares of co–production of heat and power, it is of importance to be able to analyze system behavior when planning the expansion of CHP systems. This has been done by using probability production simulations, in which results show that a method based on power-only systems can be extended to include both a power supply area as well as multiple heat supply areas.

Bibliography

Aronsson, S. (1996). *Fjärrvärmekunders värme och effektbehov*. Dissertation, Chalmers Tekniska Högskola.

Bellman, R. E. (1964). *Applied Dynamic Programming*. Princeton University Press.

Benonysson, A. (1991). *Dynamic Modelling and Operational Optimization of District Heating Systems*. PhD thesis, Laboratory of Heating and Air Conditioning, Technical University of Denmark. ISBN 87-88038-24-6.

Bøhm, B. (1988). Energy-economy of Danish district heating systems: A technical and economic analysis. Technical report, Technical University of Denmark, Laboratory of Heating and Air Conditioning.

Bøhm, B. (1999). *Heat losses from buried district heating pipes*. Polyteknisk Press. ISBN 87-502-0820-9.

Bøhm, B. et al. (1994). *Optimum Operation of District Heating Systems*. Technical University of Denmark, Lyngby, Denmark.

Energistyrelsen (1998). Energistatistik (e. energy statistics). Technical report, The Dansih Energy Agency.

Eriksson, H. (1994). *Short Term Operation of District Heating Systems An Application of Mathematical Programming*. Dissertation, Chalmers University of Technology. Department of Energy Conversion.

Frederiksen, S. and Werner, S. (1996). *Fjärrvärme. Teori, teknik och funktion*. Studentlitteratur, Lund, Sweden.

Hansson, T. (1990). Driftsoptimering af fjernvarmeværker. Master's thesis, Danmarks Tekniske Højskole. Laboratoriet for Varme- og Klimateknik.

Horlock, J. H. (1987). *Cogeneration - Combined Heat and Power (CHP), Thermodynamics and Economics*. Pergamon, Oxford.

Horlock, J. H. (1992). *Combined Power Plants, Including Combined Cycle Gas Turbine Plants*. Pergamon.

Jeppson, R. W. (1976). *Analysis of Flow in Pipe Networks*. Butterworth Publishers, Boston, Massachusetts, USA.

Jørgensen, C. and Ravn, H. F. (1994). Optimal scheduling of heat production with storage and stochastic demands. In Kangas, M. and Lund, P., editors, *CALORSTOCK '94, 6th Int. Conference on Thermal Energy Storage*, pages 411–418, Espoo, Finland.

Larsen, H. V., Pálsson, H., and Ravn, H. F. (1997). Probabilistic production simulation including CHP plants. Technical report, Risø National Laboratory, Denmark. RISØ-R–968(EN).

Madsen, H. (1995). *Tidsrækkeanalyse (E. Timeseries Analysis)*. Institute for Mathematical Modelling, Technical University of Denmark.

Madsen, H., Pálsson, Ó. P., Sejling, K., and Søgaard, H. T. (1990). Models and methods for optimization of district heating systems, Part I: Models and indentification methods. Technical Report 1323/89-14, Energiministeriets Forskningsudvalg for produktion og fordeling af el og varme. Printed by IMSOR at the Technical University of Denmark.

Nielsen, H. A., Andersen, K. K., and Madsen, H. (1998). Empirisk bestemt model for elforbruget i Østdanmark (e. empirical model of the power usage in eastern denmark). Technical Report IMM-REP-1998-18, Institute for Mathematical Modelling, Technical University of Denmark.

Nielsen, H. B. (1994). Algorithms for computing pipe network "loops". Technical Report IMM-REP-1994-04, Institute of Mathematical Modelling, Technical University of Denmark.

Pálsson, Ó. P. (1993). *Stochastic Modeling, Control and Optimization of District Heating Systems*. PhD thesis, Technical University of Denmark.

Pálsson, Ó. P. and Ravn, H. F. (1994). Stochastic heat storage problem solved by the progressive hedging algorithm. *Energy Conversion and Management*, 35(12):1157–1171.

Pálsson, H. (1999). Optimizing the use of heat storage in an engine-based CHP plant. In *7th International District Heating and Cooling Symposium*.

Pálsson, H., Larsen, H., Bøhm, B., Ravn, H. F., and Zhou, J. (1999). Equivalent models of district heating systems. Technical report, Department of Energy Engineering, Technical University of Denmark. ISBN 87-7475-221-9.

Ravn, H. F. and Rygaard, J. M. (1994). Optimal scheduling of coproduction with a storage. *Engineering Optimization*, 22:267–281.

Ravn, H. F. (1999). *Discrete time optimal control*. Dissertation, Technical University of Denmark.

Sejling, K. (1993). *Modelling and Prediction of Load in District Heating Systems*. PhD thesis, Technical University of Denmark.

Søndergren, C. and Ravn, H. F. (1996). A method to perform probabilistic production simulation involving combined heat and power units. *IEEE Trans. PWRS-11*, (2):1031–1036.

Valdimarsson, P. (1993). *Modelling of Geothermal District Heating Systems*. Dissertation, University of Iceland.

Yang, L. (1994). District heating house stations with hot water storage. simulation and evaluation of dynamic performance. Technical report, Technical University of Denmark, Laboratory of Heating and Air Conditioning. ISBN 87-88038-30-0.

Zhao, H. (1995). *Analysis, Modelling and Operational Optimization of District Heating Systems*. PhD thesis, Laboratory of Heating and Air Conditioning, Technical University of Denmark. ISBN 87-88038-31-9.

Zhao, H. and Holst, J. (1997). Study on network aggregation in DH systems. In Pálsson, Ó. P., editor, *6th International Symposium on District Heating and Cooling Simulation*, Reykjavik, Iceland. ISBN 9979-54-203-9.

Appendix A:
Analysis of Numerical Methods for Simulating Temperature Dynamics in District Heating Pipes

Halldór Pálsson

Abstract

According to recent publications, two methods have mainly been used for physical modelling and simulation of temperature dynamics in district heating (DH) networks. They are referred to as the element method and the node method. The element method seems to be more frequently applied in practice, but the node method has been found to be faster and more accurate in some cases.

The purpose of this study is to analyze and compare the element method and the node method, with special attention on numerical properties. Comparisons involve theoretical aspects of accuracy and stability, but furthermore the methods are compared to two higher order numerical schemes.

Results from the theoretical analysis show that the node method is unconditionally stable, but has problems with artificial diffusion at Courant number around 3/4. This diffusion is though reduced proportionally to the inverse square of the Courant number. Results from test simulations indicated that the higher order schemes were more accurate, in where a node method based on cubic interpolation gave the best results.

The node method has been proven to be unconditionally stable, in numerical sense, and very accurate at low Courant numbers. Furthermore it is concluded that schemes based on cubic interpolation should be used as a mathematical basis to physical models of DH networks.

Keywords: District heating, convective transport, net simulations, numerical schemes, finite difference methods.

1   Introduction

District heating (DH) provides an efficient method for house heating and has become increasingly popular during recent years. The efficiency is obtained by producing heat in large scale at central power plants, in contrast to the case where each heat consumer produces heat locally. In general, this results in better utilization of fuel, but also makes co-generation of heat and electricity very favorable, which in turns increases total fuel efficiency considerable.

The heat generated at production plants is supplied to DH customers' house stations or larger substations, using hot water as a transport media. The water is transported in DH networks, which consists in most cases of both supply and return pipes. The pipes are well insulated, but nevertheless some of the heat is transferred to the surroundings, as well as from supply to return pipes. At the end of the network lines, that is at the customer's stations, the water is cooled and the internal thermal energy is released. Finally, the cooled water mass is transported back through the return pipes to the production plants.

The rate of energy transport in the network is determined by the water flow, as well as the temperature difference between supply and return pipes. The flow is driven by pressure differences along the pipes and any dynamic changes in the flow are quickly transferred to the whole network in form of pressure waves, typically in matter of seconds. The temperature is on the other hand combined to the mass of water, which leads to the fact that effects from temperature changes in the DH network are transferred relatively slowly in relation to changes in the flow. Thus, the response time from a production plant to a customer station, with respect to temperature changes, can in some cases be up to several hours. The large difference in response time between temperature and flow gives a good argument for assuming that temperature– and flow– dynamics are independent with respect to time. Based on this argument, the flow in the network is assumed to be static, relative to the dynamic temperature changes. This situation allows the flow to be determined explicitly at every point of time, and is referred to as a *quasi–dynamic* situation.

Several approaches have been used for mathematical modelling of temperature dynamics in DH networks. The two main types of approach involve:

1. Black box models, where the physical composition of the network is disregarded and the modelling is in form of standard transfer function models (parametric or non–parametric) or neural networks.

2. Physical models, where all the important components in a DH network are modelled explicitly and the whole structure of the network is taken

into account.

Parametric black box models were studied and tested in [1], [2] and [3]. A model, suggested for DH simulations, was of the type: Auto–Regressive Moving Average with eXtraneous input (ARMAX). The estimation and tracking of time delays in the network played an important role in these models and were reported to be the main source of problems, especially if temperatures were changed abruptly. A neural network model was studied in [3] and reported to be of similar quality as standard parametric models.

Based on the physical approach (item 2 above), Benonysson [4] and Zhao [3] studied and compared methods for quasi-dynamic modelling of DH networks. Two types of methods were considered in [4], which are referred to as *the element method* and *the node method*. The element method was found to be inferior to the node method, both with respect to accuracy and computational cost. The main reasons for the poor performance of the element method were found to be problems regarding artificial diffusion of temperature profiles along the pipe, which in turns could result in abnormal smoothing of sharp temperature profiles. On the other hand, the node method had no severe difficulties regarding artificial diffusion. Zhao [3] introduced an analytical solution to the quasi-dynamic model, assuming constant water velocity over time. A node method (similar to the one in [4]), based on the analytical solution was presented in [3] and found to be at least as good as the one in [4].

Although the element and node methods have been tested and compared, both on standard temperature profiles and with real data, see [3, 4], no theoretical comparisons of the methods seem to have been performed. These theoretical aspects regard primarily the numerical accuracy and stability of the methods. The numerical basis of the element method is equivalent to a well known numerical approach to convection–dominated problems in fluid dynamics, and has therefore been analyzed thoroughly, see [5, 6, 7]. But the node method is based on somewhat different numerical background and should therefore be analyzed as well. As mentioned before, artificial diffusion is found to be the main problem regarding element method, but this problem has been studied in the field of fluid dynamics, and methods found there should therefore be applicable for improvements of the element method.

The purpose of this study is to analyze the numerical background of the node method and compare it numerically to the element method. Furthermore, the problem with artificial diffusion is resolved by incorporating a specially designed method for convective fluid transport. In order to ensure that only numerical properties are compared, all methods are used to solve a single representative mathematical model, which also has an analytical

solution.

The paper is organized as follows. Section 2 describes the physical origin of a quasi–dynamic model with heat loss incorporated. Based on the physical situation, a mathematical problem is presented in form of an initial value problem (IVP). In Section 3, the element and node methods are analyzed from numerical point of view. Alternative methods for temperature dynamics are also discussed. Finally in Section 4, the methods are compared, a predefined temperature profile, mainly with regard to pure water transport.

2   Mathematical modelling of DH pipes

A mathematical model, which is used as basis in the element method mentioned before, is presented in this section. A reference to this model is found in [3] and [4].

Two layouts for the placement of DH pipe pairs, relative to the surface, are most frequently used. In the first one, both the supply and return pipes are positioned in rectangular concrete ducts, which can either be buried in ground or positioned at the surface. Many old DH systems consists of such layout, where the pipes are insulated inside the ducts. In [8], it was reported that thermal interaction between the supply and return pipes tends to be large when using concrete ducts. The second layout is more common in new DH networks. In this case, the pipes are pre–insulated and buried in ground, side by side. This typical setup is shown in Figure 1. The interaction between supply and return pipes is relatively small in this case and in [8] it was reported that the interaction could be disregarded without introducing significant model errors.

In [4], a heat transmission model is presented for the pre-insulated pipe pair in ground. The model defines thermal resistances between the different materials in Figure 1, that is water, steel, insulation and surrounding ground. As a result, a coupled set of differential equations is derived, resembling a consistent heat balance for a given length of a pipe branch. The temperature of the steel pipe is assumed to follow the water temperature, which was recommended in [8] since the thermal conductivity of both materials is relatively large (with respect to insulation and surroundings). In [4], it recommended that diffusive heat transfer in axial direction should be neglected, which means that there should not be any axial diffusion of the temperature profiles along the pipe.
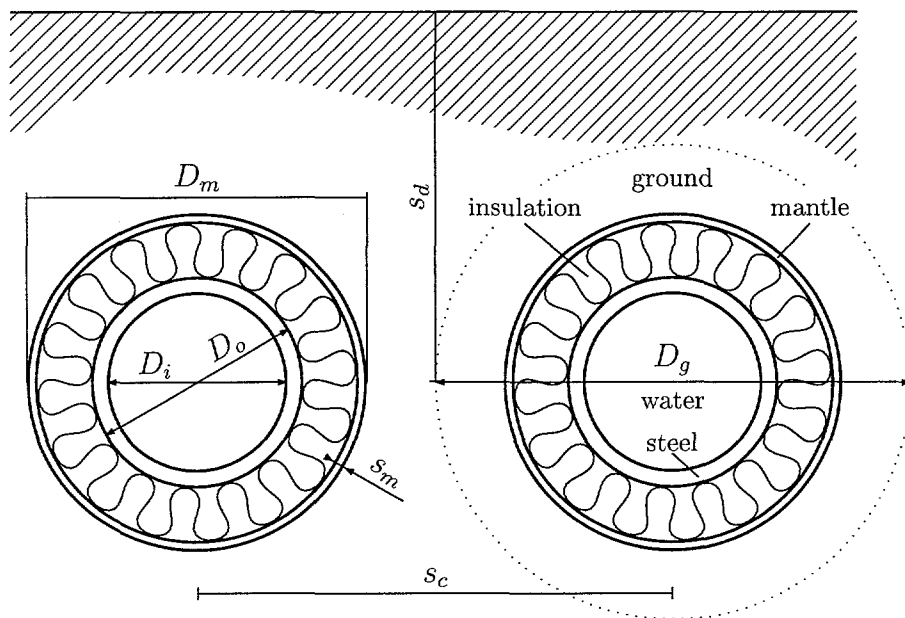
Figure 1: Cross section of a pipe pair buried in ground.

2.1 The modelling of the element method

Here the mathematical part of the element method is described as presented in [4], distinguishing it from the numerical part. This mathematical part will be referred to as the *element model* in the rest of the paper. Note that some of the nomenclature differs from the one used in [4]. Any symbols that are not described in the subsequent text are referred to in Figure 1.

In the element model, the cross section of each of the two supply and return pipes is divided into three parts, representing the surrounding ground, the insulation, and the combined steel and water mass. The specified temperatures in these parts are referred to as T^w, T^i and T^g for water–steel, insulation and surrounding ground, respectively.

The procedure of obtaining a mathematical model of the element method is divided into three phases representing the flow of energy, energy storage and energy balance. A pipe branch of length Δx is chosen as a fixed control volume, with a cross section as shown in Figure 1.

2.1.1 Heat transmission

To start with, thermal resistances are defined for the insulation material and the surrounding ground. The subscripts used in the text are i for insulation, m for mantle cover and g for surrounding ground. The thermal resistances,

R, are defined as

$$R_i = \frac{1}{2\pi K_i} \ln \frac{D_m - 2s_m}{D_o} + \frac{1}{2\pi K_m} \ln \frac{D_m}{D_m - 2s_m} \qquad (1a)$$

and

$$R_g = \frac{1}{2\pi K_g} \ln \left(\frac{4H}{D_m} \right) \qquad (1b)$$

where K denotes the thermal conductivity of the material types and $H = s_d + 0.0685K_g$. A third thermal resistance, R_h, is presented to take into account the effect of having two pipes in the ground. Assuming identical supply and return pipes, this resistance is given as

$$R_h = \frac{1}{4\pi K_g} \ln \left(1 + \left(\frac{2H}{s_c} \right)^2 \right) \qquad (2)$$

The following equations are used to determine the mutual thermal resistance between the three sections with *wi*, *gu* and *ig* denoting *water–insulation*, *ground–surroundings* and *insulation–ground* connections.

$$R_{wi} = \frac{1}{2\pi K_i} \ln \frac{1 + D_m/D_o}{2} \qquad (3a)$$

$$R_{gu} = \frac{1}{2\pi K_g} \ln \left(\frac{4H}{D_m + D_g} + \sqrt{\left(\frac{4H}{D_m + D_g} \right)^2 - 1} \right) \qquad (3b)$$

$$R_{ig} = R_i + R_g - R_{wi} - R_{gu} \qquad (3c)$$

The final result is in the form of heat transfer coefficients, h that are scaled with a factor θ. The scale factor is used in order to obtain the true steady state heat loss. The coefficients are given as

$$h_\beta = \frac{\Delta x}{R_\beta} \theta \qquad (4)$$

where β is one of *wi*, *gu* and *ig*, and Δx is the length of the pipe section, which is under consideration.

Let ΔT_s denote the temperature difference between the supply water and a surrounding ground not affected by the pipes and let ΔT_r denote the corresponding difference for the return pipe. By defining $\gamma = \frac{\Delta T_r}{\Delta T_s}$ for a

supply pipe and $\gamma = \frac{\Delta T_s}{\Delta T_r}$ for a return pipe, the correction factor for each pipe is given as

$$\theta = (R_i + R_g)\frac{(R_i + R_g) - \gamma R_h}{(R_i + R_g)^2 - R_h^2} \tag{5}$$

Note that the heat transfer coefficients are not defined per unit length, but for a pipe branch of length Δx.

2.1.2 Heat capacities

In order to determine temperature dynamics in each of the three parts (water–steel, insulation and ground), total heat capacities are defined for the pipe section. By using the same subscripts as before, the capacities, C, are given as

$$C_{ws} = \Delta x \frac{\pi}{4}\left(D_i^2 \rho_w c_{p_w} + (D_o^2 - D_i^2)\rho_s c_{p_s}\right) \tag{6a}$$

$$C_i = \Delta x \frac{\pi}{4}\left(\left((D_m - 2s_m)^2 - D_o^2\right)\rho_i c_{p_i} + \left(D_m^2 - (D_m - 2s_m)^2\right)\rho_m c_{p_m}\right) \tag{6b}$$

$$C_g = \Delta x \frac{\pi}{4}\left((D_g^2 - D_m^2)\rho_g c_{p_g}\right) \tag{6c}$$

where ρ and c_p denote the density and specific heat, respectively.

2.1.3 Heat balance equations

By requiring consistent heat balance in a pipe section of length Δx, three heat balance equations are defined, using the results from the first two phases. These equations form a system of partial differential equations, which can be written as

$$\begin{bmatrix} C_{ws} & 0 & 0 \\ 0 & C_i & 0 \\ 0 & 0 & C_g \end{bmatrix}\begin{bmatrix} \dot{T}^w \\ \dot{T}^i \\ \dot{T}^g \end{bmatrix} + \begin{bmatrix} \dot{m}c_{p_w}\Delta x \\ 0 \\ 0 \end{bmatrix}\frac{\partial T^w}{\partial x}$$
$$+ \begin{bmatrix} h_{wi} & -h_{wi} & 0 \\ -h_{wi} & h_{wi} + h_{ig} & -h_{ig} \\ 0 & -h_{ig} & h_{ig} + h_{gu} \end{bmatrix}\begin{bmatrix} T^w \\ T^i \\ T^g \end{bmatrix} = \begin{bmatrix} 0 \\ 0 \\ h_{gu}T^u \end{bmatrix} \tag{7}$$

where $\dot{T}$ denotes the time derivative $\frac{\partial T}{\partial t}$.

If proper initial (temperatures at some starting time) and inflow (temperature at the pipe entrance) conditions are given, then (7) will represent an initial value problem, which can be solved to obtain future values of temperature in the corresponding pipes.

2.2　A general flow formulation with a source

The modelling of DH pipes, which is described in the preceding subsection, belongs to a class of models referred to as *convective transport* models, see [5, 6, 9]. These type of models have been studied extensively, since they play an important role in fluid dynamic problems.

It is possible to write the element model as a one dimensional (with respect to space) transport model with a source term. For simplifying purposes, we define a relative temperature, ϕ, as the difference between absolute temperatures in the pipe cross section and the temperature of undisturbed ground. Defining x as a space variable along the pipe branch and t as time, the general transport model is defined by the initial value problem

$$\frac{\partial \phi}{\partial t} + v\frac{\partial \phi}{\partial x} + a\phi = 0 \tag{8a}$$

$$\phi(x,0) = \phi_o(x) \tag{8b}$$

$$\phi(0,t) = \phi_i(t) \tag{8c}$$

where ϕ_o and ϕ_i denote inflow and initial conditions, respectively. The parameters v and a represent a flow velocity term and a source term (heat loss in the case of DH pipes), and are both assumed to be greater than zero. In general, ϕ can be a vector of length n, with v and a as $n \times n$ matrices. If $n = 3$, then this model represents the element model in (7) exactly.

It should be noted that the flow velocity term v does not necessarily denote the physical velocity of the water. In the case where the water temperature and steel temperature are kept equal, as in the element model, an expression showing the connection between v and the true water velocity v_w is given in [10], as

$$v_w = v\left(1 + \frac{\rho_s c_{p_s}}{\rho_w c_{p_w}}\frac{4d}{D_i}\left(\frac{d}{D_i} + 1\right)\right) \tag{9}$$

where $d = (D_o - D_i)/2$ is the thickness of the steel pipe. Other parameters in (9) are referred to in Subsection 2.1 and in Figure 1. The physical effect from this, is that sharp temperature fronts along a pipe do not necessary travel with the water flow. For a thorough analysis of this effect see [10].

If we consider the case $n = 1$, with a constant source parameter a and constant flow velocity along the pipe branch, a simple analytical solution of (8) can be found. This is done by introducing a function $f(x)$, which can represent both initial and boundary conditions. The solution, including

initial and boundary conditions, is presented as

$$\phi(x,t) = f(x - \psi(t))e^{-a(t-\psi^{-1}(\psi(t)-x))} \qquad (10a)$$

$$\phi_i(x) = f(x)e^{a\psi^{-1}(-x)} \qquad (10b)$$

$$\phi_0(t) = f(-\psi(t)) \qquad (10c)$$

This solution can be verified by calculating the partial derivatives with respect to time and space, and inserting the result into (8). The function $\psi(t)$ represents the integrated velocity such that $v = d\psi/dt$. The purpose of deriving this analytical solution is to be able to compare numerical (and thus approximated) solutions to a correct solution.

3   Numerical methods

In this section, numerical methods are studied, which can be applied to calculate time varying temperature profiles in DH pipes. The first method considered, is the equivalent to the numerical part of the element model shown in (7). The second method represents the b–node method, described in [4], but is presented here in somewhat different manner, with the purpose of comparing it to other methods. A state of the art method from fluid dynamics, referred to as *quadratic upwind interpolation for convective kinematics* (QUICKEST), see [5], is also described with the purpose to compare it to the element method and the node method. Finally, an alternative method is presented shortly, which is based on the b–node method and a third order interpolation scheme, referred to as the *cubic node method.*

All the methods are finite difference methods, and therefore the first step is to define a discrete computational grid, where a numerical solution can be approximated. Figure 2 shows a computational grid with one space variable x, and a time variable t. The indices i and j denote steps in space and time, respectively. This figure is used to represent all numerical methods considered in the section.

In the case of no axial diffusion (no diffusion along the x–axis in Figure 2), every 'point' mass of water flows along the pipe without interference with other neighboring 'point' masses. This is observed as paths on the space–time computational grid, which are called *characteristics.* If the water velocity is constant with respect to time, these paths are straight and called characteristic lines, as shown in Figure 2. The reason for this discussion is that the characteristic line helps understanding the interpolatory nature of the different numerical schemes.
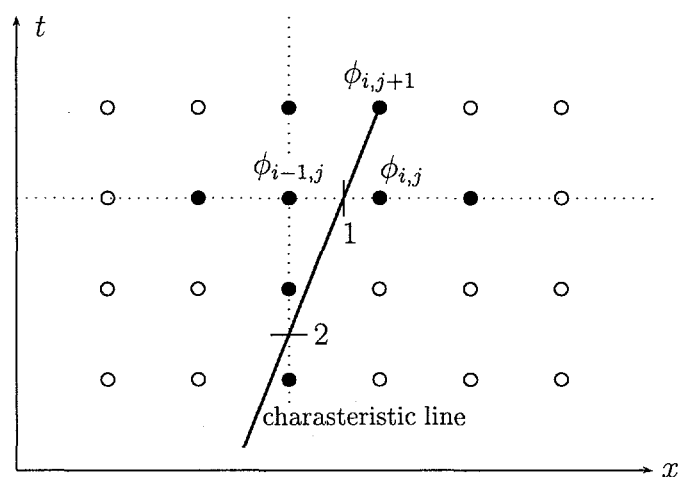
Figure 2: The computational grid.

A crucial parameter in convective dominated flow where axial diffusion is nonexistent or small, is the dimensionless Courant number. It is defined as

$$c = v\frac{\Delta t}{\Delta x} \tag{11}$$

and indicates how fast temperature information travels on the computational grid. This number is the most important parameter when regarding the performance of numerical methods for convective flow. In fact, the characteristic line and the Courant number are related in such way that the slope of the characteristic line in Figure 2 is equal to $1/c$.

3.1   The element method

As being the most simple of the methods mentioned in the beginning of this section, the numerical part of the element method is analyzed first.

In [4], an implicit numerical approximation of (7) is given. The term implicit means that the temperature at a new time–step is known before it is computed (this poses no problem when the problem is discretized). First, the partial derivatives in (7) are approximated by finite differences (discretized), such that $\dot{T} = \frac{1}{\Delta t}(T_{i,j+1} - T_{i,j})$ and $\frac{\partial T}{\partial x} = \frac{1}{\Delta x}(T_{i,j} - T_{i-1,j})$. This results in

the following three equations:

$$T^w_{i,j+1} - T^w_{i,j} + \frac{mc_{pw}(T^w_{i,j} - T^w_{i-1,j})\Delta t}{C_{ws}} + \frac{h_{wi}(T^w_{i,j+1} - T^i_{i,j+1})\Delta t}{C_{ws}} = 0 \qquad (12a)$$

$$T^i_{i,j+1} - T^i_{i,j} + \frac{h_{wi}(T^i_{i,j+1} - T^w_{i,j+1})\Delta t}{C_i} + \frac{h_{ig}(T^i_{i,j+1} - T^g_{i,j+1})\Delta t}{C_i} = 0 \qquad (12b)$$

$$T^g_{i,j+1} - T^g_{i,j} + \frac{h_{ig}(T^g_{i,j+1} - T^i_{i,j+1})\Delta t}{C_g} + \frac{h_{gu}(T^g_{i,j+1} - T^u)\Delta t}{C_g} = 0 \qquad (12c)$$

As an initial condition, we assume that $T_{i,j}$, $T_{i-1,j}$ (with superscripts w, i and g) and the temperature of undisturbed ground, T^u, are known at some point of time. Using a time step of length Δt, the linear system in (12) can be solved for the unknown temperatures $T^w_{i,j+1}$, $T^i_{i,j+1}$ and $T^g_{i,j+1}$ at the end of each time step.

In the rest of the Section, the simplified formulation in (8) will only be considered. As mentioned below equation (8c), this formulation is perfectly valid for the element model if v and a are matrices, but these parameters will be considered as scalars from now on, in order to simplify the analysis. Using finite difference approximations, a numerical approach for the simplified element model becomes

$$\frac{\phi_{i,j+1} - \phi_{i,j}}{\Delta t} + v\frac{\phi_{i,j} - \phi_{i-1,j}}{\Delta x} + a\phi_{i,j+1} = 0 \qquad (13)$$

By defining $\alpha = a\Delta t$ and introducing the Courant number, c, then a solution for $\phi_{i,j+1}$ is given as

$$\phi_{i,j+1} = (1 + \alpha)^{-1}\big((1 - c)\phi_{i,j} + c\phi_{i-1,j}\big) \qquad (14)$$

If (14) is compared to the variables shown in Figure 2 (assuming that $\alpha = 0$), it is observed that $\phi_{i,j+1}$ is in fact a linear interpolation at point 1 in the figure. Thus, a numerical scheme can be obtained, not only by concerning finite difference approximations, but also by studying the characteristics.

The type of discrete approximation of $\partial\phi/\partial x$ observed here, is often referred to as a *first order upwind scheme*. The term upwind is used because the $\phi_{j,i-1}$ is evaluated upstream in the flow, and 'first order' means that only linear interpolation is used.

3.1.1 Error analysis

Now the attention is turned towards an analysis of the errors introduced by the discretization in (13). The purpose is to estimate the artificial diffusion in

the scheme, and therefore the analysis only incorporates the transport term of (8a), so that $\alpha = 0$.

To start with, Taylor expansions are introduced for ϕ. The point $(i, j+1)$ in Figure 2 is used as a reference point and the function $\phi(x,t)$ is assumed to be analytic (continuous and infinitely many times differentiable). Two dimensional Taylor approximations for the points in time–step j are given as

$$\phi_{i,j} = \phi - \Delta t\frac{\partial \phi}{\partial t} + \frac{\Delta t^2}{2}\frac{\partial^2 \phi}{\partial t^2} + O(\delta^3) \tag{15a}$$

$$\phi_{i-1,j} = \phi - \Delta t\frac{\partial \phi}{\partial t} - \Delta x\frac{\partial \phi}{\partial t} + \frac{\Delta t^2}{2}\frac{\partial^2 \phi}{\partial t^2} + \frac{\Delta x^2}{2}\frac{\partial^2 \phi}{\partial x^2} + \Delta t\Delta x\frac{\partial^2 \phi}{\partial x\partial t} + O(\delta^3) \tag{15b}$$

where δ denotes a discretization step in either time or space (or mixed). This usage of δ instead of Δt and Δx is valid if both Δt and Δx are assumed to be connected proportionally (e.g. by the velocity and the Courant number, see equation (11)). If the source term in (8a) is discarded, then (8a) is found to give the following connection between time and space derivatives:

$$\frac{\partial u}{\partial t} = -v\frac{\partial u}{\partial x} \tag{16a}$$

$$\frac{\partial^2 u}{\partial t\partial x} = -v\frac{\partial^2 u}{\partial x^2} \tag{16b}$$

$$\frac{\partial^2 u}{\partial t^2} = v^2\frac{\partial^2 u}{\partial x^2} \tag{16c}$$

The Taylor expansions in (15) are put into (14) and by using (16) the resulting approximated partial differential equation becomes

$$\frac{\partial u}{\partial t} + v\frac{\partial u}{\partial x} = v\frac{(1-c)\Delta x}{2}\frac{\partial^2 u}{\partial x^2} + O(\Delta x^2) \tag{17}$$

The right hand term in (17) is a mathematical interpretation of diffusion along the x–axis, which should not be there when compared to the mathematical model in (8a). It is observed that this diffusion term is proportional to Δx, which confirms the first order nature of the scheme, and the problems with artificial diffusion.

3.1.2   Stability

It is important that the numerical scheme is stable for all values of c and α that are of interest. Consequences of instability are observed in that the method "blows up" numerically, with increasing number of time–steps taken.

A common way to proof stability is to use von Neumann stability analysis, which is based on a solution representation with Fourier series terms. For information on von Neumann analysis, see [7]. In the analysis, an arbitrary Fourier mode is defined such that $\phi_{i,j} = g^j e^{ikx_i}$, where $i = \sqrt{-1}$, k is an arbitrary integer and g is a magnifying factor.

The application for the element method is relatively simple. The Fourier modes are inserted into (14), which results in $(\alpha + 1)g = (1 - c) + ce^{-ik\Delta x}$. The von Neumann stability criteria requires that $|g| \leq 1$ for all k, which gives the following stability condition for the element method, with respect to α and c:

$$-\frac{\alpha}{2} \leq c \leq 1 + \frac{\alpha}{2} \tag{18}$$

Observe that the source term increases the stability of the element method, but the Courant number is generally not allowed to exceed one.

3.2 The node method

Here the numerical properties of the b–node method are analysed, in similar way as for the element method. Two node methods were presented in [4] and referred to as 'a' and 'b' methods. There, it was found that the 'b' method was somewhat better than the 'a' method, with respect to accuracy. Consequently, the b–method will only be treated here.

The main principle in the node method is to use temperature values at different time–steps to determine the current temperature situation. This is different from the element method, where the temperature at each time–step is determined only from the time–step before. A pipe section of some predefined length is considered, accommodated by two nodes. The nodes, which are placed at the inflow and outflow ends of the pipe section, contain a time history of the corresponding temperatures. Thus, the temperature at the outflow node is obtained by using the time history at the inflow node, which in turn must be approximated. The need for an approximation rises from the fact that a water mass at the outflow node was possibly in between time–steps at the inflow node. Temperature dynamics in the radial direction of the pipes are computed separately, and thus do not affect the axial transport properties of the method.

A short description of the b–node method is given in the following list, based on the description in [4].

1. At time–step number N, find the smallest integer n and a corresponding

variable R, which fulfills

$$R = \sum_{k=N-n}^{N} (v_k \Delta t) > Z \quad n \in [0, 1, \dots] \tag{19}$$

where Z is the length of the pipe element and v_k is the flow velocity at time–step k.

2. Find the smallest integer m which fulfills,

$$\sum_{k=N-m}^{N} (v_k \Delta t) > Z + v_N \Delta t \quad m \in [0, 1, \dots] \tag{20}$$

3. Compute the variables Y and S, given by

$$Y = \sum_{k=N-m+1}^{N-n-1} v_k T_{n_k} \Delta t \tag{21}$$

$$S = \begin{cases} \sum_{k=N-m+1}^{N} v_k \Delta t & \text{if } m > n \\ R & \text{if } m = n \end{cases} \tag{22}$$

where T_{n_k} is the temperature at the inflow end.

4. Compute the temperature of the water flowing from the pipe, denoted as $T_{o_N}^*$, using

$$T_{o_N}^* = \frac{(R - Z)T_{n_{N-n}} + Y + (v_N \Delta t - S + Z)T_{n_{N-m}}}{v_N \Delta t} \tag{23}$$

In [4], temperature dynamics in radial direction are treated in two separate steps. First the heat capacity of the steel pipe is accounted for, by introducing a dynamic steel temperature that interacts with the water. Secondly, the heat loss from the pipe to the surroundings is computed explicitly, assuming that the steel temperature is uniform over the axial section of the pipe. The exact procedure for radial temperature dynamics is not shown here, refer to [3] and [4], but a simple source is included, which corresponds to the simplified model in (8). The treatment of this source factor will be considered later in this subsection.

As well as for the element method, the computational grid shown in Figure 2 is used as a basis for the node method. Each column of circles in the figure resembles a time series for the inflow and outflow nodes, so that

the x–directional spacing, Δx, is equivalent to the length, Z, of a pipe section in the node method.

For the purpose of simplifying further analysis, the velocities v_k are assumed to be constant for all k. This yields $(n+1)c > 1$ if (19) and (20) are divided by Z and $v_k \Delta t/Z$ is replaced by the Courant number from (11). The fulfillment of n in step 1 above would result in higher n if $(n+1)c \leq 1$, so the condition $nc \leq 1$ must also be fulfilled. Thus, if c is given, then n should be chosen such that

$$n \leq \frac{1}{c} < n+1 \qquad (24)$$

Comparison of equations (19) and (20) yields $m = n+1$, so that the expressions in list items 2 and 3 become $R = (1+n)c$, $Y = 0$ and $S = (1+n)c$. Now let $\phi_{i,j+1}$ denote the reference temperature, defined in Subsection 2.2, at the outflow node with $N = j+1$. By inserting R, Y and S into (23) and dividing by Z, the equation can be written as

$$\phi_{i,j+1} = \left(n+1-\tfrac{1}{c}\right)\phi_{i-1,j-n+1} + \left(\tfrac{1}{c}-n\right)\phi_{i-1,j-n} \qquad (25)$$

The characteristic line in Figure 2 crosses the $(i-1)$–th column at point '2' in the figure. The slope of the line is equal to $1/c$, which in turn indicates that point '2' is placed $1/c$ time–steps from step $j+1$. Referring to Figure 2, it is found that the distance from point '2' to the points $(i-1, j-n+1)$ and $(i-1, j-n)$ is equal to $1/c-n$ and $n+1-1/c$, respectively. Comparing this result to (25) reveals the fact that the temperature at point '2' is a linear interpolation between points $(i-1, j-n+1)$ and $(i-1, j-n)$.

The heat loss model in [4] uses the total time of the water traveling from inflow to outflow node to determine the exponential decay of temperature. Here, a similar approach is used, which incorporates the source coefficient a in (8a) to the transport model, such that

$$\hat{\phi}_{i,j+1} = \phi_{i,j+1} e^{-a\bar{t}} \qquad (26)$$

where $\hat{\phi}$ denotes the solution with the source term included and $\bar{t}$ is the total travelling time of a water mass through the pipe. The characteristic line in Figure 2, which cuts the inflow column at $1/c$, indicates that $\bar{t} = \Delta t/c$ and thus, $\hat{\phi}_{i,j+1} = \phi_{i,j+1} e^{-\alpha/c}$.

3.2.1   Error analysis

Analysis of discretization errors in the node method is in principle similar to the analysis performed for the element method in Subsection 3.1. Taylor

expansions are used for approximating $\phi_{i-1,j-n+1}$ and $\phi_{i-1,j-n}$, with respect to the reference $\phi_{i,j+1}$, and the only difference from preceding analysis is that the steps in time can be much larger (e.g. $j - n$ instead of j).

First, the point above point '2' in Figure 2 is considered, that is $(i-1, j-n+1)$. The distance from this point on the grid to the reference point $(i, j+1)$ is $-\Delta x$ in the x–direction and $-n\Delta t$ in the t–direction. The resulting Taylor expansion, with δ defined as in (15), is

$$
\begin{aligned}
\phi_{i-1,j-n+1} = \phi - n\Delta t \frac{\partial \phi}{\partial t} - \Delta x \frac{\partial \phi}{\partial x} \\
+ n\Delta t \Delta x \frac{\partial^2 \phi}{\partial t \partial x} + \frac{n^2 \Delta t^2}{2} \frac{\partial^2 \phi}{\partial t^2} + \frac{\Delta x^2}{2} \frac{\partial^2 \phi}{\partial x^2} + O(\delta^3) \quad (27)
\end{aligned}
$$

Similarly, the expansion for the point below '2', where the distances are $-\Delta x$ and $-(n+1)\Delta t$ for x and t respectively, is given as

$$
\begin{aligned}
\phi_{i-1,j-n} = \phi - (n+1)\Delta t \frac{\partial \phi}{\partial t} - \Delta x \frac{\partial \phi}{\partial x} \\
+ (n+1)\Delta t \Delta x \frac{\partial^2 \phi}{\partial t \partial x} + \frac{(n+1)^2 \Delta t^2}{2} \frac{\partial^2 \phi}{\partial t^2} + \frac{\Delta x^2}{2} \frac{\partial^2 \phi}{\partial x^2} + O(\delta^3) \quad (28)
\end{aligned}
$$

Next, (27) and (28) are inserted into (25), which replaces $\phi_{i-1,j-n+1}$ and $\phi_{i-1,j-n}$ by the Taylor series. This results in

$$
\begin{aligned}
\frac{\partial u}{\partial t} + \frac{c\Delta x}{\Delta t} \frac{\partial u}{\partial x} = \Delta x \frac{\partial^2 u}{\partial t \partial x} \\
+ \tfrac{1}{2}(1 + 2n - nc - n^2 c)\Delta t \frac{\partial^2 u}{\partial t^2} + \frac{c\Delta x^2}{2\Delta t} \frac{\partial^2 u}{\partial x^2} + O(\delta t^2) \quad (29)
\end{aligned}
$$

By using the identities from (16), (29) is finally written as

$$
\frac{\partial u}{\partial t} + v \frac{\partial u}{\partial x} = \frac{v\Delta x}{2}\left(1 - nc\right)\left((n+1)c - 1\right)\frac{\partial^2 u}{\partial x^2} + O(\Delta x^2) \quad (30)
$$

The right hand side of (30) gives impression of artificial diffusion, just as in the element method. This term is also first order with respect to Δx but there is one important difference from the result in (17). Here, the diffusion factor varies in steps, depending on n, which results in a series of parabolic paths with respect to c (c forms a second order polynomial). Maximum diffusion for a specific n is found to be $\frac{v\Delta x}{16n(n+1)}$, with the corresponding $c = \frac{2n+1}{2n(n+1)}$, so that the diffusion is reduced quickly when c goes to zero. The worst case of artificial diffusion is observed when $c = 0.75$, assuming that $c \leq 1$. On the other hand, a special case evolves when $n = 0$. Then the diffusion factor is equal to $\frac{v\Delta x(c-1)}{2}$, but still positive since $c > 1$ (see (24)). This last result indicates that the node method has problems with artificial diffusion for $c > 1$.

3.2.2 Stability

Now a stability analysis, corresponding to that of the element method, is performed for the b–node method. As in the error analyses above, the flow velocity is assumed to be time independent. By defining $\phi_{i,j} = g^j e^{ik\Delta x_i}$ as in Subsection 3.1 and inserting it into (25), the resulting equation with Fourier terms becomes

$$g^{n+1}e^{ik\Delta x} = \left(n + 1 - \frac{1}{c}\right)g + \frac{1}{c} - n \tag{31}$$

Considering the length of the complex factors in (31) and fulfilling the von Neumann criteria, $|g| \leq 1$, and thus $|g^{n+1}| \leq 1$, the following condition is established

$$\left|\left(n + 1 - \frac{1}{c}\right)g + \frac{1}{c} - n\right| \leq 1 \tag{32}$$

The complex number inside the brackets represents a circle in the complex plane with center at $1/c - n$ on the real axis, if $|g|$ is constant. Consequently, this circle must be inside the unit circle in the complex plane, which indicates that $|g| = 1$ is a critical condition in (32). Since the center of the circle is on the real axis, the real values of g give extreme conditions with respect to the requirement that values should be inside the unit circle.

First consider $g = 1$, which results in $n + 1 - 1/c + 1/c - n = 1$ and therefore fulfillment of (32). Secondly consider $g = -1$, which results in $-n - 1 + 1/c + 1/c = 2/c - 2n + 1$ and consequently $|2/c - 2n - 1| \leq 1$. The last expression gives $2/c - 2n - 1 \leq 1$ and $-2/c + 2n + 1 \leq 1$ which finally results in $n \leq \frac{1}{c} \leq n + 1$. This condition is equivalent to the basic condition in (24), which in turn proofs that the node method is unconditionally stable for $c > 0$.

3.3 Higher order numerical schemes

In this section, a state of the art method for convective transport is considered, with the purpose of comparing it to the element method and the node method. This method, referred to as Quadratic Upwind Interpolation for Convective Kinematics with Estimated Streaming Terms (QUICKEST), was presented in [5], where results showed good behavior of the method for all Courant numbers in the interval $0 \leq c \leq 1$. A method, similar to the b–node method, but using cubic interpolation instead of linear interpolation, see 25, is also presented here.

The first order upwind scheme, which is equivalent to the numerical procedure of the element method, has been used frequently to solve convection–dominant flow problems. Because of the problems regarding uncontrollable artificial diffusion, methods have been developed in recent years to improve accuracy and reduce the artificial diffusion. These methods can basically be put into two classes: (i) Petrov–Galerkin finite element methods, see [6, 7] and (ii) Finite difference methods, see [5, 11, 9]. The QUICKEST scheme is a finite difference method and is regarded to be one of the best methods available for convective transport, see [9].

In the QUICKEST scheme, the values at $(i, j + 1)$ in Figure 2 depend on four values in the time–step before. These values are shown in Figure 2 as filled circles at time–step j. The numerical procedure of this method, when used to solve (8), is given in the following list and corresponds to the procedure shown in [5]. As in the methods in preceding subsections, normalized temperature values are used.

1. Compute gradients by using central difference approximation between the nodes.

$$\text{GRAD}_i = \frac{\phi_{i+1,j} - \phi_{i,j}}{\Delta x_i} \tag{33}$$

   Here, Δx_i is the distance between nodes $(i + 1, j)$ and (i, j) in Figure 2.

2. Approximate the curvature at each node, using the gradients from list item 1 above.

$$\text{CURV}_i = \frac{\text{GRAD}_i - \text{GRAD}_{i-1}}{(\Delta x_i + \Delta x_{i-1})/2} \tag{34}$$

   Note that the grid spacing can vary, which is very convenient for DH applications where different pipes are connected in the DH network.

3. Approximate values of the temperature profile in between nodes $(i + 1, j)$ and (i, j), where the Courant number c_i refers to the flow situation between the same nodes.

$$\phi_i^* = \frac{\phi_{i,j} + \phi_{i+1,j}}{2} - \frac{\Delta x_i}{2} c_i \text{GRAD}_i - \frac{\Delta x^2}{6}(1 - c_i^2)\text{CURV}_i \tag{35}$$

4. Determine the temperature at node $(i, j + 1)$ by using the centered temperatures from list item 3.

$$\phi_{i,j+1} = \phi_{i,j} + \frac{2\Delta t}{\Delta x_i + \Delta x_{i-1}}(v_{i-1}\phi_{i-1}^* - v_i\phi_i^*) + \Delta t \bar{s} \tag{36}$$

The term $\bar{s}$ denotes the time average of the source $a\phi$ in (8a).

If the velocity is changing along the flow direction, the solution in (36) represents a conservative form of (8a), which means that changes in the flow velocity will affect the temperature profile. For DH applications, this gives incorrect solutions at pipe junctions or when diameters are changed. Fortunately, this problem can be overcome if v_i is replaced by v_{i-1} in (36), which then denotes a solution to the non–conservative problem. Also, for DH applications, the term $\Delta t\bar{s}$ is replaced by the time averaged source $\frac{\alpha}{2}(\phi_{i,j} + \phi_{i,j+1})$, so that (36) can be solved for $\phi_{i,j+1}$, including a source term.

For error and stability analysis of the QUICKEST scheme, refer to [5]. It is shown in this reference that the method satisfies the von Neumann stability criteria for $0 \leq c \leq 1$. Furthermore, it is pointed out that if Δx_i is constant for all i, then the QUICKEST scheme corresponds to cubic interpolation through the four filled nodes at time–step j in Figure 2, evaluated at point '1'. It is therefore evident, as reported in [5], that the method possesses third order in accuracy, with respect to Δx.

The idea of cubic interpolation can be applied to the node method as well, in order to improve accuracy. This new approach is referred to as *the cubic node method*. Numerical analysis of this method is omitted in this paper, but computations are performed and it is compared to the other methods. There is only one major difference between the cubic node method and the b–node method discussed in Subsection 3.2. By replacing (25) with

$$\phi_{i,j+1} = \frac{\xi(\xi-1)(2-\xi)}{6}\phi_{i-1,j-n+2} + \frac{(1+\xi)(1-\xi)(2-\xi)}{2}\phi_{i-1,j-n+1}$$
$$+ \frac{(1+\xi)\xi(2-\xi)}{2}\phi_{i-1,j-n} + \frac{(1+\xi)\xi(\xi-1)}{6}\phi_{i-1,j-n-1} \quad (37)$$

where $\xi = (1 - nc)/c$, a cubic interpolation scheme has been derived. The cubic node method, which is usable for $0 \leq c \leq 1$, is expected to possess third order accuracy, because of the cubic interpolation, see e.g. [12].

4   Numerical results

In this section, the numerical schemes, discussed in Section 3, are compared by using a predefined temperature profile as an initial condition and by simulating temperature dynamics on a single equidistant computational grid.

The temperature profile, which is shown in Figure 3, was recommended in [11], as being very representative for different types of profiles. The profile consists of the following three sections:

Figure 3: The analytical reference solution at time zero.

1. A sharp step, representing a discontinuity in the temperature profile.

2. A sine squared curve. This is a continuous and smooth profile and should reveal the order of accuracy in different method.

3. A half ellipse. This profile represents both a sharp discontinuity and a smooth profile, which combines the two items above and is extra challenging for the numerical schemes.

All the schemes are simulated, using a constant inflow temperature, over a time interval that gives equal displacement on the grid for different Courant numbers. In order to emphasize the errors due to convective transport, the temperature losses are assumed to be zero. It was found in Subsection 3.2 that the worst case of artificial diffusion in the node method appears at $c = 0.75$. Thus, the methods are compared for this Courant number, and for $c = 0.488$ which is the worst case for $n = 20$ in (25).

Figure 4 shows the results for the upwind scheme, which is the numerical basis of the element method. The artificial diffusion is clearly seen for $c = 0.75$ and becomes severe for the lower number $c = 0.0488$. Thus, it can be concluded that this method is quite unsatisfactory for small Courant numbers.

Figure 5 shows results for the numerical scheme, incorporated in the b–node method. At $c = 0.75$, quite large artificial diffusion is observed, which expresses that the method is not very accurate for Courant numbers between 0.5 and 1. On the other hand, when $c = 0.0488$ the method shows very good results. This confirms the results from the error analysis in Subsection 3.2, where the artificial diffusion term was found to be proportional to $1/c^2$.

Results for the QUICKEST scheme are shown in Figure 6. There is not much difference in the cases for $c = 0.75$ and $c = 0.0488$, which confirms that the method is almost unaffected by the Courant number, see [5]. The scheme is especially accurate for the smooth sine curve, but the effect from

Figure 4: The upwind scheme.

Figure 5: The b–node scheme.

Figure 6: The QUICKEST scheme.

Figure 7: The cubic node scheme.

Figure 8: Temperature losses with $c = 1$ and $a = 1$.

the discontinuities appears as small overshoots in the solution. If unwanted, these transients can be eliminated by using *universal flux limiters*, see [11].

Figure 7 shows results from a simulation with the cubic node method. The results are very good for both $c = 0.75$ and $c = 0.0488$, in contrast to the original b–node method which showed artificial diffusion for $c = 0.75$. The good results here for $c = 0.75$ are due to the high order of the cubic interpolation scheme, but some overshoots are observed at the discontinuities just as in the QUICKEST scheme. Nevertheless, these overshoots are smaller than the ones observed in Figure 6. Thus, it is concluded that the cubic node method is more accurate than any of the methods in Figures 4–6, which results from the fact that it incorporates the best properties of the b–node scheme and the QUICKEST scheme.

Finally, in order to include temperature losses in the test, a simulation with $c = 1$ is performed for the QUICKEST scheme and the element method. Choosing $c = 1$ results in exact transport solutions for all the methods. There is no point in comparing the node methods here, because (26) gives exact temperature transients in case of exact transport solution. The results are shown in Figure 8 and indicate that the temperature loss calculations are not critical, as is the case with convective transport calculations.

5   Discussion

Two numerical approaches have mainly been used for modelling and simulation of temperature dynamics in district heating pipes. The methods, referred to as the element method and the node method, have been implemented and tested on real systems, where it was found that the node method was better in some cases, with respect to accuracy and simulation time.

The two methods, mentioned above, are based on different temperature loss models. This makes it difficult to compare the methods in terms of numerical properties, only by using measured data. In other words, it is hard to see if the source of simulation errors comes from erroneous data, wrong modelling or inaccurate numerical methods.

In this paper, the element method and the node method have been analyzed, based on a single well defined mathematical model. Results from the analysis indicated clearly the problems with artificial diffusion, when using the element method. Analysis of the node method revealed that it had problems with artificial diffusion at Courant numbers close to one; worst case was found to be $c = 0.75$. But this diffusion is reduced proportional to $1/c^2$, which still makes the method very feasible at low Courant numbers. It was proven that the node method satisfies the von Neumann stability criteria for $c \geq 0$, and is therefore unconditionally stable.

The problem with inaccuracy and artificial diffusion in the element method can be resolved by using the QUICKEST scheme. Simulations showed that the QUICKEST scheme had no problems with artificial diffusion, at the cost of small overshoots in sharp temperature gradients. The idea of higher order schemes was implemented for the node method, which resulted in a very accurate method, referred to as the cubic node method.

It is concluded that the node method is especially feasible for problems with small Courant numbers. In DH applications, this corresponds to long pipe segments and small time–steps in the simulation. As being more accurate, the cubic node method offers a feasible alternative to the original b–node method.

The QUICKEST scheme offers an accurate replacement of the upwind scheme used in the original element method. The method can be used to solve the same mathematical problem as the element method, but without incorporating artificial diffusion. One advantage of the QUICKEST scheme over the node methods, is that the temperature profile at a given time–step is only dependent on the temperature at the time–step before. Thus, it could be possible to model an entire DH network as a first order difference equation, $\phi_{k+1} = \mathbf{A}(v)\phi_k$, where $\mathbf{A}(v)$ is a matrix representing both the topological structure as well as all heat transfer properties of the network. This is a

possible topic for further study, along with implementation of the higher order methods in real DH networks.

References

[1] H. Madsen, O. P. Palsson, K. Sejling, and H. T. Søgaard, "Models and methods for optimization of district heating systems, Part I: Models and indentification methods," Tech. Rep. 1323/89-14, Energiministeriets Forskningsudvalg for produktion og fordeling af el og varme, 1990. Printed by IMSOR at the Technical University of Denmark.

[2] B. Bøhm, *Optimum Operation of District Heating Systems.* Lyngby, Denmark: Technical University of Denmark, 1994.

[3] H. Zhao, *Analysis, Modelling and Operational Optimization of District Heating Systems.* PhD thesis, Laboratory of Heating and Air Conditioning, Technical University of Denmark, Feb. 1995.

[4] A. Benonysson, *Dynamic Modelling and Operational Optimization of District Heating Systems.* PhD thesis, Laboratory of Heating and Air Conditioning, Technical University of Denmark, Sept. 1991.

[5] B. P. Leonard, "A stable and accurate convective modelling procedure based on quadratic upstream interpolation," *Comp. Meths. Appl. Mech. Eng.*, vol. 19, pp. 59–98, 1979.

[6] S. R. Idelsohn, J. C. Heinrich, and E. Onate, "Petrov-galerkin methods for the transient advective-diffusive equation with sharp gradients," *Int. J. Num. Meth. Eng.*, vol. 39, pp. 1455–1473, 1996.

[7] J. J. Westerink and J. C. Shea, "Consistent higher hegree petrov-galerkin hethods for the solution of the transient convection-diffusion equation," *Int. J. Num. Meth. Eng.*, vol. 28, pp. 1077–1102, 1989.

[8] B. Bøhm, "Dynamiske temperaturforløb i fjernvarmeledninger," tech. rep., Technological Institute of Copenhagen, 1984.

[9] J. R. Manson and S. G. Wallis, "An accurate numerical algorithm for advective transport," *Comm. Num. Meth. Eng.*, vol. 11, pp. 1039–1045, 1995.

[10] G. Larsson, "Temperaturdynamik i fjärrvärmesystem," Master's thesis, Chalmers University of Technology, Gothenburg, Sweden, Feb. 1996. Department of Thermo- and Fluid Dynamics.

[11] B. P. Leonard, "The ultimate conservative difference scheme applied to unsteady one-dimensional advection," *Comp. Meths. Appl. Mech. Eng.*, vol. 88, pp. 17–74, 1991.

[12] R. L. Burden and J. D. Faires, *Numerical Analysis.* PWS-KENT Publishing Company, fourth ed., 1989.

Appendix B:
Equivalent Models for District Heating Systems

Helge V. Larsen,* Halldór Pálsson
Benny Bøhm† Hans F. Ravn‡

Abstract

Simulating the flow and transient temperatures in a district heating (DH) network can be performed in various ways and to various degrees of accuracy. However, the time needed for the computations may be excessive and it is therefore desirable to reduce this time in some way. In this paper we present a method in which an original model of a DH network is replaced by a simplified one, with the purpose of reducing simulation time, but without loosing too much accuracy in the simulation.

The simplified model, referred to as an equivalent network, is generated by gradually reducing the topological complexity of the original network. During this reduction, the relevant model parameters of the network are transformed in such a way that the dynamic behaviour of the equivalent network will resemble the original one.

In order to validate the reduction method, we perform simulation tests on real as well as equivalent systems. These tests include a simple illustrative case and a case with a real DH network involved. Furthermore, in order to verify the quality of the equivalent model parameters we compare them with parameters that are optimally estimated for a given operational case.

Results show that simple equivalent networks can maintain most of the dynamic characteristics of the original networks, but with some

---
*Systems Analysis Department, Risø National Laboratory, Denmark
†Department of Energy Engineering, Technical University of Denmark
‡Elkraft Power Company Ltd., Denmark

loss of accuracy in different situations. When applied to a real network, it is observed that a considerable network reduction is possible without introducing significant errors, which results in a good potential for a reduction of simulation time.

1   Introduction

District heating (DH) systems provide an efficient method for house heating and have become increasingly popular in recent years. In a typical DH system, the heat is produced at central stations and is then distributed by hot water to the DH customers through a network of pipes. This process involves both time dependent changes in flows and temperatures as well as in the heat losses from the pipe network. These changes make it possible to optimise the operation of the system, with respect to economy and energy preservation. See e.g. Benonysson et al. (1995) or Zhao et al. (1996) for approaches towards this.

One way of determining the optimal operational conditions in a DH system is to generate a mathematical model of the system, which can be used for simulating various operational strategies. For this purpose, two classes of models have traditionally been used for DH systems, denoted as physical models and statistical models, see e.g. Zhao (1995). Of these two, the statistical models tend to be simpler but with respect to the physical models their main drawback is a lower degree of accuracy and a more non-physical relationship to the real world.

In contrast to the statistical models, the physical ones represent the real structure of the DH system involved, and it is therefore easy to change or add new components to an existing model. Then again the physical models require a full description of the DH system, and they tend to be more computationally intensive than statistical models. In order to reduce the computational intensity it might therefore be desirable to simplify the physical model, but still retain some of the links to the real physical world.

The first obvious approach to simplify the DH network is to reduce the number of pipe branches and customers. In Hansson (1990) the problem of such network reductions has been addressed and a simple model consisting of one pipe and one consumer has been proposed. In Zhao and Holst (1997) an aggregated network model based on representative consumers is suggested and tested.

In this paper a new method for reduction of a DH network is proposed. The main procedure in this method is successive reductions of the network, which finally results in a system where all pipes are placed sequentially after
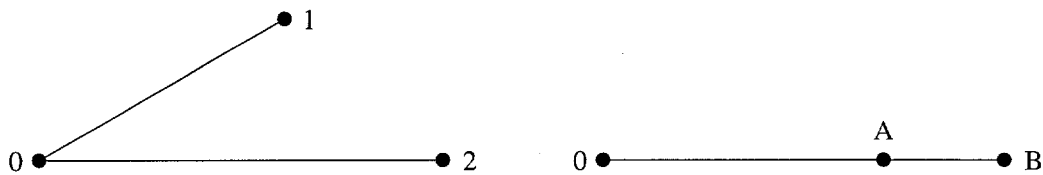
Figure 1: Original (left) and equivalent (right) networks.

each other with no side branches. Correspondingly, the various parameters defining the properties and dimensions of the pipes are transformed from the real network to equivalent parameters in the comparable equivalent network. Further reduction can then be obtained by observing that many nodes in this network are positioned close to each other, only separated by short pipes. Such nearby nodes can be collapsed to simplify the equivalent network.

The generated equivalent networks are validated by performing simulations of both original and equivalent systems, and by comparing the resulting return temperature at the production plant. Furthermore, to determine whether the equivalent network could be improved further, a least-squares minimisation algorithm is applied in which optimal values for various parameters of the network are estimated.

Finally, it should be noted that since we do not consider pressure variations in the network, the equivalent network is not applicable for calculation of pumping energy. Likewise it is not applicable to networks with loops.

2 Generation of equivalent DH network by successive reductions

A DH network with no loops can be considered as consisting of several two-branch sub-networks, as shown in the left side of Figure 1, where two branches (1 and 2) originating from the same node 0 lead to the nodes 1 and 2. Each branch represents a supply and a return DH pipe and we assume that the delay time in branch 1 is less than the delay time in branch 2. Typically, the simple network in Figure 1 is part of a more complex network, and therefore other DH networks might in principle be connected to nodes 1 and 2.

In the sequel, a method is described for transforming the sub-network mentioned above into a simpler equivalent network, as shown in the right side of Figure 1. The resulting equivalent network is simpler in the sense that there is no branching and that the total length of the branches is reduced. From now on the branch from node 0 to node A will be named branch A, and the branch between nodes A and B will be named branch B.

If we have the same supply temperature and flow at node 0 in the two networks, we *demand* that the following points are fulfilled for the equivalent network:

- The return temperature in node 0 is the same for the two networks.

- The sum of the loads in nodes A and B is equal to the sum in nodes 1 and 2.

- The total heat loss from branches A and B is equal to that from branches 1 and 2.

- The total water volume in branches A and B is equal to that in branches 1 and 2.

- Time delay in branch A must equal the delay in branch 1.

- Total time delay in branches A and B must equal the delay in branch 2.

Above it is assumed that time delay in branch 1 is less than or equal to the delay in branch 2. If this is not fulfilled, the definitions of 1 and 2 are switched.

Furthermore we *assume* that:

- The ratio between mass flows in branch 1 and 2 is constant through time.

This assumption is the main assumption in the derivation of the equivalent network. Naturally, the assumption is never fulfilled in practice. Therefore the equivalent network will not give exactly the same results as the original one, but as shown in the tests the results are close.

Finally, to obtain the equivalent network we *choose*:

- Branch B is equal to the last part of branch 2, i.e. the part of branch 2 with $\tau > \tau_1$ (τ is time delay and subscript 1 indicates branch 1). This choice does *not* take the insulation of pipe B into account.

- The mass flow in branch B is equal to that in branch 2.

- The velocity in branch A is equal to a weighted average of the velocities in branches 1 and 2. The mass flows in branches 1 and 2 are used as weight factors.

The steel pipe is included in the model by interpreting velocity and time delay as connected to the propagation of a temperature front, and by assuming that the temperature of the pipe wall and the water is equal in every cross section of the pipe.

Now using the requirements and choices above, the flow and physical dimensions (except for the insulation) for the equivalent network is found as shown in Appendix A. Below, the insulation of the pipes will be found, together with the return temperatures and heat loads in nodes A and B.

Heat loss

To this point, the insulation of the pipes has been excluded from our calculations. Here we shall address this aspect. Generally, we shall allow for different insulation thickness in the supply and return pipes.

We begin by choosing that the two networks have the same amount of heat loss on the supply side, and correspondingly the same amount of heat loss on the return side. Moreover, we demand that the equivalent loads in nodes A and B are equal to the original loads in nodes 1 and 2, respectively.

As shown in Appendix A, the above requirements and choices lead to expressions for the insulation of the equivalent network that is valid only if the following is satisfied:

- Supply side: $H_{2S}/H_{1S} \geq m_2/m_1$

- Return side: $H_{2R}/H_{1R} \geq m_2/m_1$

where H is the heat conductivity (W/°C) and m is the mass flow (kg/s). (S: Supply, R: Return, 1 and 2: Branches 1 and 2).

We manage the situation when the above restrictions on H_{2S}/H_{1S} and H_{2R}/H_{1R} are not fulfilled by imposing further assumptions on the original network. First of all we choose to let branch B have the same insulation as branch 2. Then the calculations in Appendix A show that (in excess to the hitherto main assumption that the ratio between mass flows in branches 1 and 2 is constant) we have to assume that the return temperatures in nodes 1 and 2 are equal. With this extra assumption it is shown that we are able to define an equivalent network even if $H_{2S}/H_{1S} < m_2/m_1$ and $H_{2R}/H_{1R} < m_2/m_1$.

As for the assumption that the ratio between mass flows is constant, the new assumption regarding the return temperatures is never totally fulfilled in practice. Therefore, the equivalent network will not give exactly the same results as the original network, but hopefully close enough results.

Expressions for the exact definition of the equivalent network can be found in Appendix A.

Collating nearby nodes

When a DH network consisting of many branches is converted to an equivalent network with no side branches as described above, many nodes in the equivalent network will be positioned close to each other separated by relatively short pipes. Such nearby nodes can then be collapsed to simplify the equivalent network.

3   Parameter estimation in an equivalent network

In the method described in the preceding section we assume that a total description of a DH network exists, before we perform the successive reductions. In the process of reducing the network we obtain new physical parameters, but it is difficult to validate if these parameters are optimally adjusted for a given topological reduction. Thus it is feasible for us to confirm that the equivalent network cannot be improved significantly by a further adjustment of the parameters.

The main purpose of DH simulation is to determine operational conditions at the plant, which leaves us with determining the return temperature into the plant. Thus, this temperature is an indicator of how well the equivalent network performs. Therefore we compute the sum of squared errors in a given time interval, where the error is the difference between original and equivalent network.

Minimisation of errors can be obtained by least-squares parameter estimation of the equivalent network. In other words: Minimise the squared sum of errors by changing parameters such as pipe lengths and heat loss coefficients. This is done by attaching a Levenberg-Marquardt least-squares algorithm to the simulation model, which then can be used to estimate parameters of choice. The algorithm used here is a part of the MINPACK Fortran library, obtainable at Netlib program repository (http://netlib.org).

Experiments show that if we try to estimate both optimal lengths of branches and pipe diameters, the problem becomes underdetermined, meaning that a change in length can be compensated by a change in diameter without changing the squared error. The same problem occurs when we estimate heat loss parameters for both supply and return pipes. As a result we only estimate heat loss coefficients in the return pipes, as well as the lengths of the pipe-pair branches.

Although we use parameter estimation for evaluation purposes only, it might be possible to use it to make an equivalent model of a DH network

without full information of the original network. In this paper, we leave this matter to further studies.

4 Simulation of DH networks

In the preceding sections we have described a method to generate an equivalent DH network from an original one. In order to validate this equivalent network against the original situation, we must determine the resemblance between the two in some typical operational conditions. This is of course not possible in real life, so we need a dynamic modelling tool which can be used for simulating the operation of general DH networks.

In the present work we use a simulation tool called DHSIM, which has been developed in Denmark at Risø National Laboratory. The tool is in form of a computer program which is capable of simulating changes in both flow and temperatures in a DH network with tree structure. For further information about dynamic simulation of DH networks see e.g. Benonysson (1991) and Zhao (1995).

Here we assume that there is one production plant connected to several DH substations through a network of DH branches (each branch consists of a pair of supply and return pipes). The substations are equipped with plate heat exchangers used to supply heat from our network in question to a secondary network, which can be either a distribution DH network or a single house. At each exchanger station we determine conditions for flows and temperatures by using the following equation, based on logarithmic mean temperature (see e.g. Holman (1989))

$$E = \left(\frac{kA}{m_2^{-q} + m_2^{-q}} \right) \left(\frac{(T_{S1} - T_{S2}) - (T_{R1} - T_{R2})}{\ln(T_{S1} - T_{S2}) - \ln(T_{R1} - T_{R2})} \right)$$

where T_S and T_R are supply and return temperatures, m is mass flow, and A is the cross section area, with subscripts 1 and 2 denoting primary and secondary side of the exchanger. The parameter q affects how the energy flow E is dependent on the mass flow, and k is a scaling parameter, which is typically determined for every single heat exchanger. By using this equation and enforcing preservation of energy in the exchanger, we can determine the flow and return temperature on the primary side, given the primary and secondary supply temperatures, secondary return temperature and energy flow. For further details see Benonysson (1991).

The simulation tool mentioned above is used for comparison between the original DH network and an equivalent one. By doing that we are assuming that simulation results for the original network are perfectly accurate with

respect to the real world, which is not entirely correct because of numerical errors and simplifying assumptions in the model. However, we can use the model for comparison if we assume that these errors are small in comparison with errors due to equivalent reduction.

5   Test examples

In this section, we perform tests of the method for generating equivalent networks. Two tests are performed, where the first test example consists of a very simple network and the last example is larger and represents a real DH system.

Example 1

Here we consider a small illustrative example, consisting of only 2 branches and 2 loads. The structure of the system is shown in Figure 1. To avoid dispersion the wall thickness of the steel pipes is assumed to be zero. All data describing the original network as well as the equivalent one are given in Appendix B. For this DH network we observe several test situations, as follows:

Test A

The supply temperature from the plant at node N0 is 80°C, but is suddenly increased to 100°C, whereas the return temperature at the two load nodes N1 and N2 is 40°C on the primary side of the heat exchangers. Flows through the heat exchangers are 30 kg/s and 20 kg/s as used in the reduction of the DH network. With these data the assumptions made when developing the method for the equivalent network are fulfilled. Therefore, the equivalent network should give the same simulation results as the original one.

Test results: Figure 2 shows a comparison of the supply temperature at the 3 nodes. As expected there is a perfect correspondence between the original and equivalent network, and therefore the curves for the two networks cannot be distinguished. Steep temperature fronts at nodes N1 and N2 (no dispersion) are observed. On the other hand, if the thickness of the steel pipes is not ignored, expected dispersion is observed as shown in Figure 3. Now the curves for node N2 can be distinguished.
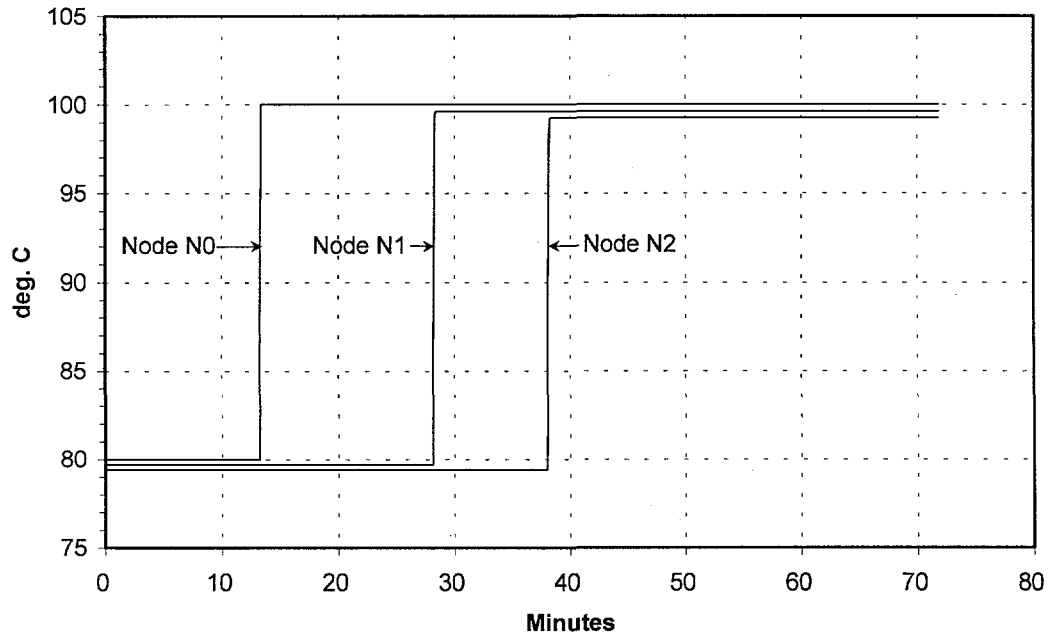
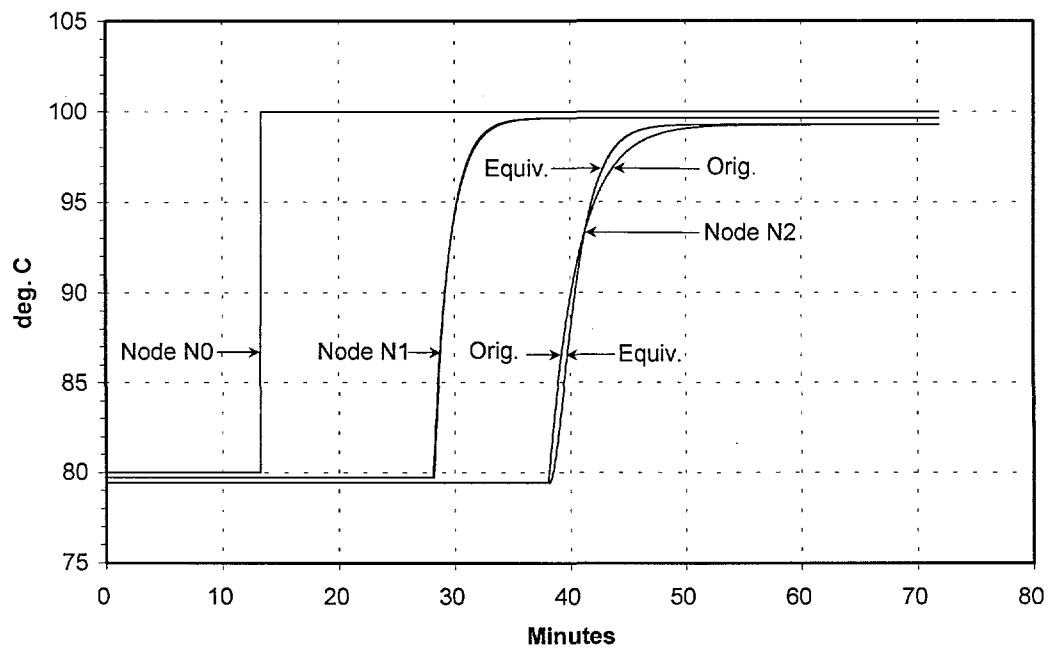Figure 2: Supply temperatures from the plant. Steel pipes not included.

Figure 3: Supply temperatures from the plant. Steel pipes included.

Test B

We supply water with temperature of 80°C at node N0 and introduce heat exchangers (see Section 4) at both load nodes N1 and N2. Supply and return temperatures are set to 70 and 40°C respectively on the secondary side of the heat exchangers and the heat load at Node N2 is constant, 3.379 MW.

Now we introduce some dynamic conditions for the heat load. At node N1 the heat load is constant (5 MW) at the beginning and at the end of the simulation period, but in the middle of the period the load is increased to 7 MW, following a sine curve. With the values of the heat load set to 5 and 3.379 MW and with a temperature drop of 80 - 40 = 40°C, we obtain flows of magnitude 34.20 kg/s and 22.80 kg/s in pipes P01 and P02. Since 34.20/22.80 = 30/20 (the flows used in the reduction of the DH network), our assumptions are (almost) fulfilled in the two ends of the simulation period, but not in the middle. Finally it should be noted that the thickness of the steel pipes is ignored in this case.

Test results: Figure 4 shows the return temperatures into the plant. Due to the sine variation of the load at node N1, the assumption regarding a constant ratio between mass flows is violated. Therefore, during the time in which the load in node N1 follows a sine curve we observe a small difference between the original and equivalent networks.

Test C

The current test situation is as in B with the only difference that the supply temperature from the plant at node N0 is 80°C at the beginning, but is suddenly increased to 100°C. As before we simulate the operation of both the original and equivalent network. Moreover we perform a least-squares parameter estimation in order to determine if the equivalent network could be further improved under these specific test conditions, see Section 3. Data for the network found by estimation can be found in Appendix B.

Test results: Figure 5 shows the return temperature into the plant for the original, equivalent and estimated networks. It is seen that the estimation has improved the network, since the standard deviation of the error has been reduced from 0.38°C to 0.27°C. This improvement is expected since the equivalent network obtained by successive reductions is found under stationary conditions and with a constant ratio between the flows in the two pipes. It should be noted that the superiority of the estimated network is only valid under the conditions used here, regarding supply temperature and loads.
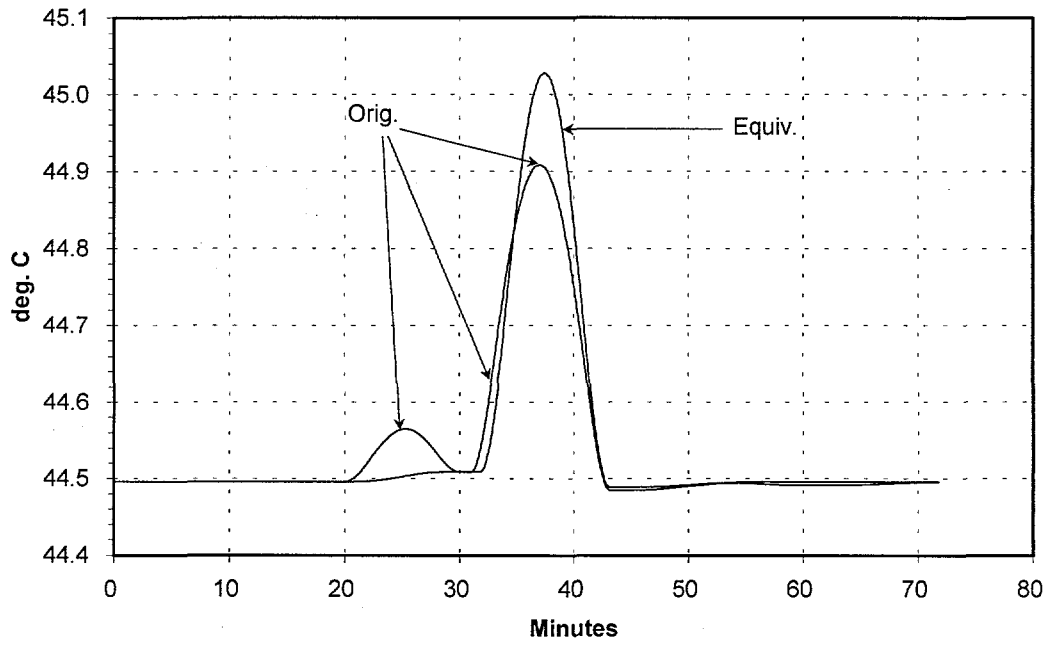
Figure 4: Return temperatures into the plant.
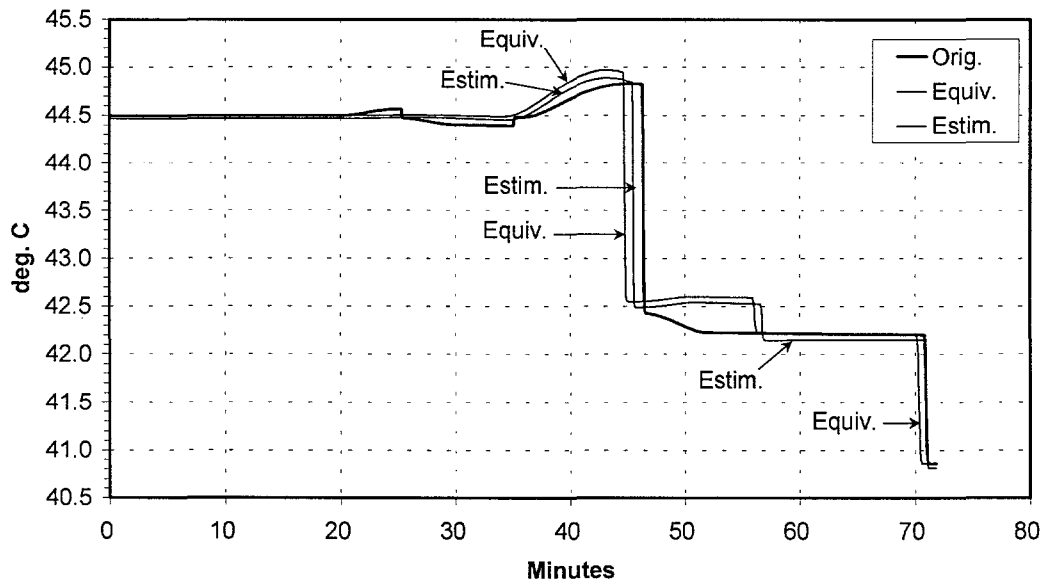
Figure 5: Return temperatures into the plant.
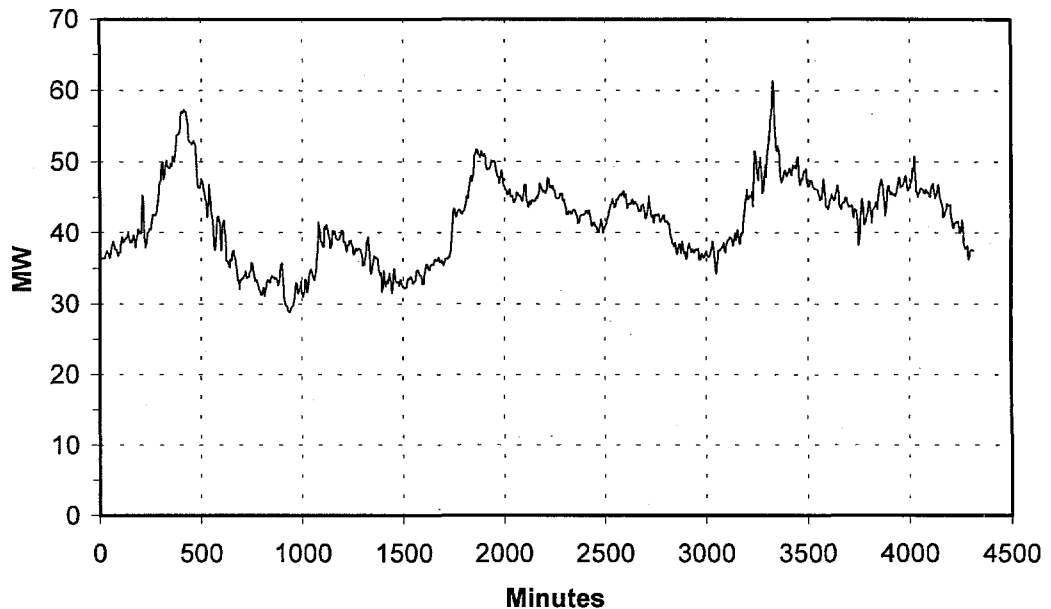
Figure 6: Total heat load.

5.1   Example 2

Here we consider a larger example consisting of 30 branches and 17 loads
(heat exchangers) which corresponds to the DH system at Ishøj, Denmark,
with minor simplifications. Data regarding the network and the annual heat
loads are obtained from Zhao (1995), while time series for load variations are
measurements from the VEKS DH company, also in Denmark. Since the data
from VEKS only include time series for 5 heat exchangers, the variations for
the remaining 12 heat loads are constructed as simple linear combinations of
these 5 series. Figure 6 shows the total heat load for a simulation period of
three days.

Test A

In the first test the plant is connected to node N0 with a constant supply
temperature of 80°C. We model the heat exchangers at the load nodes with
secondary supply and return temperatures set to 70°C and 40°C respectively.
Time steps of 5 minutes are used in the simulations.

Test results: We only consider the return temperature into the plant, since
it is the most important variable from an operational point of view. While
maintaining all heat loads, we begin by reducing the original network to a
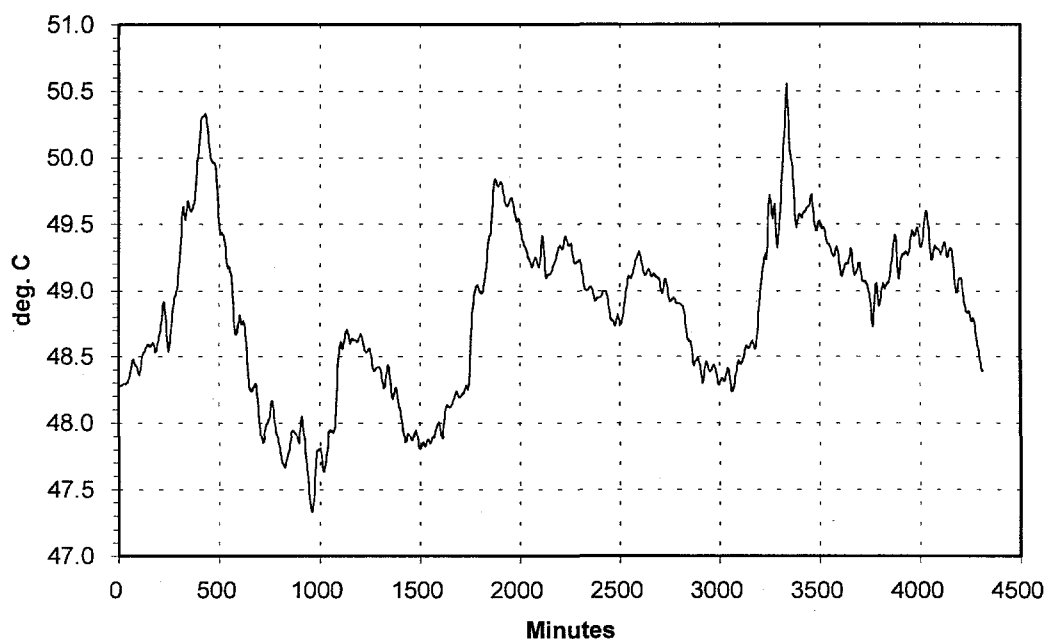
Figure 7: Return temperatures into the plant for the original network.

system where all pipes are placed sequentially after each other with no side branches. Figure 7 shows the temperature for the original network, while Figure 8 shows the difference between equivalent and original networks. It is seen that the error is always smaller than 0.04°C, and since the error is oscillating between positive and negative numbers, the average error is extremely small (0.00007°C). This indicates that the calculation of heat loss is very accurate in the equivalent case.

To determine whether the equivalent network could be further improved under these specific test conditions, a least-squares estimation of pipe lengths and return pipe insulation has been performed. A plot of the temperature difference like Figure 8 shows that there is no significant improvement, since the standard deviation has only been reduced from 0.0076°C to 0.0074°C.

Test B

Now we modify test A by introducing a sudden change in supply temperature from the plant, where the temperature is increased from 80 to 100°C after the first day (1440 minutes).

Test results: Figures 9 and 10 show the return temperature into the plant and the corresponding error. Again it is observed that the error is always
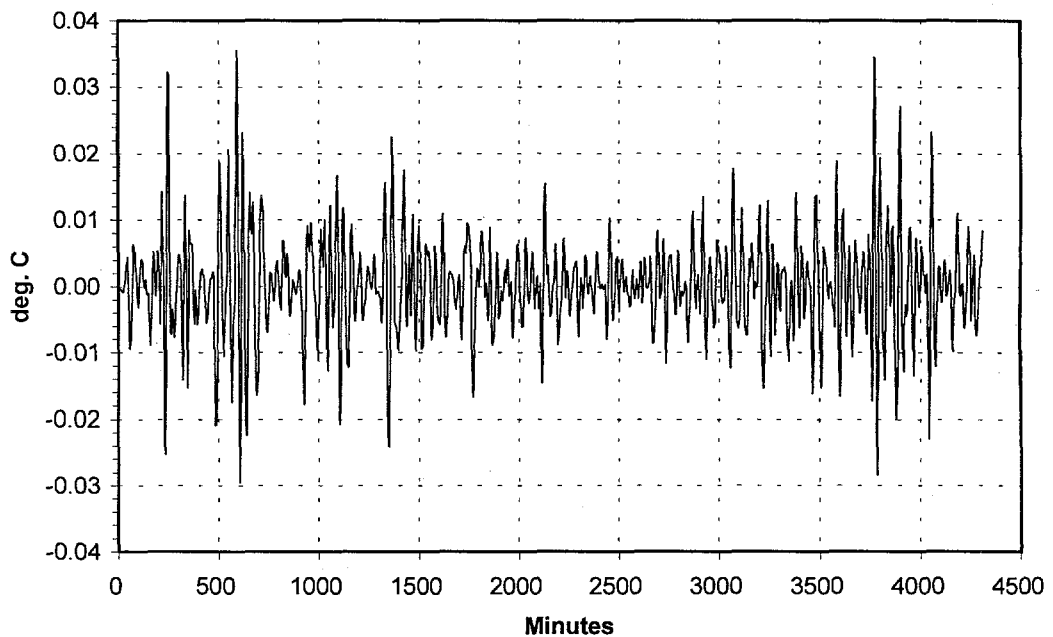
Figure 8: Error in return temperature into the plant for the equivalent network.

smaller than 0.04°C except for a spike around 1500 minutes. At this time the temperature front has moved to the heat exchangers and back to the plant, and the very short spike shows that the delay time for the equivalent network is only slightly inaccurate. The average error in return temperature into the plant is -0.0009°C, again a very small number.

Like in test A, a least-squares parameter estimation is performed, reducing the standard deviation from 0.0146°C to 0.0105°C. Since the situation in test B, as compared to test A, is farther from the general assumption regarding a constant ratio between mass flows, the estimation brings about a larger reduction of the error.

Test C

In the last test we consider a situation like in test B, but gradually reduce the network by removing the branches with the smallest delay time. When each branch is removed, the lengths of the preceding and succeeding branches are increased in order to maintain the correct time delay and heat loss. For each of these equivalent networks we perform a least-squares parameter estimation in order to determine if the equivalent network could be further improved under these specific test conditions.
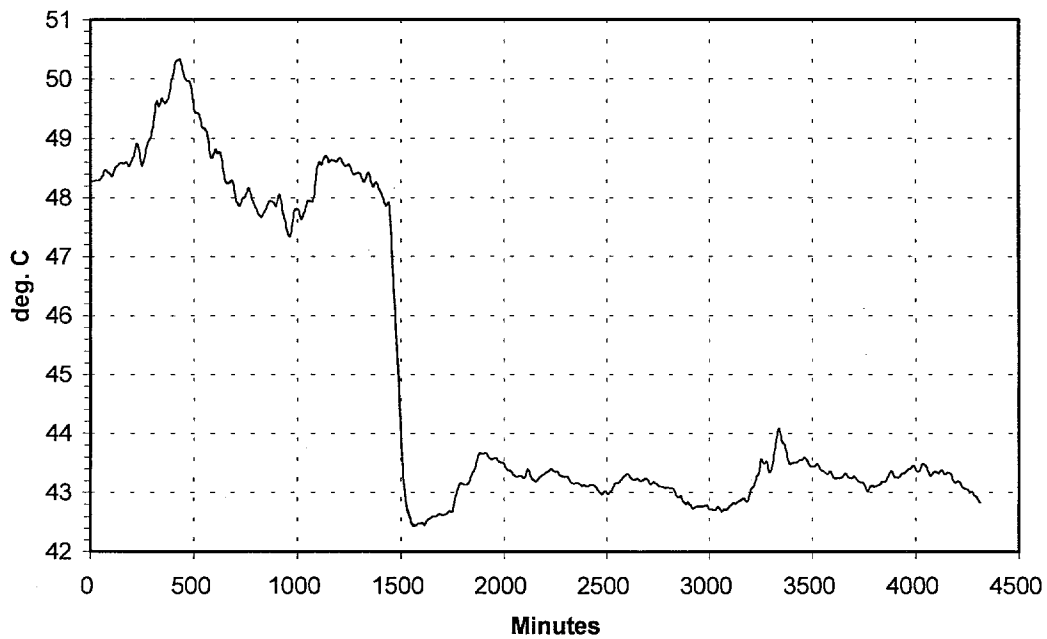
Figure 9: Return temperatures into the plant.
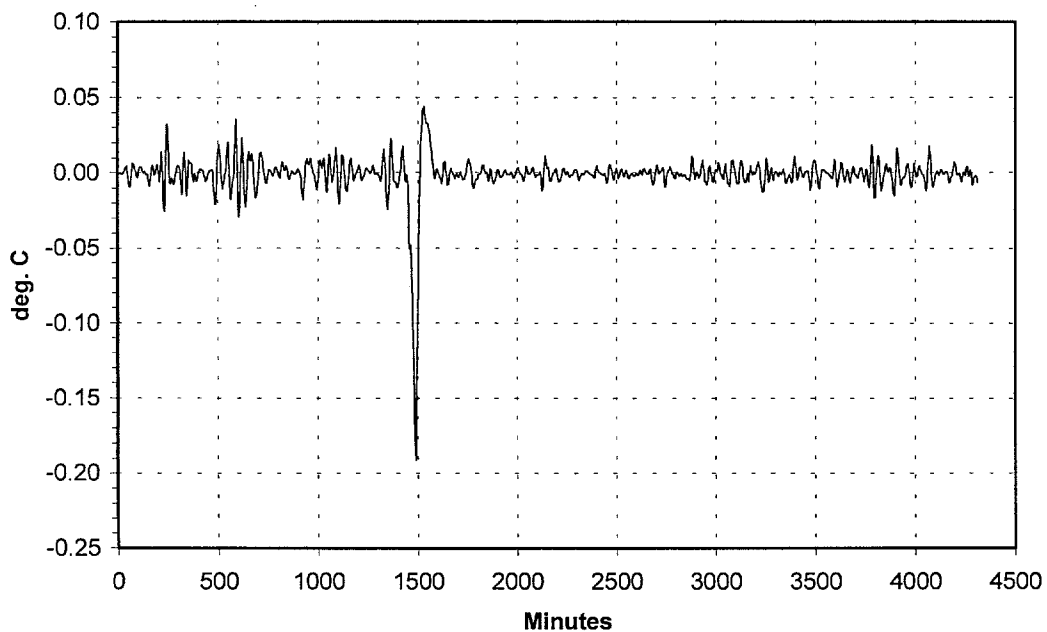
Figure 10: Error in return temperature into the plant for the equivalent network.
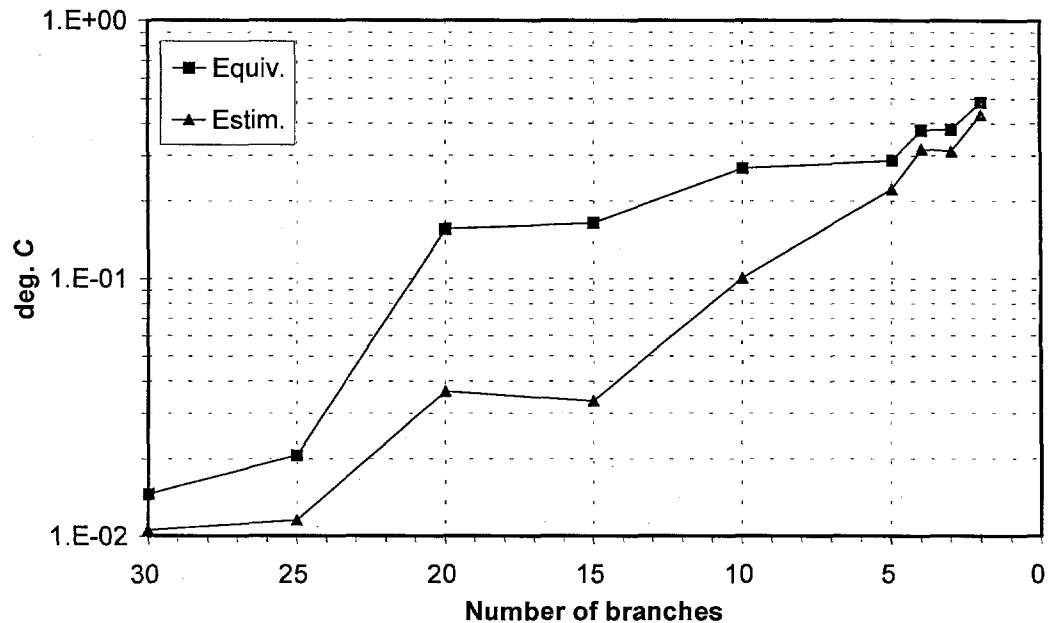
Figure 11: Standard deviation of error in return temperature into the plant when reducing the number of branches.

Test results: In Figure 11 the standard deviation of the plant return temperature error between the original and equivalent networks is shown. It is observed that the standard deviation of 0.0146°C, obtained when all 30 branches are present, is increased to 0.164°C when the branches are reduced to 15, and further increased to 0.38°C with only 3 branches remaining.

As long as the number of branches is not reduced, a least-squares estimation cannot significantly improve the equivalent network, as already seen in test B above. If however the network is reduced to e.g. 15 branches, an estimation will reduce the standard error by a factor of 5. If the network is reduced to only a few branches, the benefit of the estimation is again reduced.

6 Conclusion

It is shown in the paper that the method for aggregating a complex DH network with no loops gives a very good approximation to the original network. The approximation is good even if the very strong assumptions are not fulfilled regarding a constant ratio between mass flows and equal return temperatures at all heat exchangers.

When finding the equivalent network the complexity of the DH network is reduced by gradually changing the tree structure into a chain structure

with no branches. Correspondingly the various parameters which define the branches are transformed from the real network to equivalent parameters in the corresponding equivalent network.

Two main assumptions are made to be able to define the equivalent network mathematically. All mass flows are assumed to vary proportionally, i.e. there is a constant ratio between mass flows. Moreover, it is assumed that the return temperatures on the primary side of all heat exchangers are equal. Naturally, the assumptions are never fulfilled in practice. This means that the equivalent network will not give exactly the same results as the original network, but as the tests show we get results close to the original network.

The equivalent network is reduced further by observing that many nodes in this network are positioned close to each other separated by short pipes. Such nearby nodes are collapsed to simplify the equivalent network. Finally, to find out whether the equivalent network could be further improved, a least-squares minimisation is performed in which optimal values for various parameters (pipe length and insulation) of this network are found.

The equivalent DH network is tested by simulating some examples using the original network as well as the equivalent network. It is shown that the return temperatures into the plant as calculated for the equivalent network are very close to the return temperature for the original network.

Since the return temperatures into the plant seem to be accurate, the models could be used in an optimisation of the operation of a DH system including a CHP plant where the return temperature is an important parameter, and where computational costs might be of concern.

Acknowledgement

References

Benonysson, A. (1991). *Dynamic Modelling and Operational Optimization of District Heating Systems*. PhD thesis, Laboratory of Heating and Air Conditioning, Technical University of Denmark.

Benonysson, A., Bøhm, B., and Ravn, H. F. (1995). Operational optimiza-

tion in a district heating system. *Energy Conversion and Management*, 36(5):297–314.

Hansson, T. (1990). Driftsoptimering af fjernvarmeværker. Master's thesis, Danmarks Tekniske Højskole. Laboratoriet for Varme- og Klimateknik.

Holman, J. P. (1989). *Heat Transfer*. McGraw-Hill Book Company, Singapore.

Zhao, H. (1995). *Analysis, Modelling and Operational Optimization of District Heating Systems*. PhD thesis, Laboratory of Heating and Air Conditioning, Technical University of Denmark.

Zhao, H., Bøhm, B., and Ravn, H. F. (1996). Optimum operation of a CHP-based district heating system by mathematical modelling. *Euroheat & Power Fernwärme Int.*, 24(11):618, 620–622.

Zhao, H. and Holst, J. (1997). Study on network aggregation in DH systems. In Pálsson, Ó. P., editor, *6th International Symposium on District Heating and Cooling Simulation*, Reykjavik, Iceland. ISBN 9979-54-203-9.

A Generation of equivalent DH network by successive reductions

This appendix describes how the expressions for the equivalent network are deduced. Since it should be possible to read the appendix independently of Section 2, some of the verbal statements given in Section 2 will be repeated here, possibly in a more precise way. Before we describe the network reduction method in detail, we shall define some symbols:

Physical variables:

Sym.	Unit	Definition
T	°C	Temperature
P	kW	Heat load
m	kg/s	Mass flow
v	m/s	Velocity of water (temp. front)
τ	s	Delay in pipe (temp. front)
L	m	Length of pipe
D	m	Inner diameter of steel pipe
D_P	m	Outer diameter of steel pipe
V	m^3	Water volume
A	m^2	Inside area of pipe
h	W/(m°C)	Specific heat conductivity
H	W/°C	Heat conductivity
Q	kW	Heat loss
c	kJ/(kg°C)	Specific heat capacity
C	kJ/(m°C)	Heat capacity per meter pipe
ρ	kg/m^3	Density

Subscripts:

Sym.	Definition
0	Node 0
1	Branch or node 1
2	Branch or node 2
A	Branch or node A
B	Branch or node B
S	Supply
R	Return
G	Ground
W	Water
P	Steel pipe

Note:

Flow in branch A: $m_A + m_B$

Auxiliary variables.

Symbol	Definition	Condition
α	m_2/m_1	$\alpha > 0$
β	$1 + \alpha$	$\beta > 1$
φ	$C_w/(C_w + C_p)$	$0 < \varphi < 1$
ψ	φ_2/φ_1	
γ	$(V_1/V_2)(m_2/m_1) = (V_1/V_2)\alpha$	$0 < \gamma \leq 1/\psi$
δ	$1 - (V_1/V_2)(m_2/m_1) = 1 - \gamma$	$1 - 1/\psi \leq \gamma < 1$
A	H_{AR}/H_{1R}	$A > 0$
B	H_{BR}/H_{1R}	$B > 0$
θ_R	H_{2R}/H_{1R}	$\theta_R > 0$
θ_S	H_{2S}/H_{1S}	$\theta_S > 0$

The steel pipe is included in the model by interpreting the velocity v and the delay τ as connected to the propagation of a temperature front, and by assuming that the temperature of the pipe wall and the water is equal in every cross section of the pipe.

We will define the equivalent network so that the return temperature in node 0 is the same for the original network and the equivalent one if we have the same supply temperature and flow at node 0 in the two networks. We will start out by assuming the following:

- $\tau_1 \leq \tau_2$. If this is not fulfilled, the definitions of 1 and 2 are switched.

- $\alpha = m_2/m_1$ is constant through time.

The second assumption above, concerning a constant ratio between mass flows, implies that the variables α, β, γ, and δ are also constant, which is the main assumption in the derivation below. Moreover, it is a necessary assumption because violating it will result in time dependent physical data for the pipes in the equivalent network. Naturally, the assumption is never fulfilled in practice meaning that the equivalent network found below will not give exactly the same results as the original network, but hopefully close results.

We proceed in obtaining our equivalent network by demanding the following:

- $\tau_A = \tau_1$: Time delay in branch A must equal delay in branch 1.

- $\tau_B = \tau_2 - \tau_1$: Delay in branches A and B must equal delay in branch 2.

- $V_A + V_B = V_1 + V_2$: Water volume must be conserved.

- $m_A + m_B = m_1 + m_2$: Mass flow must be conserved.

- $P_A + P_B = P_1 + P_2$: Heat load must be conserved.

- $Q_A + Q_B = Q_1 + Q_2$: Heat loss from the pipes must be conserved.

Finally, to obtain the equivalent network we choose:

- Branch B is equal to the last part of branch 2, i.e. the part of branch 2 with $\tau > \tau_1$. This choice does not take the insulation of pipe B into account.

- The mass flow in branch B is equal to that in branch 2.

- The velocity in branch A is equal to a weighted average of the velocities in branches 1 and 2. The mass flows in branches 1 and 2 are used as weight factors.

Using the results from above, the equivalent network is defined by:

$$
\begin{aligned}
m_B &= m_2 & m_A &= m_1 \\
V_B &= V_2(1 - \gamma\psi) & V_A &= V_1(1 + \alpha\psi) \\
A_B &= A_2 & A_A &= \beta(1 + \alpha\psi)A_1 A_2/(A_2 + A_1\alpha^2\psi) \\
L_B &= L_2(1 - \gamma\psi) & L_A &= L_1(1 + \alpha^2\psi A_1/A_2)/\beta \\
D_B &= D_2 & D_A &= 2\sqrt{A_A/\pi} \\
\varphi_B &= \varphi_2 & \varphi_A &= (\varphi_1 + \alpha\varphi_2)/(1 + \alpha) \\
D_{PB} &= D_{P2} & D_{PA} &= D_A\sqrt{[(1 - \varphi_A)/\varphi_A][(\rho_W c_W)/(\rho_P c_P)] + 1}
\end{aligned}
$$

Now the flow and physical dimensions (except for the insulation) for the equivalent network have been determined. Below, the insulation of the pipes will be found, together with the return temperatures and heat loads in nodes A and B.

Heat loss

To this point, the insulation of the pipes has been excluded from our calculations. Here we shall address this aspect. Generally, we shall allow for different insulation thickness in the supply and return pipes. Hence we have four quantities to find: H_{AS}, H_{BS}, H_{AR}, and H_{BR}. When calculating the heat loss from a pipe we use the temperature at the inlet to the pipe. Since the heat loss in a pipe and the temperature drop along the pipe are small, the error introduced by using the inlet temperature is acceptable.

We begin by choosing that the two networks have the same amount of heat loss on the supply side, which results in:

$$H_{AS} + H_{BS} = H_{1S} + H_{2S}$$

Considering the return side, we define three new symbols as:

$$A = H_{AR}/H_{1R}$$
$$B = H_{BR}/H_{1R}$$
$$\theta_R = H_{2R}/H_{1R}$$

By demanding that the total heat loads in the two systems are equal, we can express the conservation of heat loss by the two following equations:

$$P_A = K_{A1}P_1 + K_{A2}P_2$$
$$P_B = K_{B1}P_1 + K_{B2}P_2$$

where

$$K_{A1} = (A\alpha/\beta + B - \alpha)/B \qquad K_{B1} = \alpha(1 - A/\beta)/B$$
$$K_{A2} = (A\alpha/\beta + B - \theta_R)/B \qquad K_{B2} = (\theta_R - A\alpha/\beta)/B$$

It is seen that P_A and P_B are given by linear expressions in P_1 and P_2 with constant coefficients. These equations for PA and PB are equivalent to the following equations for T_{RA} and T_{RB}:

$$T_{RA} = C_{A1}T_{R1} + C_{A2}T_{R2} \qquad (1)$$
$$T_{RB} = C_{B1}T_{R1} + C_{B2}T_{R2} \qquad (2)$$

where

$$C_{A1} = (A\alpha/\beta + B - \alpha)/B \qquad C_{B1} = (1 - A/\beta)/B \qquad (3)$$
$$C_{A2} = \alpha(A\alpha/\beta + B - \theta_R)/B \qquad C_{B2} = (\theta_R - A\alpha/\beta)/B \qquad (4)$$

As before, it is seen that T_{RA} and T_{RB} are given by linear expressions in T_{R1} and T_{R2} with constant coefficients. T_{RA} is the return temperature in node A before mixing with the water from branch B.

Now the problem consists of assigning values to A and B (or H_{AR} and H_{BR}) so that one gets reasonable values for T_{RA}, T_{RB}, P_A, and P_B as defined in the above linear identities. At this point it should be noted that nodes 1 and 2 represent sub-trees of the DH network in general and the constant coefficients C_{Xi} and K_{Xi} should thus be equal to 1 or 0:

$$C_{A1} = C_{B2} = K_{A1} = K_{B2} = 1 \qquad C_{A2} = C_{B1} = K_{A2} = K_{B1} = 0 \qquad (5)$$

This leads to the following expressions for the return side of the equivalent network:

$$H_{AR} = (1 + \alpha)H_{1R} \qquad\qquad H_{BR} = H_{2R} - \alpha H_{1R} \qquad (6)$$

Since heat conductivity H_{BR} should not be negative, it is seen that with the assumptions made so far, it is possible to find a viable equivalent network only if $\theta_R \geq \alpha$ or $H_{2R}/H_{1R} \geq m_2/m_1$.

Since $K_{A1} = K_{B2} = 1$, the loads in nodes A and B of the equivalent network are equal to the original loads in nodes 1 and 2, respectively.

We manage the situation $\theta_R < \alpha$ (equivalent to $H_{2R}/H_{1R} < m_2/m_1$) by imposing further assumptions on the original network. We start by demanding that the loads and return temperatures in nodes A and B should equal loads and return temperatures in nodes 1 and 2, respectively. Moreover, we choose to let branch B have the same insulation as branch 2. Then the conservation of heat loss on the return side can be expressed as:

$$H_{AR} = (H_{1R} + H_{2R}\gamma\psi\Omega)(1 + \alpha)/(1 + \alpha\Omega) \qquad H_{BR} = H_{2R}(1 - \gamma\psi) \qquad (7)$$
$$\Omega = (T_{R2} - T_G)/(T_{R1} - T_G) \qquad (8)$$

As can be seen, in excess to the hitherto main assumption that $a = m_2/m_1$ is constant, we have to assume that $\Omega = (T_{R2} - T_G)/(T_{R1} - T_G)$ is constant, T_G being the ground temperature. If we furthermore assume that $T_{R1} = T_{R2}$ we get:

$$H_{AR} = H_{1R} + \gamma\psi H_{2R} \qquad\qquad H_{BR} = H_{2R}(1 - \gamma\psi) \qquad (9)$$

As for the assumption that $\alpha = m_1/m_2$ is constant, the new assumptions regarding T_{R1} and T_{R2} are never totally fulfilled in practice. Therefore, the equivalent network will not give exactly the same results as the original network, but hopefully close enough results.

We will now address the supply side of the DH system. It is stated above that the sum of heat conductivities $(H_{AS} + H_{BS})$ for the supply pipes of the equivalent network should equal the sum for the original network $(H_{1S}+H_{2S})$. To have the same formulas for the supply and the return sides, we choose to divide the heat conductivity on the supply side between branches A and B in the same ratio as on the return side. Therefore, we have the following expressions for the supply side of the equivalent network:

If $\theta_S \geq \alpha$ or $H_{2S}/H_{1S} \geq m_2/m_1$:

$$H_{AS} = (1+\alpha)H_{1S} \qquad\qquad H_{BS} = H_{2S} - \alpha H_{1S} \qquad (10)$$

If $\theta_S < \alpha$ or $H_{2S}/H_{1S} < m_2/m_1$:

$$H_{AS} = H_{1S} + \gamma\psi H_{2S} \qquad\qquad H_{BS} = H_{2S}(1 - \gamma\psi) \qquad (11)$$

B   Data for test example 1

Network	Branch	Node		Pipe diamter		Length	Heat transf. coeff.		Flow
		1	2	Inner	Outer		Supply	Return	
				m	m		W/(mC)	W/(mC)	kg/s
Original	P1	N0	N1	0.185	0.185	1000	0.461	0.426	30
	P2	N0	N2	0.159	0.159	1500	0.420	0.389	20
Original	P1	N0	N1	0.185	0.185	1000	0.461	0.426	30
	P2	N0	N2	0.159	0.159	1500	0.420	0.389	20
Equivalent	P1	N0	N1	0.244	0.244	961	0.800	0.739	50
	P2	N1	N2	0.159	0.159	597	0.540	0.501	20
Estimated	P1	N0	N1	0.244	0.244	981	0.800	1.202	50
	P2	N1	N2	0.159	0.159	596	0.540	2×10^{-5}	20

Appendix C:
An aggregated dynamic simulation model of district heating networks

Helge V. Larsen,[*] Halldór Pálsson,[†] Benny Bøhm[‡] and Hans F. Ravn[§]

Unpublished

Abstract

Dynamic properties of district heating (DH) networks include e.g. water flow and propagation of heat from production plants to consumers. Mathematical models of such networks can be applied either for general understanding of DH systems, or in combination with production planning and optimization.

One type of mathematical models involve a full physical modeling of the network, taking into account individual pipes, dimensions, material properties, etc. Such full models tend to be computationally intensive when applied in network simulations, which can be a problem when considering large DH systems.

In the current paper a method is presented in which a fully described model of a DH network is replaced by a simplified one, with the purpose of reducing simulation time. This is done in a way such that the dynamic properties of the system are preserved as well as possible. The simplified model is generated by gradually reducing the topological complexity of the original network.

The method is validated by applying it on a real case study, in which a network with over 1000 pipes is reduced to less than 10 pipes. Results show that such relatively simple network can maintain most of the dynamic characteristics of the original networks. Furthermore, since simulation time is in general directly proportional to the number of pipes, there is a great potential for reducing computational time in model applications.

[*]Risø National Laboratory, Denmark
[†]Risø National Laboratory and Technical University of Denmark
[‡]Technical University of Denmark
[§]Elkraft System A.m.b.a

Nomenclature

Original variables

Sym.	Unit	Definition
T	°C	Temperature
P	kW	Heat load
m	kg/s	Mass flow in heat-exch.
v	m/s	Velocity
τ	s	Time delay
L	m	Length of pipe
d	m	Inner diam. of steel pipe
D	m	Outer diam. of steel pipe
V	m^3	Water volume
A	m^2	Inside area of pipe
h	W/(m°C)	Specific heat cond.
H	W/°C	Heat conductivity
Q	kW	Heat loss
c	kJ/(kg°C)	Specific heat capacity
C	kJ/(m°C)	Heat capacity per meter
ρ	kg/m^3	Density

Subscripts

Sym.	Definition
0	Node 0
1	Branch or node 1
2	Branch or node 2
A	Branch or node A
B	Branch or node B
G	Ground

Superscripts

Sym.	Definition
s	Supply
r	Return
w	Water
p	Steel pipe

Auxiliary variables.

Symbol	Definition	Condition
α	m_2/m_1	$\alpha > 0$
β	$1 + \alpha$	$\beta > 1$
φ	$C^w/(C^w + C^p)$	$0 < \varphi < 1$
ψ	φ_2/φ_1	$\psi > 0$
γ	$(V_1/V_2)(m_2/m_1) = (V_1/V_2)\alpha$	$0 < \gamma \le 1/\psi$
δ	$1 - (V_1/V_2)(m_2/m_1) = 1 - \gamma$	$1 - 1/\psi \le \gamma < 1$
θ_A^r	H_A^r/H_1^r	$\theta_A^r > 0$
θ_B^r	H_B^r/H_1^r	$\theta_B^r > 0$
θ_2^r	H_2^r/H_1^r	$\theta_2^r > 0$
θ_2^s	H_2^s/H_1^s	$\theta_2^s > 0$

1   Introduction

District heating (DH) systems provide an efficient method for house heating and is widely used, particularly in the Nordic countries. In a typical DH system, the heat is produced at central plants and is then distributed by hot water to the DH customers through a network of pipes. Such centralized production has advantages in form of high efficiency and the possibility of combined heat and power production (CHP), see e.g. Horlock (1987).

The process of transporting the heat to the customers involves both time dependent changes in flows and temperatures, as well as in the heat losses

from the pipe network. These heat losses should be kept at minimum, which is possible by lowering the supply temperature from the plant. However, lowering the supply temperature could result in unacceptably low temperature levels at the customers. Furthermore, if the supply temperature is reduced, the water flow in the system increases, resulting in higher pumping costs. Hence, an appropriate balance between these effects should be attained. Refer to this as operational optimization of the DH supply temperature.

One way of determining the optimal operational conditions in a DH system is to generate a mathematical model of the system, which can be used for simulating various operational strategies. For this purpose, two classes of models have mainly been used for DH systems: (i) Physical models and (ii) Statistical models. The statistical models, based on time-series or neural networks, are generally quite simple when compared to physical models, but require the availability of measurements for model estimation and validation, see Pálsson (1993) and Zhao (1995).

In contrast to the statistical models, the necessary data for a physical description (network topology, pipe diameter and insulation, pump characteristics, etc.) are often available. Moreover, the physical models often represent the whole structure of the DH system involved, and it is therefore easy to change or add new components to an existing model. Since these models require a full description of the DH system, they tend to be much more computationally intensive than statistical models. Thus, in order to reduce this intensity it might be desirable to simplify the physical description, but without loosing the relation of the model to the real pipe network in consideration.

The problem of operational optimization has been treated in various references. In Pálsson (1993) an optimal controller based on statistical methods was developed, with the single aim of lowering the supply temperature without discomforting the customers. In Benonysson (1991) and Zhao (1995) operational optimization based on physical models was performed, including the pumping costs. It was reported that the problem became quite large and complex, when regarding a relatively small reference network. Network simplifications were furthermore suggested in Zhao (1995).

The first obvious approach to simplify a physical model of a DH network is to reduce the number of model components, such as pipes, nodes and customer stations. In Hansson (1990) the problem of such network reductions was addressed and a simple model consisting of one pipe and one consumer was proposed. In Zhao and Holst (1997) an aggregated network model based on representative consumers was suggested and tested.

In this paper a new method for reduction of a DH network is proposed. A typical DH network, to which the presented method applies, has a tree

like structure, where the production plant is at the root with branches going
to the leaves, or customers. The main procedure in this new method is a
successive reduction of a network tree, which results in a system where all
the DH pipes are placed sequentially after each other on a single pipe branch.
Correspondingly, the various parameters that determine the properties and
dimensions of the pipes, are transformed in a way such that the reduced
network will be similar to the original one. Further reduction is then obtained
by cumulating customers which are geometrically close on the single branch.
Refer to this simplification as an *equivalent network*.

The reduction method is validated by performing simulations of both
original and equivalent systems, using a real case study as a reference. The
simulation results are compared at the production plant, since the main
application of the method is in the field of operational optimization. It
is essential that the equivalent network model should give results that are
adequately close to a full network model.

The paper is organized as follows. In Section 2 dynamic modeling of DH
networks is briefly introduced and discussed. In Section 3 the method for
reducing a tree network to a single branch is presented and in Section 4 the
additional process of removing internal nodes is presented. In Section 5 the
method is illustrated and tested on a DH network located in the town of
Hvalsø in Denmark and finally in Section 6 conclusions are drawn.

2 Mathematical modeling of DH networks

A typical DH distribution system consists of one production unit, a pipe
network, and customer stations. The customers can be of several different
types which include

- Single family houses. The radiators in the houses can be connected
  directly to the DH system, or there can be a secondary system with a
  heat exchanger connection to the DH network.

- Large housing blocks with several flats. The same two possibilities of
  a connection to the radiators as in the preceding item apply here.

- Public buildings such as schools and institutions. The heat usage here
  can be quite different from residential houses with respect to diurnal
  variations.

- Special customers, such as industries.

The plant produces heat to fulfill a given demand and transports it through the pipes to the various customers, where heat is extracted and the cooled water returned. In order to be able to simulate dynamic changes in the system, mathematical models can be posed which describe system components as well as their interactions.

Here, the main focus is on mathematical modeling of the pipes, as well as the customer stations where it is assumed that heat is extracted by heat-exchangers. Detailed models have been developed by considering the actual topology of the network as well as the physical layout and properties of the DH pipes. This involves using mathematical methods for computing the flow distribution as well as the temperature distribution in the network, taking into account pressure drop as well as heat losses, see e.g. Benonysson (1991) and Pálsson et al. (1999).

Simulation of the flows and temperatures in a DH network in connection with operational optimization is traditionally done by assuming a quasi-dynamic condition between flow and temperature, see e.g. Benonysson (1991). This implies that the flow can be computed independently from the temperature distribution, and the temperature is computed by assuming constant flow in the whole network.

Nevertheless, the first step is to determine the flows at the customer stations which are determined from the heat demand (load) as well as the temperature conditions in the DH pipes. At each customer station conditions are determined for flows and temperatures by using an equation based on logarithmic mean temperature, see e.g. Holman (1989) and Pálsson et al. (1999).

$$Q = \left(\frac{kA}{m_1^{-q} + m_2^{-q}} \right) \left(\frac{(T_{s1} - T_{s2}) - (T_{r1} - T_{r2})}{\ln(T_{s1} - T_{s2}) - \ln(T_{r1} - T_{r2})} \right) \tag{1}$$

where Q is the heat flow, m is mass flow, T_s is the supply temperature and T_r is the return temperature. The subscripts 1 and 2 denote primary and secondary side of the exchanger.

In the present work, a special simulation tool has been used for computation of flow and temperature dynamics, see Pálsson et al. (1999). There are basically three steps involved in computing all flows, pressures and temperatures in the system, at any given time.

1. Given the temperature distribution in the network, compute the flow and return temperature at the customers stations

2. Compute flow in every branch in the network tree and the corresponding pressures in every branch junction (node).

3. Use the computed flows to determine how much the water has moved in the pipes and how much heat is lost to the surroundings.

4. Go to step 1.

This concludes the brief discussion on DH network simulation. For further information refer to Benonysson et al. (1995), Zhao et al. (1994) and Pálsson (1997).

3   Collapsing a network tree into one branch

Consider a DH network with a pure tree structure, i.e. there is no circular connection in the network and there is only one production plant. Here a method is presented in which an original tree network is gradually reduced to an equivalent single branch network such that all pipes are connected consecutively, and with heat consumers connected to pipe junctions along the branch. By using this method of reduction, the total number of pipe branches and nodes (junctions) is not reduced, but the total length of pipes is reduced. Thus, the resulting branch typically consists of very short pipes. In Section 4, a further reduction of the DH network is performed, in form of gradually removing these short pipes.

In the definition of the equivalent network it is assumed that the mass flow, water volume, temperature, time delay, and heat loss are conserved. On the other hand, these assumptions are only valid if some rather strong assumptions are made regarding the flows and return temperatures in the system. Although these assumptions are not fulfilled in practice, it is shown by examples that results from the equivalent model are still reasonably good.

3.1   Transformation of lengths and diameters

A DH network with no circular loops can be considered as consisting of several two-branch sub-networks, as shown in the left side of Figure 1 where two branches (1 and 2) originating from the same node 0 lead to the nodes 1 and 2. Each branch represents a pair of a supply and a return DH pipes, see Figure 2.

Let the *delay time* be the time it takes the water to go through a pipe branch. It is assumed that the delay time in branch 1 is less than the delay time in branch 2. Typically, the simple network in Figure 1 is part of a more complex network, and therefore other DH network trees might in principle be connected to nodes 1 and 2.
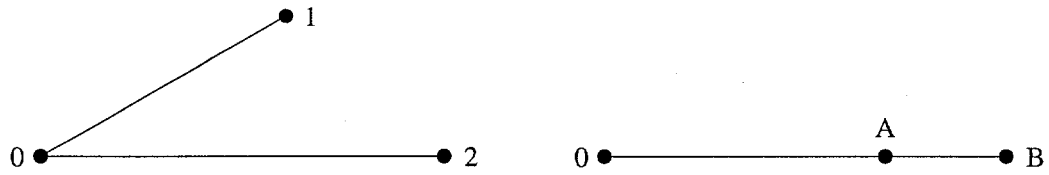
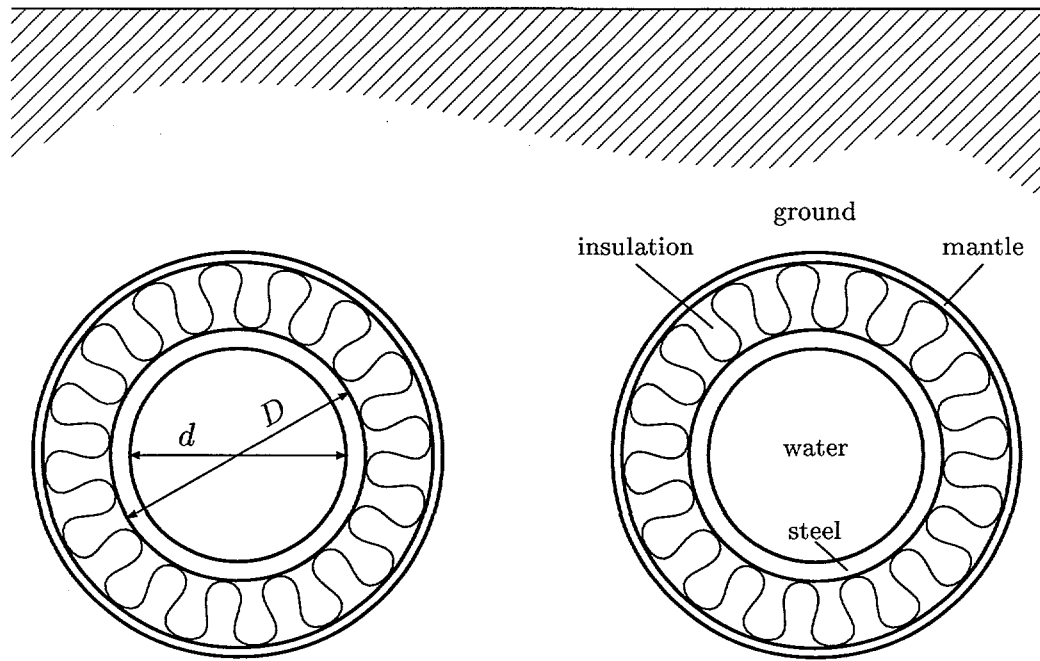Figure 1: Original and equivalent networks

Figure 2: Cross section of a pipe pair buried in ground.

In the sequel, the sub-network mentioned above is transformed into a simpler equivalent network, as shown in the right side of Figure 1. The resulting equivalent network is simpler in the sense that there is no branching and that the total length of the branches is reduced. From now on the branch from node 0 to node A will be named branch A, and the branch between nodes A and B will be named branch B.

If it is assumed that the supply temperature and flow are the same at node 0 in the two networks, then the following main conditions are fulfilled for the equivalent network:

- The return temperature in node 0 is the same for the two networks.

- The sum of the loads in nodes A and B is equal to the sum of the loads in nodes 1 and 2.

- The total heat loss from branches A and B is equal to that from branches 1 and 2.

- The total water volume in branches A and B is equal to that in branches 1 and 2.

The steel in the DH pipes is included in the model by interpreting velocity v and delay τ as connected to the propagation of a temperature front, and by assuming that the temperatures of the pipe wall and the water are the same in every cross section of the pipe. Ignoring the steel pipe is equivalent to assigning the value one to the variables $\varphi = C^w/(C^w + C^p)$ and $\psi = \varphi_2/\varphi_1$. The following is now assumed:

- The time delay in branch 1 is less or equal to the time delay in branch 2, or $\tau_1 \leq \tau_2$. (If this is not fulfilled, the definitions of branches 1 and 2 are switched.)

- Mass flows in branches 1 and 2 are varying proportionally with time, i.e. $\alpha = m_2/m_1$ is constant through time.

- Time delay in branch A is equal to the delay in branch 1:

$$\tau_A = \tau_1 \tag{2}$$

- Time delay in branches A and B is equal to the delay in branch 2:

$$\tau_B = \tau_2 - \tau_1 \tag{3}$$

- Water volume is conserved:

$$V_A + V_B = V_1 + V_2 \qquad (4)$$

- Mass flow is conserved (notice that m denotes mass flow in a heat exchanger, not a DH pipe):

$$m_A + m_B = m_1 + m_2 \qquad (5)$$

- Heat load is conserved:

$$P_A + P_B = P_1 + P_2 \qquad (6)$$

- Heat loss from the pipes is conserved:

$$Q_A + Q_B = Q_1 + Q_2 \qquad (7)$$

Finally, to obtain the equivalent network we choose

- Branch B is equal to the last part of branch 2, i.e. the part of branch 2 with $\tau > \tau_1$. This choice does not take the insulation of pipe B into account.

$$d_B = d_2 \qquad (8)$$
$$D_B = D_2 \qquad (9)$$
$$A_B = A_2 \qquad (10)$$
$$\varphi_B = \varphi_2 \qquad (11)$$

- The mass flow in branch B is equal to that in branch 2:

$$m_B = m_2 \qquad (12)$$

- The velocity in branch A equals a weighted average of the velocities in branches 1 and 2. To give priority to the branch with the bigger flow, the mass flows are used as weight factors.

$$v_A = \frac{m_1 v_1 + m_2 v_2}{m_1 + m_2} \qquad (13)$$

The choices above regarding branch B (physical dimensions and mass flow) and the velocity in branch A could have been made in other ways. But as shown in the sequel these rather simple choices make it possible to define an equivalent network.

We now derive the remaining characteristics of the equivalent network, which follow from the above definitions. From (5) and (12) follows that

$$m_A = m_1 \tag{14}$$

Generally, by assuming a perfect temperature equilibrium across the water and pipe wall, the time delay of the temperature front can be expressed by

$$\tau = \frac{\rho^w V}{m\varphi} \tag{15}$$

Combining (2) and (15), and remembering that the flow in branch A is $m_A + m_B$, gives

$$\frac{\rho^w V_A}{(m_A + m_B)\varphi_A} = \frac{\rho^w V_1}{m_1 \varphi_1} \tag{16}$$

By inserting (12) and (14), the definition of the auxiliary variable α gives

$$V_A = V_1(1+\alpha)(\varphi_A/\varphi_1) \tag{17}$$

Likewise, combining (3) and (15) gives

$$\frac{\rho^w V_B}{m_B \varphi_B} = \frac{\rho^w V_2}{m_2 \varphi_2} - \frac{\rho^w V_1}{m_1 \varphi_1} \tag{18}$$

Using (11) and (12) and the definitions of the auxiliary variables α and ψ gives

$$V_B = V_2 - V_1 \alpha \psi \tag{19}$$

Introducing the definition of the auxiliary variable γ gives

$$V_B = V_2(1 - \gamma\psi) \tag{20}$$

Because of (8), we furthermore have

$$L_B = L_2(1 - \gamma\psi) \tag{21}$$

Replacing V_B in (4) by the expression in (19) gives

$$V_A = V_1(1 + \alpha\psi) \tag{22}$$

We combine (17) and (22) and eliminate V_A to get

$$(1 + \alpha)(\varphi_A/\varphi_1) = 1 + \alpha\psi \tag{23}$$

This can be solved for φ_A, which yields

$$\varphi_A = \frac{\varphi_1 + \alpha\varphi_2}{1 + \alpha} \tag{24}$$

Generally, the velocity of the temperature front can be expressed by

$$v = \frac{\varphi m}{\rho^w A} \tag{25}$$

Combining (13) and (25), and remembering that the flow in branch A is $m_A + m_B$, gives

$$\frac{\varphi_A(m_A + m_B)}{A_A} = \frac{m_1\varphi_1 m_1/A_1 + m_2\varphi_2 m_2/A_2}{m_1 + m_2} \tag{26}$$

Substituting the expressions for φ_A and $m_A + m_B$ from (24) and (5) gives

$$\left(\frac{\varphi_1 + \alpha\varphi_2}{1 + \alpha}\right)\left(\frac{m_1 + m_2}{A_A}\right) = \frac{m_1\varphi_1 m_1/A_1 + m_2\varphi_2 m_2/A_2}{m_1 + m_2} \tag{27}$$

Using $\beta = 1 + \alpha$, this can be solved for A_A to get

$$A_A = \frac{\beta(1 + \alpha\psi)A_1 A_2}{A_2 + A_1\alpha^2\psi} \tag{28}$$

Substituting $L_A A_A$ for V_A in (22) gives

$$L_A A_A = V_1(1 + \alpha\psi) \tag{29}$$

Here, L_A can be found by inserting the expression for A_A from (28), which gives

$$L_A = \frac{V_1(1 + \alpha\psi)}{\frac{\beta(1+\alpha\psi)A_1 A_2}{A_2 + A_1\alpha^2\psi}} = L_1\frac{(1 + \alpha^2\psi A_1/A_2)}{\beta} \tag{30}$$

The inner diameter of the steel pipe can be found from the area, which results in

$$d_A = 2\sqrt{\frac{A_A}{\pi}} = 2\sqrt{\frac{\beta(1 + \alpha\psi)A_1 A_2}{(A_2 + A_1\alpha^2\psi)\pi}} \tag{31}$$

Finally, the outer diameter, D_A, of the steel pipe can be found by using the general definition of φ_A, which gives

$$\varphi_A = \frac{C_A^w}{C_A^w + C_A^p} = \frac{1}{1 + C_A^p / C_A^w} \tag{32}$$

The heat capacity per meter pipe C_A^w and C_A^p are given by

$$C_A^w = \tfrac{1}{4}\pi d_A^2 \rho^w c^w \tag{33}$$

$$C_A^p = \tfrac{1}{4}\pi (D_A^2 - d_A^2)\rho^p c^p \tag{34}$$

Inserting (33) and (34) in (32) gives

$$\varphi_A = \left(1 + \frac{(D_A^2 - d_A^2)\rho^p c^p}{d_A^2 \rho^w c^w}\right)^{-1} \tag{35}$$

This equation can be solved for D_A to give

$$D_A = d_A \sqrt{1 + \left(\frac{\rho^w c^w}{\rho^p c^p}\right)\left(\frac{1 - \varphi_A}{\varphi_A}\right)} \tag{36}$$

The results found above are summarized as follows. In order to find the length, inner diameter, time delay coefficient and outer diameter for branch A, use (30), (31), (24) and (36). Branch B is almost identical to branch 2, but with the exception of the length given in (21).

The dimensions (except for the insulation) for the equivalent network have been determined here. In the next subsection, the insulation of the equivalent pipes will be found, together with the return temperatures and heat loads in nodes A and B.

3.2   Including heat loss

To this point, the insulation of the pipes has been excluded from our calculations. In this section we shall address this aspect. When calculating the heat loss from a pipe we use the temperature at the inlet to the pipe. Since the heat loss in a pipe and the temperature drop along the pipe are small, the error introduced by using the inlet temperature is acceptable. Moreover, we will allow for different insulation thickness in the supply and return pipes.

We begin by stating that the total heat loss in the two systems should be equal, which imposes that

$$(T^s - T_G)(H_A^s + H_B^s) + (T_{AB} - T_G)H_A^r + (T_B^r - T_G)H_B^r$$
$$= (T^s - T_G)(H_1^s + H_2^s) + (T_1^r - T_G)H_1^r + (T_2^r - T_G)H_2^r \tag{37}$$

While T_A^r is the return temperature from the load in node A before mixing with the water from branch B, T_{AB} is the temperature in node A after mixing has taken place. By demanding that both networks have the same return temperature in node 0, we can use $\alpha = m_2/m_1$ and $\beta = 1 + \alpha$ to obtain

$$T_{AB} = \frac{m_A T_A^r + m_B T_B^r}{m_A + m_B} = \frac{m_1 T_1^r + m_2 T_2^r}{m_1 + m_2} = \frac{T_1^r + \alpha T_2^r}{\beta} \tag{38}$$

We choose to let the two networks have the same amount of heat loss on the supply side, which results in the following equation for the heat conductivity out of the supply pipes

$$H_A^s + H_B^s = H_1^s + H_2^s \tag{39}$$

Inserting this in (37) gives

$$(T_{AB} - T_G)H_A^r + (T_B^r - T_G)H_B^r = (T_1^r - T_G)H_1^r + (T_2^r - T_G)H_2^r \tag{40}$$

Furthermore, inserting (38) in (40) gives

$$T_B^r H_B^r = T_1^r \left(H_1^r - H_A^r/\beta\right) + T_2^r \left(H_2^r - H_A^r \alpha/\beta\right) \\ + T_G \left(H_A^r + H_B^r - H_1^r - H_2^r\right) \tag{41}$$

Now we demand that the total heat load in the equivalent network should equal the total load in the original network. This is expressed as

$$(T^s - T_A^r)m_A + (T^s - T_B^r)m_B = (T^s - T_1^r)m_1 + (T^s - T_2^r)m_2 \tag{42}$$

Since $m_A = m_1$ and $m_B = m_2$ we furthermore have

$$T_A^r = T_1^r + (T_2^r - T_B^r)(m_2/m_1) = T_1^r + (T_2^r - T_B^r)\alpha \tag{43}$$

We combine (41) and (43) and eliminate T_B^r to get

$$T_A^r H_B^r = T_1^r \left(H_A^r \alpha/\beta + H_B^r - H_1^r \alpha\right) \\ + T_2^r \left(H_A^r \alpha/\beta + H_B^r - H_2^r\right)\alpha \\ + T_G \left(H_1^r + H_2^r - H_A^r - H_B^r\right)\alpha \tag{44}$$

Introducing the auxiliary variables $\theta_A^r = H_A^r/H_1^r$, $\theta_B^r = H_B^r/H_1^r$, and $\theta_2^r = H_2^r/H_1^r$, (44) and (41) can be expressed as

$$T_A^r = T_1^r \frac{\theta_A^r \alpha/\beta + \theta_B^r - \alpha}{\theta_B^r} + T_2^r \frac{(\theta_A^r \alpha/\beta + \theta_B^r - \theta_2^r)\,\alpha}{\theta_B^r} \\ + T_G \frac{(1 + \theta_2^r - \theta_A^r - \theta_B^r)\,\alpha}{\theta_B^r} \tag{45}$$

$$T_B^r = T_1^r \frac{1 - \theta_A^r/\beta}{\theta_B^r} + T_2^r \frac{\theta_2^r - \theta_A^r \alpha/\beta}{\theta_B^r} + T_G \frac{\theta_A^r + \theta_B^r - \theta_2^r - 1}{\theta_B^r} \qquad (46)$$

Equations (45) and (46) give T_A^r and T_B^r as linear expressions in T_1^r and T_2^r with constant coefficients, which is expressed as

$$T_A^r = C_{A1}T_1^r + C_{A2}T_2^r + C_{AG}T_G \qquad (47)$$
$$T_B^r = C_{B1}T_1^r + C_{B2}T_2^r + C_{BG}T_G \qquad (48)$$

where the coefficients are defined by

$$C_{A1} = (\theta_A^r \alpha/\beta + \theta_B^r - \alpha)/\theta_B^r \qquad\qquad = -\alpha C_{B1} + 1 \qquad (49)$$
$$C_{A2} = \alpha(\theta_A^r \alpha/\beta + \theta_B^r - \theta_2^r)/\theta_B^r \qquad\quad = -\alpha C_{B2} + \alpha \qquad (50)$$
$$C_{AG} = -\alpha(\theta_A^r + \theta_B^r - \theta_2^r - 1)/\theta_B^r \qquad = -\alpha C_{BG} \qquad (51)$$
$$C_{B1} = (1 - \theta_A^r/\beta)/\theta_B^r \qquad (52)$$
$$C_{B2} = (\theta_2^r - \theta_A^r \alpha/\beta)/\theta_B^r \qquad (53)$$
$$C_{BG} = (\theta_A^r + \theta_B^r - \theta_2^r - 1)/\theta_B^r \qquad (54)$$

Now we will show that the heat loads P_A and P_B in the equivalent network in the same way can be stated as linear expressions in P_1 and P_2. The heat loads can be written as

$$P_1 = m_1(T^s - T_1^r)c^w \qquad (55)$$
$$\Rightarrow \quad T_1^r = T^s - P_1/(m_1 c^w) \qquad (56)$$
$$P_2 = m_2(T^s - T_2^r)c^w \qquad (57)$$
$$\Rightarrow \quad T_2^r = T^s - P_2/(m_2 c^w) \qquad (58)$$
$$P_B = m_B(T^s - T_B^r)c^w \qquad (59)$$

Now we take (59) and substitute T_B^r by the definition in (48). We furthermore substitute T_1^r and T_2^r found in (48) by the definition in (56) and (58), respectively. After inserting relevant C_B coefficients and re-arranging the equation we finally get

$$P_B = P_1 \frac{\alpha(1 - \theta_A^r/\beta)}{\theta_B^r} + P_2 \frac{\theta_2^r - \theta_A^r \alpha/\beta}{\theta_B^r} + P_G \frac{\theta_A^r + \theta_B^r - \theta_2^r - 1}{\theta_B^r} \qquad (60)$$

where $P_G = m_2(T^s - T_G)c^w$ is the heat load that would be delivered in node 2 if the DH water was cooled to ground temperature T_G instead of T_2^r. (Below we will assume that the coefficient to P_G in (60) is zero, and therefore P_G disappears from the formulas.)

By using the fact that the total heat load in the equivalent network should equal the total load in the original network (we insert (60) in this equality $P_A + P_B = P_1 + P_2$) we get

$$P_A = P_1 \frac{\theta_A^r \alpha/\beta + \theta_B^r - \alpha}{\theta_B^r} + P_2 \frac{\theta_A^r \alpha/\beta + \theta_B^r - \theta_2^r}{\theta_B^r} - P_G \frac{\theta_A^r + \theta_B^r - \theta_2^r - 1}{\theta_B^r} \tag{61}$$

By introducing symbols for the constant coefficients, (61) and (60) can be written respectively as

$$P_A = K_{A1}P_1 + K_{A2}P_2 + K_{AG}P_G \tag{62}$$
$$P_B = K_{B1}P_1 + K_{B2}P_2 + K_{BG}P_G \tag{63}$$

where

$$
\begin{aligned}
K_{A1} &= (\theta_A^r \alpha/\beta + \theta_B^r - \alpha)/\theta_B^r & &= C_{A1} & &= 1 - \alpha C_{B1} & &(64) \\
K_{A2} &= (\theta_A^r \alpha/\beta + \theta_B^r - \theta_2^r)/\theta_B^r & &= C_{A2}/\alpha & &= 1 - C_{B2} & &(65) \\
K_{AG} &= -(\theta_A^r + \theta_B^r - \theta_2^r - 1)/\theta_B^r & &= -C_{BG} & & & &(66) \\
K_{B1} &= (1 - \theta_A^r/\beta)\alpha/\theta_B^r & &= \alpha C_{B1} & & & &(67) \\
K_{B2} &= (\theta_2^r - \theta_A^r \alpha/\beta)/\theta_B^r & &= C_{B2} & & & &(68) \\
K_{BG} &= (\theta_A^r + \theta_B^r - \theta_2^r - 1)/\theta_B^r & &= C_{BG} & & & &(69)
\end{aligned}
$$

In the equations for C_{Xi} and K_{Xi} the symbols α, β, and θ_x^r are constant and defined from the original network as

$$\alpha = m_2/m_1 \tag{70}$$
$$\beta = 1 + \alpha \tag{71}$$
$$\theta_x^r = H_x^r/H_1^r \tag{72}$$

The fact that α is constant is the main assumption as mentioned before.

Now the problem consists of assigning values to θ_A^r and θ_B^r (or $H_A^r = \theta_A^r H_1^r$ and $H_B^r = \theta_B^r H_1^r$) so that one gets reasonable values for T_A^r, T_B^r, P_A, and P_B as defined in the above linear identities (47), (48), (62) and (63). At this point it should be noted that nodes 1 and 2 in general represent sub-trees of the DH network. To avoid to have to split a sub-tree (e.g. the sub-tree at node 1) in the original network into two equivalent sub-trees connected to nodes A and B in the equivalent network, the constant coefficients C_{Xi} and K_{Xi} should equal 1 or 0. By demanding that

$$C_{A1} = C_{B2} = K_{A1} = K_{B2} = 1 \tag{73}$$
$$C_{A2} = C_{B1} = K_{A2} = K_{B1} = 0 \tag{74}$$

the sub-tree in node 1 in the original network is simply moved to node A in the equivalent network, and likewise the sub-tree in node 2 is moved to node B.

By looking at (49)–(54) and (64)–(69) it can be shown that (73) and (74) are fulfilled if and only if

$$\theta_A^r = 1 + \alpha \qquad \Leftrightarrow \qquad H_A^r = (1 + \alpha)H_1^r \qquad (75)$$
$$\theta_B^r = \theta_2^r - \alpha \qquad \Leftrightarrow \qquad H_B^r = H_2^r - \alpha H_1^r \qquad (76)$$

Equations (75) and (76) imply that

$$\theta_A^r + \theta_B^r = \theta_2^r + 1 \qquad \Leftrightarrow \qquad H_A^r + H_B^r = H_1^r + H_2^r \qquad (77)$$

Therefore the coefficients to T_G and P_G are zero, as can be seen by combining (77) with (66) and (69), and thus we have

$$C_{AG} = C_{BG} = K_{AG} = K_{AB} = 0 \qquad (78)$$

We will now for a moment leave the return side of the DH system and address the supply side. Equation (39) gives the sum of the heat conductivities H_A^s and H_B^s for the supply pipes. To have the same formulas for the supply and the return sides, we choose to divide the heat conductivity on the supply side between branch A and B in the same ratio as on the return side. Therefore, from (75) and (76) we get

$$H_A^s = (1 + \alpha)H_1^s \qquad (79)$$
$$H_B^s = H_2^s - \alpha H_1^s \qquad (80)$$

This extra degree of freedom on the supply side as compared to the return side stems from the fact that we assume the same temperature in the supply pipes 1, 2, A, and B. By the choice made, we achieve to have $H_A^s = H_A^r$ and $H_B^s = H_B^r$ if $H_1^s = H_1^r$ and $H_2^s = H_2^r$.

Equations (75), (76), (79), and (80) give the heat conductivity of the pipes in the equivalent network. Since heat conductivity should not be negative, the supply side of the equivalent network defined above is valid only if

$$\theta_2^s \geq \alpha \quad \Leftrightarrow \quad H_2^s/H_1^s \geq m_2/m_1 \qquad (81)$$

Likewise, the return side of the equivalent network defined above is valid only if

$$\theta_2^r \geq \alpha \quad \Leftrightarrow \quad H_2^r/H_1^r \geq m_2/m_1 \qquad (82)$$

We manage the situations $\theta_2^s < \alpha$ and $\theta_2^r < \alpha$ (equivalent to $H_2^s/H_1^s < m_2/m_1$ and $H_2^r/H_1^r < m_2/m_1$) by imposing further assumptions on the original network. We start by demanding that loads and return temperatures in nodes A and B should equal loads and return temperatures in nodes 1 and 2 respectively, as was the case for $\theta^s \geq \alpha$ and $\theta^r \geq \alpha$. If we did not demand this, the equivalent network could change drastically for only minor changes in the original network. Moreover, we choose to let branch B have the same insulation thickness as branch 2. This is a natural choice, since it has been chosen earlier (see (8)–(11)) to let branch B have the same steel pipe as branch 2. These statements can be expressed by

$$P_A = P_1 \qquad\qquad P_B = P_2 \tag{83}$$

$$T_A^r = T_1^r \qquad\qquad T_B^r = T_2^r \tag{84}$$

$$h_B^r = h_2^r \qquad\qquad h_B^s = h_2^s \tag{85}$$

We start out by looking at the return branches. From (21) and (85) we find the heat conductivity for branch B, given as

$$H_B^r = H_2^r(1 - \gamma\psi) \quad \Leftrightarrow \quad \theta_B^r = \theta_2^r(1 - \gamma\psi) \tag{86}$$

Conservation of heat loss can be expressed as

$$(T_{AB} - T_G)H_A^r + (T_B^r - T_G)H_B^r = (T_1^r - T_G)H_1^r + (T_2^r - T_G)H_2^r \tag{87}$$

To simplify the formulas we introduce relative temperatures, which are defined as

$$\Delta T_1 = T_1^r - T_G \tag{88}$$

$$\Delta T_2 = T_2^r - T_G \tag{89}$$

$$\Delta T_B = T_B^r - T_G = T_2^r - T_G = \Delta T_2 \tag{90}$$

$$\Delta T_{AB} = T_{AB} - T_G = (\Delta T_1 + \alpha\Delta T_2)/\beta \tag{91}$$

These relative temperatures are inserted in (87), which results in

$$\frac{\Delta T_1 + \alpha\Delta T_2}{\beta}H_A^r + \Delta T_2 H_B^r = \Delta T_1 H_1^r + \Delta T_2 H_2^r \tag{92}$$

Equation (86) is substituted for H_B^r to find H_A^r, which results in

$$H_A^r = \frac{(\Delta T_1 H_1^r + \Delta T_2 H_2^r \gamma\psi)\beta}{\Delta T_1 + \alpha\Delta T_2} \tag{93}$$

By using $\beta = 1 + \alpha$ and $\theta_2^r = H_2^r/H_1^r$ and defining Ω by

$$\Omega = \frac{\Delta T_2}{\Delta T_1} = \frac{T_2^r - T_G}{T_1^r - T_G} \tag{94}$$

then H_A^r can be written as

$$H_A^r = \frac{(H_1^r + H_2^r \gamma\psi\Omega)(1 + \alpha)}{1 + \alpha\Omega} \quad\Leftrightarrow\quad \theta_A^r = \frac{(1 + \theta_2^r \gamma\psi\Omega)(1 + \alpha)}{1 + \alpha\Omega} \tag{95}$$

As can be seen, in excess to the hitherto main assumption that $\alpha = m_2/m_1$ is constant, we have to assume that $\Omega = (T_2^r - T_G)/(T_1^r - T_G)$ is constant, T_G being the ground temperature.

We now address the supply side of the DH system. From (21) and (85) we find the heat conductivity for branch B, given as

$$H_B^s = H_2^s(1 - \gamma\psi) \tag{96}$$

Moreover, since $H_A^s + H_B^s = H_1^s + H_2^s$ we have

$$H_A^s = H_1^s + \gamma\psi H_2^s \tag{97}$$

If we furthermore assume that $T_1^r = T_2^r$, we get the following for the supply and return sides of the equivalent network

$$H_A^s = H_1^s + \gamma\psi H_2^s \qquad\qquad H_B^s = H_2^s(1 - \gamma\psi) \tag{98}$$
$$H_A^r = H_1^r + \gamma\psi H_2^r \qquad\qquad H_B^r = H_2^r(1 - \gamma\psi) \tag{99}$$

It is seen that the heat conductivity on the supply side is divided between branch A and B in the same ratio as on the return side.

As for the assumption that $\alpha = m_2/m_1$ is constant, the new assumptions regarding T_1^r and T_2^r are never totally fulfilled in practice. Therefore, the equivalent network will not give exactly the same results as the original network, but hopefully close enough results.

For the return side, the results above can be summarized as follows:

- If $\theta_2^r \geq \alpha \Leftrightarrow H_2^r/H_1^r \geq m_2/m_1$ and we assume that $\alpha \equiv m_2/m_1$ is constant, then

$$H_A^r = (1 + \alpha)H_1^r$$
$$H_B^r = H_2^r - \alpha H_1^r$$

- If $\theta_2^r < \alpha \Leftrightarrow H_2^r/H_1^r < m_2/m_1$ and we assume that both $\alpha \equiv m_2/m_1$ and $\Omega \equiv \frac{T_2^r - T_G}{T_1^r - T_G}$ are constant, then

$$H_A^r = \frac{(H_1^r + H_2^r \gamma\psi\Omega)(1 + \alpha)}{1 + \alpha\Omega}$$
$$H_B^r = H_2^r(1 - \gamma\psi)$$

On the other hand if we assume that $\alpha \equiv m_2/m_1$ is constant, and $T_1^r = T_2^r$, then

$$H_A^r = H_1^r + \gamma\psi H_2^r$$
$$H_B^r = H_2^r(1 - \gamma\psi)$$

For the supply side the results can be summarized as follows:

- If $\theta_2^s \geq \alpha \Leftrightarrow H_2^s/H_1^s \geq m_2/m_1$ and we assume that $\alpha \equiv m_2/m_1$ is constant, then

$$H_A^s = (1 + \alpha)H_1^s$$
$$H_B^s = H_2^s - \alpha H_1^s$$

- If $\theta_2^s < \alpha \Leftrightarrow H_2^s/H_1^s < m_2/m_1$ and we assume that $\alpha \equiv m_2/m_1$ is constant, then

$$H_A^s = H_1^s + \gamma\psi H_2^s$$
$$H_B^s = H_2^s(1 - \gamma\psi)$$

4   Removing internal nodes

When a DH network consisting of many branches is converted to an equivalent network as described above, many nodes in the equivalent network will be positioned close to each other separated by relatively short pipes. Following the method described in the sequel, such nearby nodes can be collapsed to further simplify the equivalent network. The method can also be used to reduce the equivalent network to only a few or just one branch. This will of course reduce the quality of the resulting network model.

We look upon a situation as shown in Figure 3 with a short branch (branch 2) in-between branches 1 and 3. Loads may be present at both ends of branch 2 as indicated in the figure. Below a method for removing this short branch and at the same time changing branches 1 and 3 will be given. During this process the two loads are also transformed as described in the following.

Let indices 1, 2, and 3 describe the three branches in the original DH network while indices A and B describe the slightly changed replacements for branches 1 and 3 as shown in Figure 3. We will divide branch 2 in two parts and let branch A represent branch 1 and the first part of branch 2 while branch B shall represent the other part of branch 2 and branch 3.

In this section we will use μ to indicate flow in branches while m as in the previous sections indicates flow to heat exchangers. This leads to the following identities

$$m_1 = \mu_1 - \mu_2 \tag{100}$$

$$m_2 = \mu_2 - \mu_3 \tag{101}$$

Branch 2 is not divided in equal parts. Instead it is divided so that the length of the first part is $f_A L_2$ and the length of the second part is $f_B L_2$ where

$$f_A = m_2/(m_1 + m_2) \tag{102}$$

$$f_B = m_1/(m_1 + m_2) = 1 - f_A \tag{103}$$

By defining factors f_A and f_B in this way, the larger part of branch 2 is included in branch B if load 1 is much bigger than load 2, and therefore in this case branch A will be almost identical to branch 1.

The load (or more correctly flow to the heat exchanger) in node 1 is split in two parts. Symbols g_{AA} and g_{AB} indicate the fractions of the load that are moved to the first and to the last end of branch A. Likewise, g_{BA} and g_{BB} indicate the fractions of the load in node 2 that are moved to the first and to the last end of branch B. Figure 3 shows how the g–factors are used. We choose to use time delay τ to define the g–factors

$$g_{AA} = \frac{f_A \tau_2}{\tau_1 + f_A \tau_2} \qquad\qquad g_{AB} = \frac{\tau_1}{\tau_1 + f_A \tau_2} \tag{104}$$

$$g_{BB} = \frac{f_B \tau_2}{\tau_3 + f_B \tau_2} \qquad\qquad g_{BA} = \frac{\tau_3}{\tau_3 + f_B \tau_2} \tag{105}$$

By defining the g–factors in this way, the major part of the load is moved to the closest node in the simplified network. It is readily seen that

$$g_{AA} + g_{AB} = g_{BB} + g_{BA} = 1 \tag{106}$$

The flow in branches A and B can be expressed by

$$\mu_A = \mu_1 - g_{AA} m_1 \tag{107}$$

$$\mu_B = \mu_2 - g_{BA} m_2 \tag{108}$$
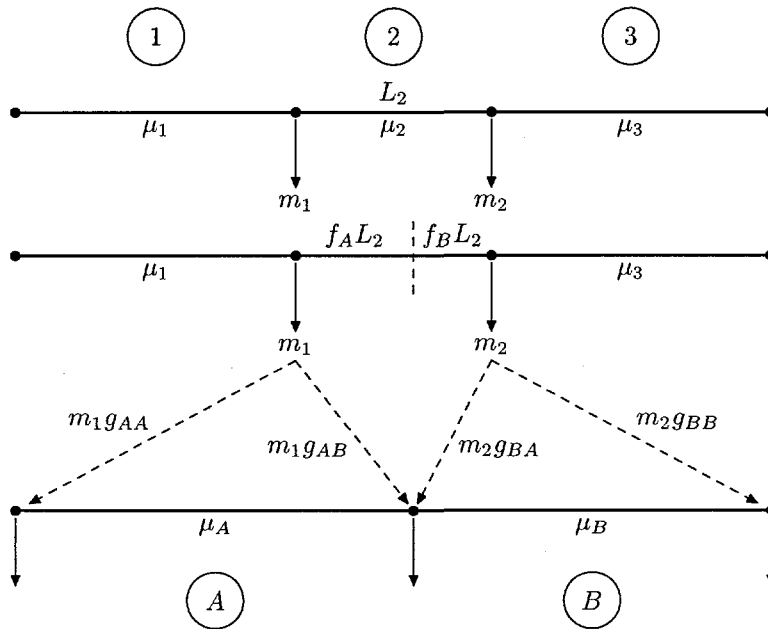
Figure 3: Collapsing nodes

To find branch A from the data describing branches 1 and 2, and branch B from the data describing branches 2 and 3, we demand that total length, time delay, and heat loss should be preserved. It can be shown that this leads to preservation of the total water volume, too.

First we will look at branch A. The preservation of length can be expressed

$$L_A = L_1 + f_A L_2 \tag{109}$$

Generally, time delay in a branch is given by

$$\tau = \frac{\rho^w V}{\mu \varphi} \tag{110}$$

Then preservation of time delay can be expressed as

$$\tau_A = \tau_1 + f_A \tau_2 \quad \Leftrightarrow \quad \frac{V_A}{\mu_A \varphi_A} = \frac{V_1}{\mu_1 \varphi_1} + \frac{f_A V_2}{\mu_2 \varphi_2} \tag{111}$$

$$\Leftrightarrow \quad V_A = V_1 \frac{\mu_A}{\mu_1} \frac{\varphi_A}{\varphi_1} + f_A V_2 \frac{\mu_A}{\mu_2} \frac{\varphi_A}{\varphi_2} \tag{112}$$

Except for φ_A, all variables on the right side of (112) are known. To find φ_A, the general expression for φ is used

$$\varphi = \frac{C^w}{C^w + C^p} = \frac{1}{1 + C^p/C^w} = \frac{1}{1 + XV^p/V} \tag{113}$$

where $X = \frac{\rho^p c^p}{\rho^w c^w}$.

Inspired by (113), we use the following expression for φ_A

$$\varphi_A = \frac{1}{1 + X \frac{V_1^p + f_A V_2^p}{V_1 + f_A V_2}} \tag{114}$$

Now by inserting (114) in (112) it is possible to find V_A. The resulting expression for V_A will not be given here.

By using (113) for branch A we get

$$\varphi_A = \frac{1}{1 + X V_A^p / V_A} \tag{115}$$

which can be reformulated as

$$V_A^p = V_A \frac{1 - \varphi_A}{\varphi_A X} \tag{116}$$

From V_A and V_A^p the inner and outer diameters of the steel pipe are readily found, resulting in

$$d_A = 2\sqrt{\frac{V_A}{\pi L_A}} \qquad\qquad D_A = 2\sqrt{\frac{V_A + V_A^p}{\pi L_A}} \tag{117}$$

Assuming constant temperature, preservation of heat loss is expressed by

$$h_A = \frac{h_1 L_1 + f_A h_2 L_2}{L_A} \tag{118}$$

In this section we will not distinguish between specific heat conductivities h^s and h^r. Therefore, the expressions for h_A and h_B can be used for the supply side as well as the return side.

Now the length, the inner and outer diameter of the steel pipe, and the heat loss coefficient have been found for branch A. In a similar way these data can also be found for branch B. The result is summarized by the following procedure.

Assume that we have an original network described by the following data:

- Branch 1: d_1, D_1, L_1, h_1, and μ_1.

- Branch 2: d_2, D_2, L_2, h_2, and μ_2.

- Branch 3: d_3, D_3, L_3, h_3, and μ_3.

Then first calculate

$$V_1 = \tfrac{1}{4}\pi L_1 d_1^2 \qquad V_2 = \tfrac{1}{4}\pi L_2 d_2^2 \qquad V_3 = \tfrac{1}{4}\pi L_3 d_3^2$$

$$V_1^p = \tfrac{1}{4}\pi L_1 D_1^2 - V_1 \qquad V_2^p = \tfrac{1}{4}\pi L_2 D_2^2 - V_2 \qquad V_3^p = \tfrac{1}{4}\pi L_3 D_3^2 - V_3$$

$$\varphi_1 = \frac{1}{1 + X V_1^p / V_1} \qquad \varphi_2 = \frac{1}{1 + X V_2^p / V_2} \qquad \varphi_3 = \frac{1}{1 + X V_3^p / V_3}$$

$$\tau_1 = \rho^w V_1 / (\mu_1 \varphi_1) \qquad \tau_2 = \rho^w V_2 / (\mu_2 \varphi_2) \qquad \tau_3 = \rho^w V_3 / (\mu_3 \varphi_3)$$

where

$$X = \frac{\rho^p c^p}{\rho^w c^w}$$

and then calculate

$$m_1 = \mu_1 - \mu_2 \qquad m_2 = \mu_2 - \mu_3$$

$$f_A = m_2 / (m_1 + m_2) \qquad f_B = m_1 / (m_1 + m_2)$$

$$g_{AA} = \frac{f_A \tau_2}{\tau_1 + f_A \tau_2} \qquad g_{BA} = \frac{\tau_3}{\tau_3 + f_B \tau_2}$$

$$\mu_A = \mu_1 - g_{AA} m_1 \qquad \mu_B = \mu_2 - g_{BA} m_2$$

Then branches A and B are defined by

$$L_A = L_1 + f_A L_2 \qquad L_B = L_3 + f_B L_2$$

$$\varphi_A = \left(1 + X \frac{V_1^p + f_A V_2^p}{V_1 + f_A V_2}\right)^{-1} \qquad \varphi_B = \left(1 + X \frac{V_3^p + f_B V_2^p}{V_3 + f_B V_2}\right)^{-1}$$

$$V_A = V_1 \frac{\mu_A}{\mu_1} \frac{\varphi_A}{\varphi_1} + f_A V_2 \frac{\mu_A}{\mu_2} \frac{\varphi_A}{\varphi_2} \qquad V_B = V_3 \frac{\mu_B}{\mu_3} \frac{\varphi_B}{\varphi_3} + f_B V_2 \frac{\mu_B}{\mu_2} \frac{\varphi_B}{\varphi_2}$$

$$V_A^p = V_A \frac{1 - \varphi_A}{\varphi_A X} \qquad V_B^p = V_B \frac{1 - \varphi_B}{\varphi_B X}$$

$$d_A = 2 \sqrt{\frac{V_A}{\pi L_A}} \qquad d_B = 2 \sqrt{\frac{V_B}{\pi L_B}}$$

$$D_A = 2 \sqrt{\frac{V_A + V_A^p}{\pi L_A}} \qquad D_B = 2 \sqrt{\frac{V_B + V_B^p}{\pi L_B}}$$

$$h_A = \frac{h_1 L_1 + f_A h_2 L_2}{L_A} \qquad h_B = \frac{h_3 L_3 + f_B h_2 L_2}{L_B}$$

Before choosing the above method for removing short branches, several alternative methods have been examined. These alternatives describe a gradual refinement that leads to the one described above, see Pálsson et al. (1999).
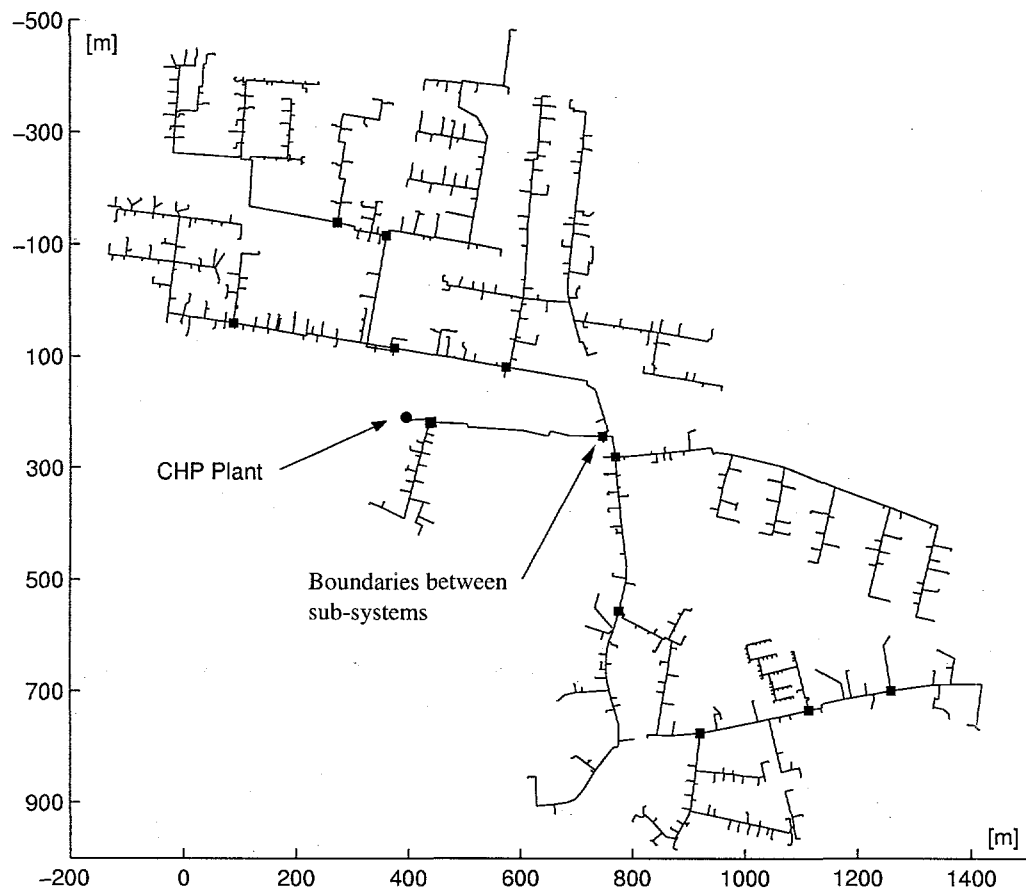
Figure 4: The Hvalsø district heating system

5   Results from a case study

5.1   The DH system

The district heating system in this case study is the system in Hvalsø, which is a small town located in the center of Zealand in Denmark. The DH system consisting of pre-insulated pipes has no loops, i.e. it is a pure tree structure as shown in Figure 4, and is modeled all the way out to the individual consumers.

The system is characterized by the following:
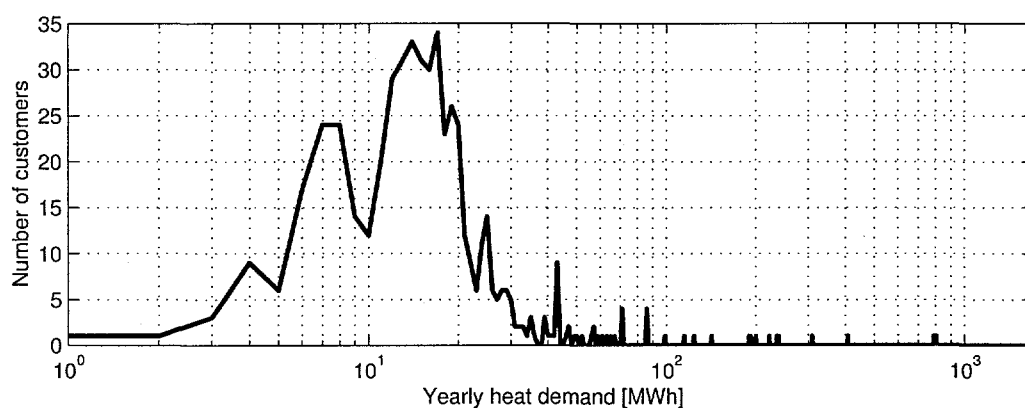
Figure 5: Frequency diagram showing the distribution between various yearly heat demands for consumers in Hvalsø

Number of consumers	535	
Yearly heat consumption	14.95	GWh
Maximum heat production	9.6	MW
Number of DH branches	1079	
Total length of DH branches	20.2	km
Number of pipe dimensions	32	

Most consumers live in single family houses, but some large consumers exist as Figure 5 shows.

5.2 Models of the DH system

To verify the accuracy of the method for creating equivalent systems, several models of the Hvalsø DH system were made and compared by simulations. The following systems have been modeled and simulated by the method described in Pálsson et al. (1999):

A The original system with 535 loads and 1079 branches. A pure tree structure (see Figure 4).

B An equivalent system with all 535 loads and 1079 branches – but no side branches.

C1 to C12 Reduced equivalent systems created by removing the shorter branches of model B. Systems with 500, 200, 100, 50, 25, 12, 6, 5, 4, 3, 2, and 1 branch are modeled.

Figure 6: Total heat load at the plant and for the consumers, when the supply temperature is changed suddenly at the plant.

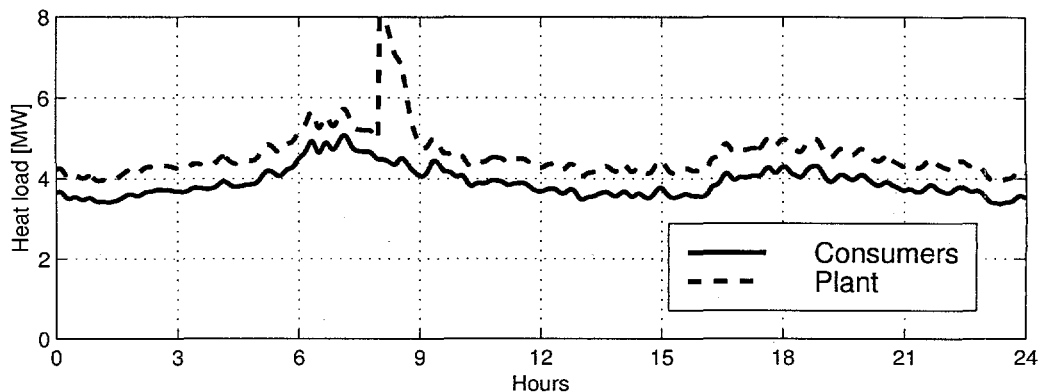**D1 to D3** An equivalent system generated by dividing the original system in model A into 24 sub-systems (see the dots in Figure 4 which determine the subsystems boundaries) each of which is then transformed to a structure with no side branches and subsequently reduced to 10, 5, and 1 branch (or nodes).

5.3   Simulations

Since no measurements are available at the individual consumers, except for the annual heat consumption (this is the normal situation for many DH systems in Denmark), simulations of the equivalent systems are compared to a simulation of the full original system.

The simulations cover a period of 24 hours with a time step of 2 minutes. Time series for the 535 heat loads are calculated by scaling a measured time series of the total load at the plant with the yearly loads at each consumer. If for instance the yearly load at a consumer amounts to 1% of the total yearly load, this consumer is assigned 1% of the measured time series. In this way all heat loads in the simulations vary proportionally. However, because of time delays in the DH system, the loads do not vary proportionally as 'seen' from the plant. Moreover, tests have shown that the results are only slightly changed if the loads at one third of the consumers are delayed by one hour, and another third is delayed by two hours. Figure 6 shows the total customer heat load, as well as the load at the plant. The peak at the plant is due to a sudden change in supply temperature as described below.

In all simulations, the supply temperature from the plant is constant 80 °C, and then 8 hours after starting the simulations it is suddenly raised
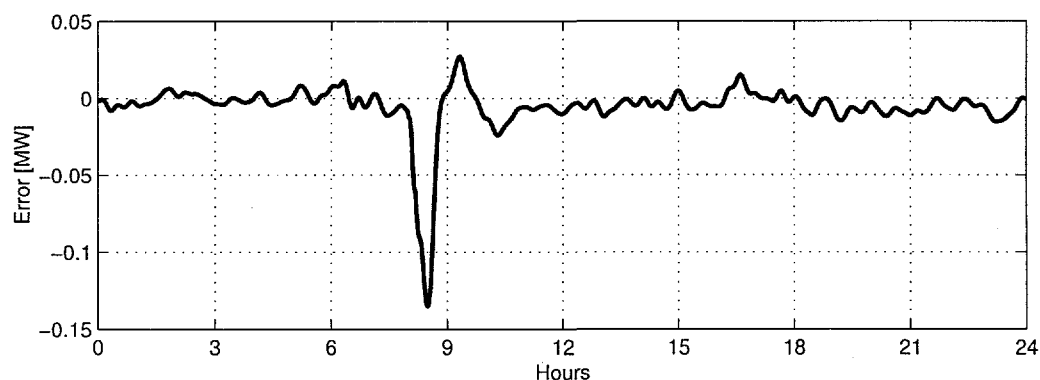
Figure 7: Heat production difference for the full equivalent system (model B) as compared to the original system (model A)

to 100 °C, which results in the peak in Figure 6. The criteria which is used in the sequel for computing error is the standard deviation of error in energy flow from the plant.

The result for the original system (model A above), when subject to a sudden increase of the supply temperature from the plant, is shown in Figure 6. It can be seen that the load at the plant rises suddenly when the temperature is raised from 80 °C to 100 °C, and then decreases when the systems becomes stable again.

The same simulation has been performed for an equivalent system (model B above) with no branches removed. Figure 7 shows the difference in heat production from the simulations with models A and B.

Similar simulations have been performed for models C1 to C12 and models D1 to D3 mentioned above. The results are summarized in Figure 8, which shows the standard deviation of error in heat production, as compared to a simulation of the original system.

In Figure 8 the curve indicated by "Models B and C1 to C12" shows the situation, as the number of branches is gradually reduced. The other curve indicated by "Models D1 to D3" shows the situation when the original system is divided into 24 sub-areas, as shown in Figure 4. For each of these sub-areas an equivalent system is found and then short branches are removed, so that each sub-model has no more than 10 (model D1), 5 (model D2), and 1 branches (model D3). This results in 201, 108, and 24 branches respectively.

It should be noted that the error in Figure 8 is slightly decreasing when moving from model C1 to C6. This can be explained by numerical errors in the simulation model, which can give problems for very short pipes like in model B and C1. See Pálsson (1997) for a discussion about these numerical
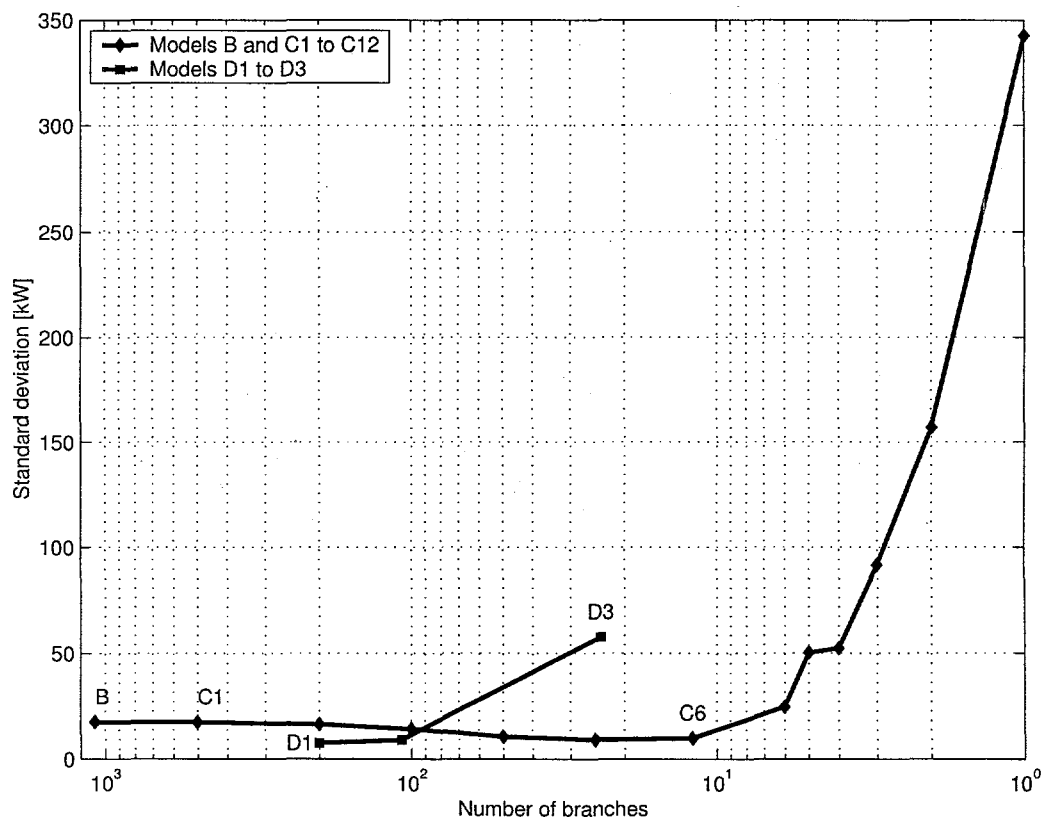
Figure 8: Standard deviation of error in heat production for models B, C1 to C12, and D1 to D3 as compared to model A (the original system)

errors.

Figure 8 shows that the number of branches in the equivalent model can be reduced to approximately 10 branches without affecting the accuracy. If more branches are removed the error increases more significantly. Since the original system has 1079 branches, the number of branches – and therefore the computational time for a simulation – can be reduced to approximately 1%. Also for the sub-areas, the equivalent systems should not be reduced to less than 5–10 branches in each sub-area.

Such substantial reduction of the network structure has important consequences for the calculation time spent on the simulations. In the simulation method applied, see Pálsson et al. (1999), the calculation time is linearly dependent on the number of nodes (or branches), and hence a reduction of the number of nodes by e.g. 99% will imply almost 99% reduction in calculation time. If this reduction can be obtained without a substantial loss of accuracy, as indicated in the case study, the method of network aggregation has clearly some practical applicability. In particular, such reduction in computation time is convenient for application in daily scheduling of heat production in the DH and power companies.

6 Discussion and conclusions

The paper presents a method for reducing a complete description of a DH network into a simple one, and still preserving the most important physical properties of the network. Thus, a simple network description is sought, which is nearly equivalent to the original one.

When finding an equivalent network, the complexity of the DH network is reduced by gradually changing the tree structure into a chain structure with no branches. Correspondingly the various parameters which define the branches are transformed from the real network to equivalent parameters in the corresponding equivalent network.

Two main assumptions are made to be able to define the equivalent network mathematically. All mass flows are assumed to vary proportionally, i.e. there is a constant ratio between mass flows. Moreover, it is assumed that the return temperatures on the primary side of all heat exchangers are equal. Naturally, the assumptions are never fulfilled in practice. This means that the equivalent network will not give exactly the same results as the original network, but as the tests show, results are close to the original network.

The equivalent network is reduced further by observing that many nodes in this network are positioned close to each other separated by short pipes. Such nearby nodes are collapsed to simplify the equivalent network. This

procedure can be continued until very few pipes remain. The last pipes removed in the procedure are not necessarily short, but the resulting network could still be useful for some simulations.

It is shown in this paper that the method for aggregating a complex DH network with no loops gives a very good approximation to the original network. The approximation is good even if the very strong assumptions are not fulfilled regarding a constant ratio between mass flows and equal return temperatures at all consumers.

The equivalent DH network is tested by simulating a case study, using the original network as well as the equivalent networks. It is shown that the heat production at the plant as calculated for the equivalent network is very close to the production in the original network.

It is also shown in the case study that the number of branches in the original network can be reduced from 1079 to approximately 10 branches without affecting the accuracy. Computational effort in simulations is proportional to the number of branches, and thus the computational time in this case is reduced by approximately 99%.

Since the results of the comparisons in the case study are based on some simplifications, one should expect to get higher errors than shown in Figure 7, if consumer data are available and can be used for comparisons. But the main conclusion as shown in Figure 8 is still expected to hold for large systems similar to the case study.

The heat production at the plant appears to be sufficiently accurate and therefore simplified models could be used in simulation and optimization of a DH system. Such systems could e.g. include a CHP plant where the heat demand is an important parameter and where computational costs might be of concern.

References

Benonysson, A. (1991). *Dynamic Modelling and Operational Optimization of District Heating Systems*. PhD thesis, Laboratory of Heating and Air Conditioning, Technical University of Denmark.

Benonysson, A., Bøhm, B., and Ravn, H. F. (1995). Operational optimization in a district heating system. *Energy Conversion and Management*, 36(5):297–314.

Hansson, T. (1990). Driftsoptimering af fjernvarmeværker. Master's thesis, Danmarks Tekniske Højskole. Laboratoriet for Varme- og Klimateknik.

Holman, J. P. (1989). *Heat Transfer*. McGraw-Hill Book Company, Singapore.

Horlock, J. H. (1987). *Cogeneration - Combined Heat and Power (CHP), Thermodynamics and Economics*. Pergamon, Oxford.

Pálsson, H. (1997). Analysis of numerical methods for simulating temperature dynamics in district heating pipes. In Pálsson, Ó. P., editor, *6th International Symposium on District Heating and Cooling Simulation*, Reykjavik, Iceland. ISBN 9979-54-203-9.

Pálsson, H., Larsen, H. V., Bøhm, B., Ravn, H. F., and Zhou, J. (1999). Equivalent models of district heating systems. Technical report, Department of Energy Engineering, Technical Univerity of Denmark.

Pálsson, Ó. P. (1993). *Stochastic Modeling, Control and Optimization of District Heating Systems*. PhD thesis, Technical University of Denmark.

Pálsson, H., Larsen, H., Bøhm, B., Ravn, H. F., and Zhou, J. (1999). Equivalent models of district heating systems. Technical report, Department of Energy Engineering, Technical University of Denmark.

Zhao, H. (1995). *Analysis, Modelling and Operational Optimization of District Heating Systems*. PhD thesis, Laboratory of Heating and Air Conditioning, Technical University of Denmark.

Zhao, H., Bøhm, B., and Ravn, H. F. (1994). Operational optimization of district heating (DH) systems – using a DH network as a heat storage. In Kangas, M. and Lund, P., editors, *CALORSTOCK '94, 6th Int. Conference on Thermal Energy Storage*, pages 459–467, Espoo, Finland.

Zhao, H. and Holst, J. (1997). Study on network aggregation in DH systems. In Pálsson, Ó. P., editor, *6th International Symposium on District Heating and Cooling Simulation*, Reykjavik, Iceland. ISBN 9979-54-203-9.

Appendix D:
Optimizing the Use of Heat Storage in an Engine-based CHP Plant

Halldór Pálsson*

Abstract

For the last five years or so, a trend has been towards establishment of small decentralized combined heat and power (CHP) plants in Denmark, which provide district heating (DH) to local and relatively small urban areas. In order to optimize the operation of such a plant, a plant operator has to produce power at time intervals where the price is high, but he also has to fulfill the heat demand from DH customers. In many cases, particularly when using piston engines, the ratio between heat and power production is fixed, but by installing a heat storage this ratio can be relaxed.

The purpose of this study is to present a solution method for operational optimization of a simple CHP plant, with focus on utilization of an installed heat storage. This operational optimization is performed by using stochastic discrete dynamic programming, and thus taking the stochastic nature of the heat load into account. It is shown that this problem can be solved quite efficiently and finally the method is tested on a real case study.

---

*Systems Analysis Department, Risø National Laboratory, DK-4000 Roskilde, Denmark

Nomenclature

Variables

D	Storage diameter	t	Time
F	Cost to go function	u	Operational state
T	Water temperature	w	Stochastic variable
Q	DH heat-load	x	Relative storage contents
a	Autoregressive model parameter	ϕ	Operational strategy function
c_p	Specific heat of water	ρ	Water density
f	Trigonometric model parameter	σ	Standard deviation
g	Gas usage		
h	Storage height	*Subscripts*	
k	Heat loss coefficient	e	Engine
p	Power production	b	Boiler
q	Heat production	p	Power
r	Cost per time interval	q	Heat
		t	Time

1   Introduction

The importance of combined heat and power production (CHP) in existing power systems has become more evident in recent years. The main reason for this is the high thermal efficiency of plants producing both heat and electric power, compared to the conventional power-only plants. The residual heat from the production process in CHP plants is typically utilized for either industrial usage or district heating (DH), which is mainly the case in Denmark. This utilization results in thermal efficiency of about 85–90%, whereas the efficiency of conventional power-plants is about 40%. In Denmark, a trend has been towards small decentralized CHP plants for the last five years or so. These plants typically produce in the range 1–10 MW power and provide DH to local, and in most cases, relatively small urban areas.

The fact that the price of electric power varies, depending on the time of day and the current weekday, poses a problem for the plant operator. He must fulfill the heat demand, but at the same time try to produce when the price for power is high. This dilemma can be partly avoided by connecting a heat storage to the CHP plant. The storage is then used to store excess heat when power production is profitable, and to supply heat to the DH customers when the power price is low. Therefore the operator faces an optimization problem, which is to determine when to operate the CHP plant, taking into account the storage contents and the uncertain future heat-load. We refer to this as a stochastic heat storage problem.

Aspects of the heat storage problem have been studied and solved in

many different ways. Most of the work has been done by using deterministic optimization procedures, such as general nonlinear programming [11], mixed-integer linear programming [10] and dynamic programming [8], [4]. When considering stochastic optimization, the problem has been solved by using the so-called progressive hedging algorithm [7] and dynamic programming [5].

In this paper we pose and solve the stochastic heat storage problem, using a simple model of a small CHP plant as a reference. The optimization is performed by using a stochastic discrete dynamic programming method, where found control decisions are represented by boolean variables. This boolean structure determines which units should be operated at each time interval in the operational horizon. In most cases each unit is operated at the same level when running, which makes it sufficient to decide only if we produce in the time interval, but not how much.

The paper is organized as follows. In section 2 we present a simple mathematical model of a CHP plant, including CHP units, boilers and a single heat storage. The model results provide the operational cost of the units, based on both fixed and time varying prices. In section 3, models for the uncertain, and thus stochastic, heat-load are presented and discussed. The resulting heat-load predictions are used as an input in the optimization procedure. In Section 4 we describe an optimization approach, which can be used for solving the stochastic optimization problem efficiently. In Section 5 we perform operational optimization, using a real-life CHP plant as a case study. Finally, in Section 6, we discuss the results and draw conclusions.

2 Modeling a CHP plant

In this section we present a simple mathematical model of a CHP plant, consisting of pure CHP units with fixed heat/power ratios, heat-only boilers and a single heat storage unit. No attempt is made to model plant thermodynamics in detail and we refer to [3] for a detailed theoretical discussion of both thermodynamics and economics of general CHP plants.

2.1 General remarks about production units

Different types of CHP units are often divided into two classes: (i) Extraction units and (ii) Back-pressure units. The extraction units possess the ability to adjust the ratio between heat and power production, whereas the back-pressure units must produce at a fixed ratio. Frequently, units in class (i) are large and centralized with the obligation to fulfill the demand of power

as well as heat.

On the other hand, when considering rather small decentralized CHP plants, some aspects of the production characteristics change. The small size implies that power production on a large-scale network can be considered *stiff*, which means that the individual plant has no real effect on the power-network load and does not take part in regulating the total power production. Another characteristic is that the main priority for the plant operator is to fulfill the heat demand, which literally makes power a secondary product.

In many cases, particularly in Denmark, the CHP units consist of ordinary piston engines, driven by natural gas. The main advantages of using piston engines are the high operational efficiency along with relatively low startup costs. Each engine is connected mechanically to a power generator, but the heat is extracted from the cooling water, lubrication oil and most importantly, the exhaust gas. The direct connection to a generator requires that the engine have a constant rotation speed in order to conform to the power-network frequency, which consequently suggests that the energy production is fixed to ensure maximum efficiency of the engine. Thus if we omit the startup costs, which are the result of warming the engine up to operational temperature, we must only decide if we produce or not.

Many decentralized CHP plants are furthermore equipped with one or more heat-only boilers. The main function of these is to provide heat in case of high heat-load as well as in breakdown situations. If these units are kept warm, startup costs are generally low and are therefore disregarded in this study. Thus, the operation of a boiler is determined in the same manner as in the engine case, only with different cost structure.

2.2   The heat storage

A typical heat storage unit is in the form of a tank, filled with DH water, see Figure 1. The supply and return water is loaded/unloaded respectively through the top and bottom of the storage, which in turns generates a thermal layer between the supply and return water. This thermal layer should be as thin as possible to maximize the efficiency of the storage, but the thickness depends on the inflow conditions as well as how the storage is used.

The effect of the thermal layer thickness will not be considered here, which leads to the assumption of a clean boundary between supply and return water. The heat loss l from the storage can be estimated by calculating the heat
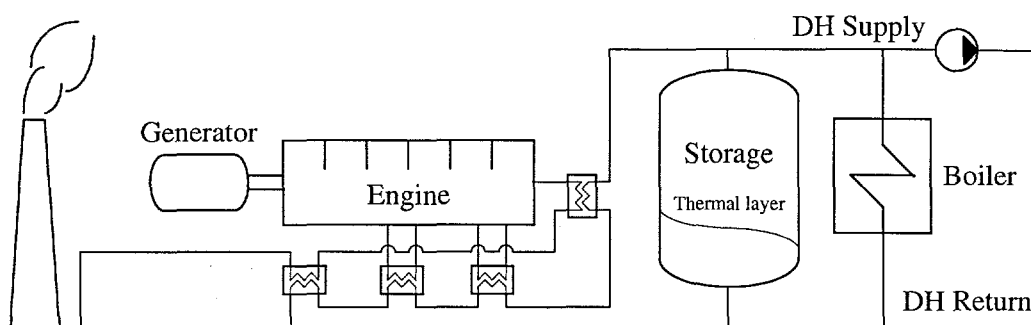
Figure 1: A CHP plant with a thermal storage and one engine

flow through the wall, top and bottom, which results in

$$l_{\text{wall}} = k_w \pi D \big(x(T_s - T_o) + (1 - x)(T_r - T_o) \big) h \tag{1}$$

$$l_{\text{top}} = k_t \pi D^2 (T_s - T_o)/4 \tag{2}$$

$$l_{\text{bottom}} = k_b \pi D^2 (T_r - T_o)/4 \tag{3}$$

where k is the thermal conductivity, h and D are the height and diameter of the storage, T is temperature (s supply, r return, o environment) and x is the relative position of the thermal layer in the storage, which satisfies $0 \le x \le 1$.

2.3 A plant operation model

In the current work, we will consider a simple plant consisting of production units and one storage tank, as shown in Figure 1. When operated, the units produce at full capacity with constant efficiency, thus disregarding the lower efficiency at startup.

If we disregard the heat production, the cost of operating the engine is mainly related to the gas usage, as well as the produced power in a negative perspective. The boiler on the other hand has only positive cost, representing the gas usage, and thus the total operating cost at a given time interval t is

$$R(t) = \underbrace{r_g g_e u_e - r_p(t) p_e u_e - r_q q_e u_e}_{\text{engine}} + \underbrace{r_g g_b u_b - r_q q_b u_b}_{\text{boiler}} \tag{4}$$

where r, g, p and q are cost, gas usage, power production and heat production per interval, respectively. The control decision u is a boolean value in both cases for engine and boiler.

The dynamic changes in the heat storage during one time interval are dependent on the production, the heat-load and to some minor extent, heat

losses from the storage. Here it is convenient to use the variable x which denotes the relative energy contained in the storage, such that $0 \le x \le 1$. This is in particular the relative height of the thermal layer in the storage, shown in Figure 1. Introducing scaling variables α and β, we write an equation for the storage dynamics

$$x(t+1) = (1-\alpha)x(t) + \beta + q_b u_b(t) + q_e u_e(t) - Q(t) \tag{5}$$

where Q is the DH heat-load and

$$\alpha = \frac{4k_w \Delta t}{\rho c_p D} \tag{6}$$

$$\beta = \frac{\Delta t}{\rho c_p} \left(\frac{k_t}{h} \left(\frac{T_s - T_0}{T_s - T_r} \right) + \left(\frac{k_b}{h} + \frac{4k_w}{D} \right) \left(\frac{T_r - T_0}{T_s - T_r} \right) \right) \tag{7}$$

To summarize the results above, we can state the following problem. Minimize, by choice of production $u(t)$ at each hour t over the coming week, the expected cost (operating cost minus income from sold power), subject to operating constraints on the plant and storage, and given that heat demand in each time step is satisfied. In the next section we discuss the stochastic heat demand.

3   Modeling the stochastic heat load

A fundamental element in a complete dynamic model of a decentralized CHP plant is the heat-load in the DH-network connected to the plant. There are two main things affecting time dependent changes, or dynamics, of the heat-load:

- House heating, which depends on e.g. the outdoor temperature, solar radiation and wind speed.

- Hot tap water usage, which is dependent on the behavior of the local inhabitants connected to the DH-network.

In our work, we must consider the future heat-load and thus make predictions with some reasonable accuracy, in order to choose an optimal operation strategy for the plant. These predictions must extend over a suitable time-horizon, so that the storage of heat can be planned with maximal utilization of the storage.

Stochastic modeling of heat-loads in DH systems has been studied extensively, see e.g. [9]. Most of the work has been focused on determining

the heat-load with the aid of known outdoor temperature (or predictions of temperature). This has for example resulted in black box models of the type: Autoregressive Moving Average with extraneous input (ARMAX) (see e.g. [6] for reference), with time dependent model parameters.

In [2], a model for long term prediction of heat-load is given. This model involves an ARMAX model with seasonal terms, plus time dependent harmonic functions, where the input is the outdoor temperature. However, in this study we consider the case where the outdoor temperature is unknown and consequently the only way to estimate the heat-load is to use old measured values of heat-load.

By analyzing the heat-load data from Hvalsø, we come to the conclusion that the following model is sufficient to describe the heat-load Q as a stochastic process

$$Q(t) = a_1 Q(t-1) + b_1 Q(t-24) + b_2 Q(t-25)$$
$$+ f_0 + f_1 \cos(\tfrac{\pi t}{12}) + f_2 \sin(\tfrac{\pi t}{12}) + f_3 \cos(\tfrac{\pi t}{6}) + f_4 \sin(\tfrac{\pi t}{6}) + e(t) \quad (8)$$

where e is the error between actual and predicted output and a, b and f are parameters to be estimated.

Given measured data for Q, it is possible to estimate the parameters once and use them for prediction. Another approach, which is used in [2], is to use recursive estimation of parameters. This approach ensures that if the dynamic properties of the heat-load change, the parameters will follow. In this study we only use the former approach.

4 The optimization method

In this section, we derive an optimization method which can be used to solve the problem posed in section 2, taking the stochastic heat-load from section 3 into account.

4.1 Dynamic programming

We use the so-called dynamic programming method, which is described e.g. in [1]. A general definition of this method, when applied to the present problem, can be written as

$$\max_{\mathbf{u}} \left\{ \sum_{t=0}^{N-1} r_t(x_t, u_t) + r_N(x_N) \right\} \quad (9)$$

subject to,

$$x_{t+1} = d_t(x_t, u_t) \tag{10}$$

$$0 \le x_t \le 1 \tag{11}$$

$$u_t \in \{0, 1\} \tag{12}$$

Here, $\mathbf{u} = [u_0, u_1, \ldots, u_{N-1}]$, and the function $d_t(x_t, u_t)$ corresponds to the definition in (5). Furthermore, x_t denotes the contents of the storage at the beginning of time t, N is the total number of periods, r_N is a given cost function which evaluates the final content of the storage, and r_t is the cost of production over period t.

The problem above can be rewritten such that instead of solving the whole optimization problem, we solve a small problem at each time-step, which conforms to the Bellman optimality principle. The steps of this separation method are given as follows:

1. Define $F_N(x_N) = r_N(x_N)$

2. Then for $t = N - 1, N - 2, \ldots, 0$ let

$$F_t(x_t) = \max_{u_t}\{r_t(x_t, u_t) + F_{t+1}(d_t(x_t, u_t))\} \tag{13}$$

$$\phi_t(x_t) = u_t^*(x_t) \tag{14}$$

    where the cost-to-go function $F_{t+1}(d_t(x_t, u_t))$ must be defined in each step and u_t^* is the optimum obtained from (13).

3. At this step, x_0 is typically supplied as present storage contents and then finally for $t = 0, 1, \ldots, N - 1$ let

$$u_t^* = \phi_t(x_t^*) \tag{15}$$

$$x_{t+1}^* = d_t(x_t^*, u_t^*) \tag{16}$$

Now u_t^* contains the optimum strategy at time t, which forms a total of $N - 1$ decision variables. The real strength of the dynamic programming method is that this solution can be obtained with computational complexity $O(N)$, with respect to N.

Another strength of the method is that if x_t changes at t, we still have information about u^* given in the strategy function $\phi_t(x_t)$. This is important in the present work, because the heat-load is stochastic and thus x^* is not known. We now proceed with an implementation of a stochastic problem, suitable to this study.

4.2 Current implementation of dynamic programming

We start by looking at the term "stochastic dynamics", which in turns means that the dynamic function $d_t(x_t, u_t)$ is exchanged for $d_t(x_t, u_t, w_t)$, where w_t is a stochastic variable with probability density function $f(w)$. As a consequence, we should substitute $\max_u\{\dots\}$ in (9) with $\max_u\{E[\dots]\}$, where $E[\dots]$ denotes the expected value of a stochastic variable.

Now, since the solution (15) is given on feed-back form depending on storage content x_t, the consequences of the realization of stochastic variables $w_0, w_1, \dots, w_{t-1}$ are already foreseen, i.e., the solution need not be recomputed at time t.

We define the optimization problem by using (4) and (5), but with the stochastic part of Q_t extracted and represented by w_t. Furthermore we use a simplified form of these two equations, which without loss of generality assumes only one production unit. This results in

$$\max_u \left\{ E\left[\sum_{t=0}^{N-1} \bigl(r_p(t)u_t + r_d(t)u_t - r_g(t)u_t\bigr) \right] \right\} \tag{17}$$

where p, d and g denote power, DH and gas, respectively, subject to

$$x_{t+1} = sx_t + pu_t - q_t - w(t) \tag{18}$$

$$0 \leq x_t \leq 1 \tag{19}$$

where $x_t \in \mathbb{R}$, $u_t \in \{0, 1\}$ and $w_t \in N(0, \sigma_t^2)$. Here we also define $s = 1 - \alpha$ and $q_t = Q_t - \beta$. The application of stochastic dynamic programming leads to the following procedure:

1. Define $F(x_N)_N = 0$, $F : R \to R$.

2. For $t = N - 1, N - 2, \dots, 0$, let

$$F_t(x_t) = \max_{u_t} \left\{ E\left[r_t u_t + F_{t+1}\bigl(sx_t + pu_t - q_t - w(t)\bigr) \right] \right\} \tag{20}$$

$$\phi_t(x_t) = u_t^*(x_t) \tag{21}$$

To proceed we compute the expected value of a function of a stochastic variable, $E[h(w)]$. By definition we have

$$E[h(w)] = \int_{-\infty}^{\infty} h(w) f_w(w)\, dw \tag{22}$$

where $f_w(w)$ is the probability density function of w.

In order to fulfill the constraint given in (19) we must place restrictions on (20) so that $0 \leq sx_t + pu_t - q_t - w_t \leq 1$. We can try to fulfill this by stopping the production if the storage is about to be filled, and start production when the storage is almost empty.

Now let us assume that we are investigating the case where $u_t = 1$, that is production is taking place. Then if the future storage $x_{t+1} = sx_t + pu_t - q_t - w_t$ is not to exceed one, we demand

$$u_t = \begin{cases} 1 & \text{if } sx_t + p - q_t - w_t \leq 1 \\ 0 & \text{if } sx_t + p - q_t - w_t > 1 \end{cases} \tag{23}$$

As an example, and without loss of generality, we assume that w is normal distributed with variance σ^2, and thus $f_w(w) = \frac{1}{\sqrt{2\pi}\sigma} \exp\left(\frac{-w^2}{2\sigma^2}\right)$. Now we can compute $E[r_t u_t]$ directly, which results in

$$E[r_t u_t]_1 = \int_{sx_t + p - q_t - 1}^{\infty} \frac{r_t}{\sqrt{2\pi}\sigma_t} \exp\left(\frac{-w^2}{2\sigma_t^2}\right) dw$$
$$= \frac{r_t \sqrt{\sigma_t}}{2}\left(1 - \text{erf}\left(\frac{sx_t + p - q_t - 1}{\sqrt{2}\sigma_t}\right)\right) \tag{24}$$

where $\text{erf}(x) = \frac{2}{\sqrt{\pi}} \int_0^x \exp(-t^2)\, dt$. Similarly, the case for $u_t = 0$, that is no production is taking place, is investigated which leads to

$$u_t = \begin{cases} 0 & \text{if } sx_t - q_t - w_t \geq 0 \\ 1 & \text{if } sx_t - q_t - w_t < 0 \end{cases} \tag{25}$$

and we compute $E[r_t u_t]$ as before, resulting in

$$E[r_t u_t]_0 = \int_{sx_t - q_t}^{\infty} \frac{r_t}{\sqrt{2\pi}\sigma_t} \exp\left(\frac{-w^2}{2\sigma_t^2}\right) dw = \frac{r_t \sqrt{\sigma_t}}{2}\left(1 - \text{erf}\left(\frac{sx_t - q_t}{\sqrt{2}\sigma_t}\right)\right) \tag{26}$$

As an example, Figure 2 shows the expected value $E[r_t u_t]$ for the two cases with $s = 0.99$, $q_t = 0.05$, $p = 0.1$, $r_t = 1$ and $\sigma_t = 0.1$. From the figure we observe that the stochasticity imposes a penalty function near $x = 0$ and $x = 1$, which can be exploited to replace the constraint in (19). This is though only possible if we assume that the production units can always satisfy the heat-load.

The next step is to evaluate $E\left[F_{t+1}(sx_t + pu_t - q_t - w_t)\right]$, in which we use the same distinctness between $u_t = 0$ and $u_t = 1$. In this case, it is typically
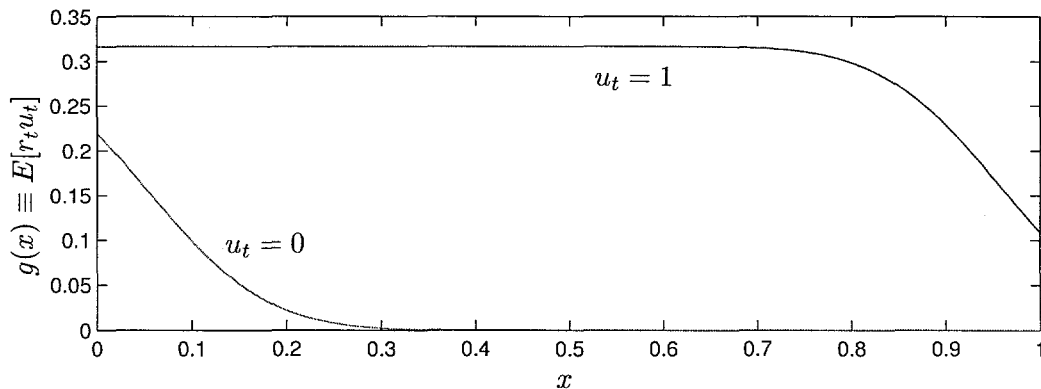
Figure 2: The cost to go function for two different strategies

impossible to compute the integrals for the expected value explicitly, but numerical integration will be appropriate.

To summarize, we can compute a function $g(x)$ for each of the possible control strategies (two in the case here, as shown in Figure 2) and then maximize the sum of these functions. The resulting function, which is piecewise continuous, provides a cost to go function $F_t(x_t)$ for the problem. So if a boiler were included then we could have three strategies: (1) No production, (2) Engine running, (3) Both boiler and engine running; with three functions, $g_1(x)$, $g_2(x)$ and $g_3(x)$.

5   A case study

In the preceding section we have presented a method for finding the optimum operational strategy of a CHP plant, spanning over a given time interval. In this section we will proceed further and apply the method to a real case, in order to validate the usefulness and robustness of the optimization method.

We will start with a short description of our case, followed by an optimization for both a summer period and a winter period. The essential difference between the two periods is that there is no house heating required during summer, just hot tap water.

5.1   Description of Hvalsø CHP plant

The case study presented in this paper is a decentralized CHP plant, located in Denmark. The plant, referred to as *Hvalsø Varmevœrk*, is equipped with a single gas engine accompanied by two heat-only boilers. The engine produces

Parameter	Unit	Value		
		low	high	peak
r_g	DKK/m^3	3.0		
g_e	m^3/h	670		
r_p	DKK/MWh	264	446	693
p_e	MW	2.9		
$r_n q$	DKK/MWh	288		
q_e	MJ/s	3.5		
R	DKK/h	208	-320	-1037
α		$7.3 \cdot 10^{-5}$		
β		$9.0 \cdot 10^{-5}$		

Table 1: Parameters regarding the production cost

3.5 MJ/s heat and 2.9 MW electricity, and the boilers have a maximum heat production of 4 MJ/s and 6 MJ/s.

The various substations parameters for operational cost, as defined in (4) and (5), are shown in Table 1. Note that the price for heat is originally taken from the price of the DH customers, but includes 20% heat-loss in the DH network. Also note that since it is always better to run the engine instead of boilers, even in low tariff periods, the boilers can be excluded in the two chosen operational time frames.

5.2   Results for a summer period

Here we choose a two week period in July 1997 and perform prediction of heat-load for the second week by using measurements for the preceding week. Figure 3 shows the heat-load during the predicted period.

In this case of heat-load in the summer it turns out that the autoregressive parts (a and b) in the heat-load model (8) are excessive, which is due to the fact that the mean heat-load over each day in summer is very stable. Therefore we choose to fit measurements with the trigonometric functions only, which is clearly observed in figure 3. But it turns out that the error is significantly biased from being a Normal distribution, so we use the following transformation formula to correct this

$$Q = q_0 + 5 \left(0.25w - 0.125 \arctan(w + 1)\right) \sigma_e; \qquad (27)$$

where q_0 is the original fit with trigonometric functions.

The results from the optimization are shown in Figure (4). The control strategy itself is not shown, but can be observed from how the storage is
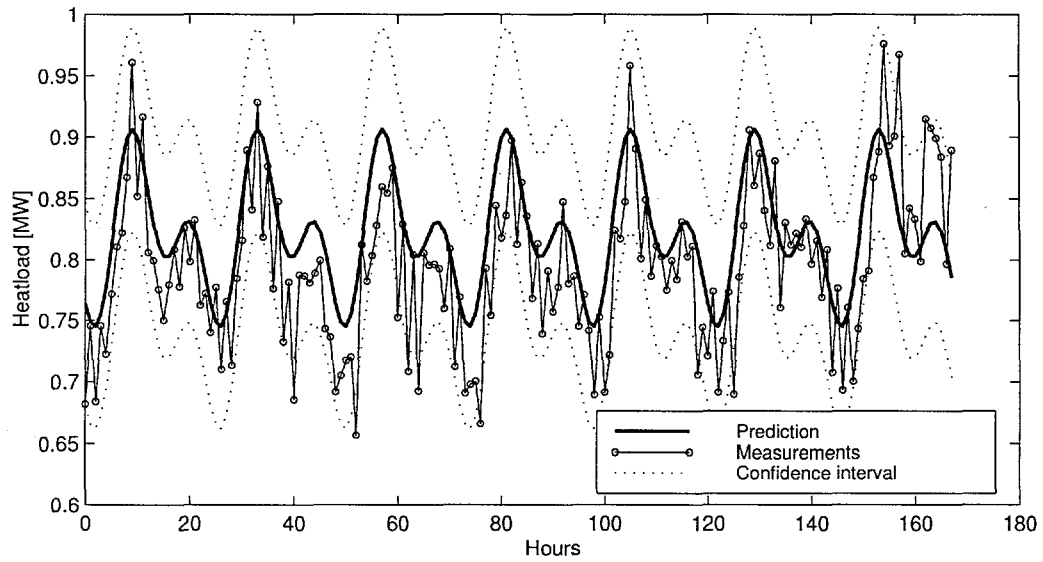
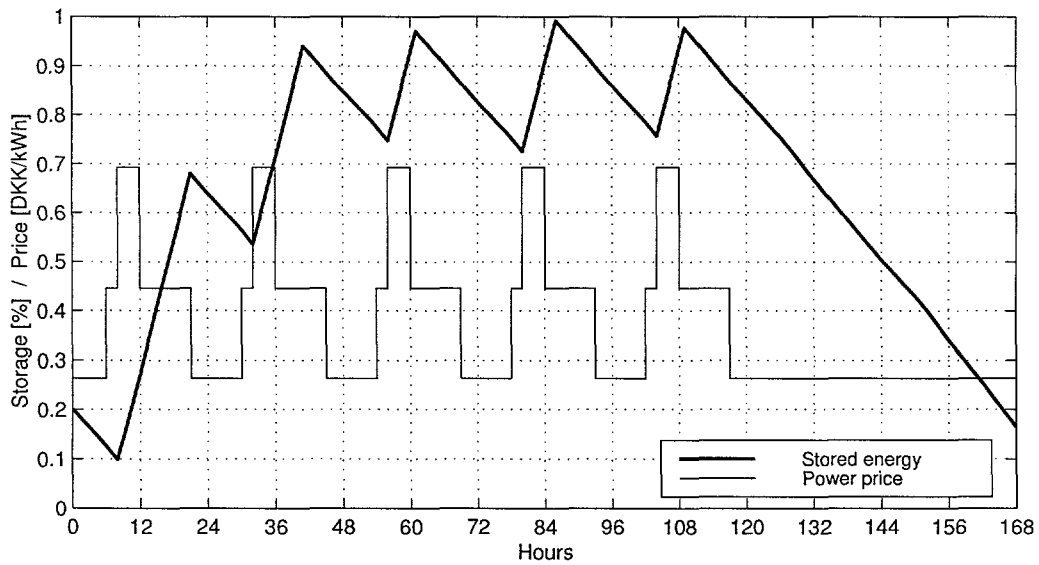Figure 3: Heat-load in July 1997, prediction versus real data

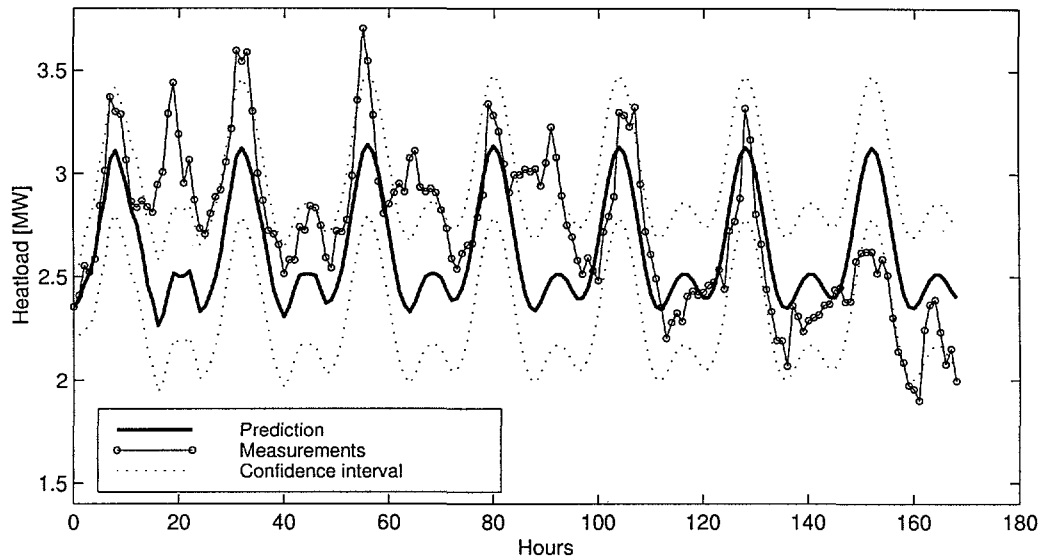Figure 4: Optimization results for July 1997

Figure 5: Heat-load in April 1997, prediction versus real data

loaded and unloaded (there is a positive slope if the engine is running). We observe that production takes place at all the peak tariff situations, never in the low tariff, and sometimes at high tariff. When not focusing on the heat losses from the storage (which are very small), we have an optimal exploitation of the high tariff periods, with a total cost of -26813.8 DKK.

It also turns out that stochastic effects do not affect the solution, which indicates that the problem can be solved by assuming equivalence between stochastic and deterministic solution. Also, in this case the cost to go functions from (20) are approximated with piecewise linear functions, each generated from 128 pieces.

5.3   Results for a winter period

In this second case of operational optimization we consider a two week period in April 1997. As before, the first week is used to estimate a prediction model for the second week, which is shown in Figure 5.

Here we use a heat-load model as shown in (8), with the autoregressive parts included (a_1, b_1, b_2). In this case the model error has a probability distribution close to a Normal one, so no transformation is performed here.

Figure 6 show the optimization results. Here the heat-load is much larger than in the summer case, which results in operation of the engine in all peak and high tariff periods. Since none of those periods are left out, the solution seems to be optimal.
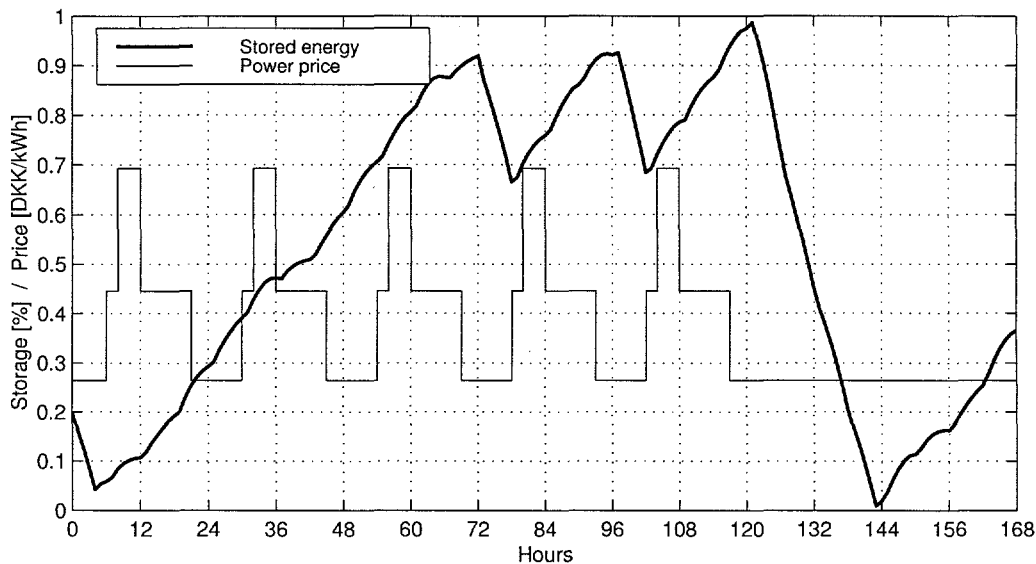
Figure 6: Optimization results for April 1997, stochastic case

There is however one difference from the summer situation. When assuming a deterministic model the total cost is -26300.2 DKK, but when stochastic optimization is performed the total cost becomes -26715.4 DKK. The difference is not great, but the reason is that at the end of Friday for the deterministic case, the storage is filled before reaching the low tariff period of the weekend. This is however taken into account in the stochastic case, resulting in a slightly better solution.

6   Discussion

Due to high efficiency, CHP plants have become more popular in recent years. In Denmark, a trend has been towards building relatively small CHP units in decentralized urban areas, in which heat is produced for use in DH and power is sold to a global power-network. Varying prices of power pose a problem for the operation of the CHP plants, which can be compensated for by installing a heat storage, which is used as a buffer between heat production and heat demand.

In the current work we propose an optimization method, especially designed to find an optimal boolean structured start-stop strategy for a simple CHP plant, consisting of piston engines and boilers. For the optimization, we use stochastic dynamic programming, focusing on the storage and the stochastic nature of the heat-load. The resulting method solves an integer

optimization problem with a computational complexity linearly connected to the number of boolean variables in the problem.

Results from case studies show that the method is computationally very efficient, solving a problem with 168 (every hour in one week) boolean variables in few seconds on an ordinary PC computer. The results are also found to be optimal for a stochastic optimization, but with a slight sub-optimality in a deterministic reference case.

We end by mentioning subjects for further study, which could be inclusion of the heat-demand as a state variable (just as the storage contents), making it possible to perform only one optimization for a long period of time (several weeks possibly). Another proposition is to include a stochastic possibility of a engine breakdown, or stochastic power prices. The latter one could be realized in a free market situation.

Acknowledgement

References

[1] R. E. Bellman. *Applied Dynamic Programming*. Princeton University Press, 1964.

[2] Benny Bøhm et al. *Optimum Operation of District Heating Systems*. Technical University of Denmark, Lyngby, Denmark, 1994.

[3] J. H. Horlock. *Cogeneration - Combined Heat and Power (CHP), Thermodynamics and Economics*. Pergamon, Oxford, 1987.

[4] K. Ito, R. Yokoyama, and T. Shiba. Optimal operation of a diesel engine cogeneration plant including a heat storage tank. *Journal of Engineering for Gas Turbines and Power*, 114:687–694, 1992.

[5] Claus Jørgensen and Hans F. Ravn. Optimal scheduling of heat production with storage and stochastic demands. In M.T. Kangas and P.D. Lund, editors, *CALORSTOCK '94, 6th Int. Conference on Thermal Energy Storage*, pages 411–418, Espoo, Finland, August 1994.

[6] Henrik Madsen. *Tidsrækkeanalyse (E. Timeseries Analysis)*. Department of Mathematical Modelling, Technical University of Denmark, 1995.

[7] O. P. Pálsson and Hans F. Ravn. Stochastic heat storage problem solved by the progressive hedging algorithm. *Energy Conversion and Management*, 35(12):1157–1171, 1994.

[8] Hans F. Ravn and Jens M. Rygaard. Optimal scheduling of coproduction with a storage. *Eng. Opt.*, 22:267–281, 1994.

[9] K. Sejling. *Modelling and Prediction of Load in District Heating Systems*. PhD thesis, IMSOR, Technical University of Denmark, 1993.

[10] R. Yokoyama and K. Ito. Optimal operational planning of cogeneration systems with thermal storage by the decomposition method. *Transactions of the ASME. Journal of Energy Resources Technology*, 117(4):337–342, 1995.

[11] H. Zhao, J. Holst, and L. Arvaston. Optimal operation of coproduction with a storage. In K. Ochifuji and K. Nagano, editors, *MEGASTOCK '97, 7th Int. Conference on Thermal Energy Storage*, pages 187–192, Sapporo, Japan, June 1997.

Appendix E:
Simulation Tool for Expansion Planning of Combined Heat and Power

Helge V. Larsen, Halldór Pálsson and Hans F. Ravn*

Abstract

Expansion planning of combined heat and power systems requires simulation tools for estimating key indicators for decision making. Probability production simulation techniques have for decades been used for power–only systems. The techniques have as well been extended to CHP systems with one heat area.

In this study, the simulation methods that include one heat area are extended to include an arbitrary number of heat areas. This can be done by either: (i) working in multidimensional probability space, (ii) aggregating all heat areas into one area and working in two dimensions, (iii) assuming that the heat demands in all heat areas are perfectly correlated and working in three dimensions.

In a simple test case, it is observed that the assumption of perfectly correlated heat areas gives results very close to a general multidimensional analysis. On the other hand, aggregating all heat areas into one large area gives rather poor results.

It is concluded that the assumption of perfect correlation of heat demand gives good results with reasonable computational complexity, while a general multidimensional method becomes much to complex with only few heat areas included.

Keywords: CHP, combined heat and power, expansion planning, district heating, probabilistic production planning

---

*Systems Analysis Department, Risø National Laboratory, DK–4000 Roskilde, Denmark.

1   Introduction

An important element in the planning of future heat and power production systems is the dimensioning of the system, that is, finding the appropriate types and capacities of production plants. The planning problem in this respect then consists of obtaining a balance between security of supply and a rarely used reserve capacity.

Traditionally, the dimensioning problem for power–only systems has been analyzed by using so-called probabilistic production simulation. In this method the power demand is represented by a probability distribution, and each power plant is represented by its capacity and forced outage rate, i.e. the probability of not being able to produce. This information is combined in a simulation, which gives results regarding the expected production of each power plant and the expected power demand that cannot be met because of failures in the plants. The method is often referred to as the Baleriaux-Booth method (see [1], [2]).

However, due to the large extent of combined heat and power production (CHP) already existing or being planned in many countries, particularly in Denmark, the production to district heating has to be considered as well. Therefore, work has been done to extend the classical method (see [3], [4], [5]).

Similar to the ideas in the classical method of probabilistic production simulation, the combined heat and power demand is here represented by a two-dimensional probability distribution, where the two dimensions are power demand and heat demand. The CHP plants are represented by their power and heat capacities and forced outage rates.

In more general terms, there is in the CHP systems a trade-off between trying to satisfy power and heat demands and trying to avoid overproduction of power and heat. Therefore, in order to analyze such systems it is necessary to develop concepts and methods that are specifically directed towards the systems' characteristics.

In the present work we extend the results on CHP systems to the situation frequently occurring where there are more than one district heating area, where [3], [4] and [5] only consider one heat area.

While this in theory may be analyzed by a direct extension of the above mentioned method for CHP systems with one heat area, the computational difficulties in this are severe. This is due to the multidimensional analysis which is demanding in terms of computation time and computer memory requirements.

We therefore in this paper propose an implementation based on a simplifying assumption. This assumption is that the heat demands in all heat

areas are perfectly correlated.

We describe how to model this and we illustrate the results for a small system. Further we compare the proposed method with the simpler approach of aggregating the heat demands to one large heat area.

The paper is organized as follows: In Section 2 we introduce the basic concepts in the two–dimen-sional analysis of CHP systems. Section 3 describes implementation aspects and gives the main theoretical results under the simplifying assumtion. Section 4 illustrates the method by application to an illustrative case.

2 Main Concepts

In this section we describe the main concepts that are necessary for the analysis. This includes the description of the system (units and demands), the convolutions, and the results in terms of expected unserved energies and expected overflow energies. The exposition largely follows [5], but includes more than one district heating areas.

2.1 Description of the units

The system considered is a combined heat and power (CHP) system. A CHP system consists of several units each producing power and/or heat.

The units in the system can be divided into two groups: units which only have one type of generation, either heat or power, and those which have a combined generation, both heat and power (CHP units). The former group consists of boiler units, which generate only heat, and condensing units, which generate only power. Within the group of CHP units we consider back pressure units and extraction units. Each heat producing unit is connected to one out of d heating areas. In many analysis a heat area will be a district heating area, however a heat area might also represent an industrial production plant if industrial CHP is considered.

Each unit is characterized by its

- working area

- forced outage rate (FOR), r

- position in the loading order list of all units in the CHP system

The relation between the possible heat and power generations for a unit is represented by the working area. The working areas of the four types of
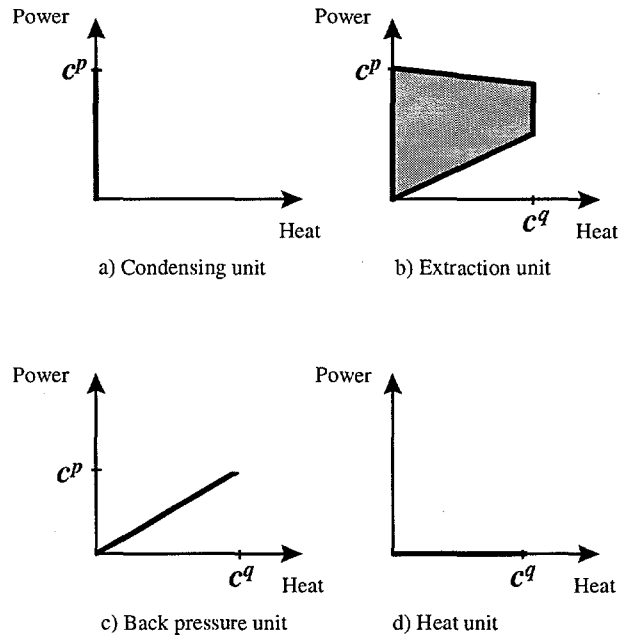
Figure 1: Working area for production units

units are sketched in Figure 1. The shape of the working area defines the possible combinations of heat and power generations.

For a heat unit the working area is characterized by the capacity c^q [MJ/s] for heat, and for a condensing unit the working area is characterized by the capacity c^p [MW] for power. It is seen that a heat unit has zero power capacity, $c^p = 0$, and that a condensing unit has zero heat capacity, $c^q = 0$.

For back pressure units, the back pressure line is defined with a slope, $c^m = c^p/c^q$, where c^q and c^p are capacities for heat [MJ/s] and power, [MW], respectively. Formally, we define $c^m = 0$ for heat units and $c^m = \infty$ for condensing units.

Extraction units permit some freedom in the choice of possible combinations of heat and power. This is in contrast to the back-pressure unit, where the combinations are fixed at the back-pressure line.

The working area of the extraction unit is a polygon, defined by four lines. Two lines limit the heat production q to the interval $0 \leq q \leq c^q$. The back-pressure line with slope c^m defines the lower limit of power production to any given heat production. The line with slope $-c^v$ (observe that c^v is positive) defines the upper limit of power production to any given heat production. The combinations (q, p) of heat and power that are within the working area

are therefore seen to satisfy the relations,

$$0 \le q \le c^q \tag{1}$$

$$c^m q \le p \le c^p - c^v q \tag{2}$$

The relations are seen to imply that $0 \le p \le c^p$.

As seen, the back-pressure and extraction units introduce a dependency between the production of heat and power. This dependency is fundamental to the method presented below since it introduces difficulties which are absent in the power–only systems. In fact, if the system contained only condensing units and heat units, then the power–only analysis could be readily extended to include also the heat production.

Each of the units is assigned a forced outage rate, i.e. the probability of non-availability of the unit.

The N units are assigned to generate in the loading order. Traditionally the loading order, or priority list, reflects the economy of the units. The generation costs of the combined units are usually lower than the heat–only and the power–only units, and therefore they might be placed first in the loading order.

For the present analysis it will be found desirable to use other loading orders that better reflect the character of the problem (see Subsection 2.5).

In the sequel lower indexes i will usually indicate unit number, e.g., r_i ,c_i^q, c_i^p and c_i^m.

2.2 Load Probability Density Function, LPDF

Based on e.g. recorded data, the power load and the d heat loads can be classified and represented as a function describing the relative frequency with which particular combinations of power and heat occurred during the period considered (typically one year), viz., the load probability density function (LPDF), $f_0 : R^{d+1} \to R$. For planning purposes the LPDF must be derived by forecasting. In practice, the data are typically represented as one-hour values over the 8760 hours of a year; multiplication of f_0 by $\tau = 8760$ hours then gives the number of hours that a particular combination of heat and power demands will occur during the year.

An example with $d = 1$, i.e. heat load in one heat area and one power load, is shown in Figure 2, left.

The occurrence depicted in Figure 2 will be considered as a two-dimensional stochastic variable. Thus, the graph in Figure 2, left, is interpreted as representing a joint probability density function of the two loads. Therefore, let the two loads, heat and power, be represented as random variables $X^q[MJ/s]$
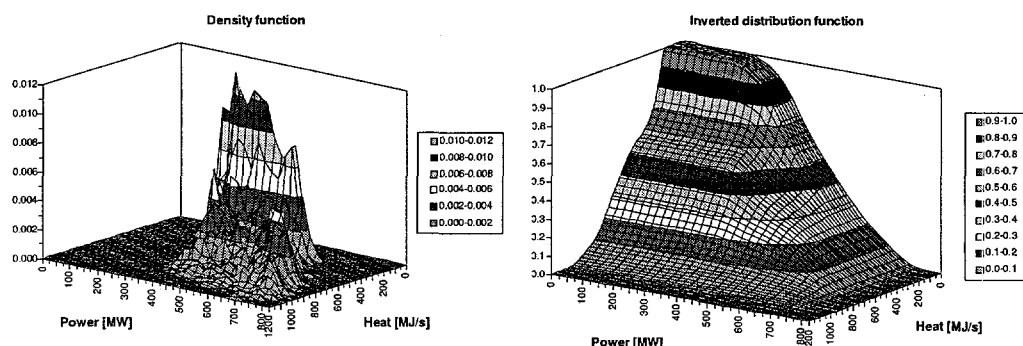
Figure 2: Density function and Inverted distribution function, with $d = 1$

and $X^p[MW]$, respectively. Thus, $f_0(x^q, x^p)$ represents their joint load probability density function LPDF; that is, $f_0(x^q, x^p)$ represents the probability that X^q takes the particular value x^q and X^p takes the particular value x^p.

Figure 2, right, shows the inverted distribution function. Observe that this function, according to the tradition of probabilistic power planning, is inverted relative to the statistical tradition. Thus, the inverted distribution function F_0, is defined as,

$$F_0(q, p) = \int_q^\infty \int_p^\infty f_0(x^q, x^p)\, dx^p dx^q \qquad (3)$$

These ideas may readily be extended for use in more than two dimensions.

2.3   Equivalent Load Probability Density Function

Now we analyze what happens when we attempt to satisfy the load by inserting the first unit in the priority list. Assume for a moment that the unit is not an extraction unit, and has capacity (c^{q_1}, c_1^p). The unit is associated with district heating area h, where $1 \le h \le d$. Assuming furthermore that the unit produces at full capacity all the time (i.e., it has no outages and thus the forced outage rate is zero, i.e., $r_1 = 0$), we get the equivalent load probability density function, ELDPC, for the remaining load, f_1 as ,

$$f_1(q^1, q^2, \ldots, q^h, \ldots, q^d, p) = f_0(q^1, q^2, \ldots, q^h + c^{q_1}, \ldots, q^d, p + c_1^p) \qquad (4)$$

Thus, the equivalent load density function f_1 is obtained by figuratively "moving" all points representing probability mass in the direction of $(0, 0, \ldots, -c^{q_1}, \ldots, 0, -c_1^p)$ when inserting unit 1. This represents the load remaining to be served by the other $N - 1$ units. This process is repeated for all N units.

Now, as the units have a FOR, $r_n > 0$ they are not available all the time but are only available with probability $(1 - r_n)$. Considering the equivalent load and the outages as independent stochastic variables, the recursive formula for the derivation of the ELPDF is obtained as the following convolution,

$$f_n(q^1, q^2, \ldots, q^h, \ldots, q^d, p) = (1 - r_n) f_{n-1}(q^1, q^2, \ldots, q^h + c_n^q, \ldots, q^d, p + c_n^p)$$
$$+ r_n f_{n-1}(q^1, q^2, \ldots, q^h, \ldots, q^d, p) \quad (5)$$

If all units considered are assumed to produce at capacity (c^q, c^p) then for some n, points with positive loads will move such that they may end up with either negative equivalent power load or negative equivalent heat load (or both). Therefore, it might be desirable to reduce the generation of a unit to a level less than (c^q, c^p).

The selection of appropriate production levels is complicated. In particular it is not even clear what production at full capacity of an extraction unit should be interpreted to mean, cf. Figure 1. We must therefore state more explicitly what combination (q, p) of heat and power will be applied during the convolution of the unit. We shall describe this in more detail in Subsection 2.5.

2.4 Energy Quantities

When all N units have been loaded, the expected unserved energies for heat in the heat area h, EUE^{q^h} and for power, EUE^p are obtained as,

$$EUE^{q^h} = \tau \int_{-\infty}^{\infty} \int_0^{\infty} \cdots \int_0^{\infty} q^h f_N(q^1, \ldots, q^d, p) \, dq^1 \ldots dq^d dp \quad (6)$$

$$EUE^p = \tau \int_0^{\infty} \int_0^{\infty} \cdots \int_0^{\infty} p f_N(q^1, \ldots, q^d, p) \, dq^1 \ldots dq^d dp \quad (7)$$

where τ is the time interval considered.

The expected heat and power overflow energies, EOE^{q^h} and EOE^p can be determined in a way similar to the expected unserved energy. The expected power overflow EOE^q is calculated as the integral of all negative values of the equivalent power load, p, multiplied by the probability that it takes that value. The expected power overflow EOE^p (non-negative by convention) can therefore be calculated as,

$$EOE^p = -\tau \int_{-\infty}^0 \int_0^{\infty} \cdots \int_0^{\infty} p f_N(q^1, \ldots, q^d, p) \, dq^1 \ldots dq^d dp \quad (8)$$

The expected heat overflows EOE^{q^h} may be calculated similarly. However, by definition of the heat priority criterion (to be presented in Subsection 2.5) EOE^{q^h} is zero in any heat area h, $h = 1, \ldots, d$. This is also why the lower limit of the integrals with respect to heat in Eqs. (6)–(8) have been taken as 0 (rather than $-\infty$).

Finally, observe that in addition to these energy quantities, the concept of loss of load probability (LOLP), known from the traditional power–only analysis, may be extended to the CHP analysis as follows,

$$LOLP^{q^h} = \int_{-\infty}^{\infty} \int_0^{\infty} \cdots \int_0^{\infty} f_N(q^1, \ldots, q^d, p)\, dq^1 \ldots dq^d dp \qquad (9)$$

$$LOLP^p = \int_0^{\infty} \int_0^{\infty} \cdots \int_0^{\infty} f_N(q^1, \ldots, q^d, p)\, dq^1 \ldots dq^d dp \qquad (10)$$

Similarly, a concept of overflow production probability (OPP) may be introduced. For the heat priority criterion $OPP^{q^h} = 0$, while

$$OPP^p = \int_{-\infty}^0 \int_0^{\infty} \cdots \int_0^{\infty} f_N(q^1, \ldots, q^d, p)\, dq^1 \ldots dq^d dp \qquad (11)$$

A distinctive feature of the CHP analysis is that relative to the power–only case, as treated in [1, 2], we have to introduce the concept of overflow energy. This is a direct consequence of the dependency between power and heat production described in Subsection 2.1.

The power overflow obtained is mathematically well defined through (8). Power overflow is simply represented by points $(q^1, \ldots, q^d, p)$ with $p < 0$, having $f(q^1, \ldots, q^d, p) > 0$, i.e., those points for which there is a positive probability that p is negative.

The physical and operational interpretation of power overflow can vary according to the circumstances. For instance, power overflow might imply that the surplus power is delivered as rotational energy (implying an increase in frequency) or it might imply that power is exported to neighboring systems. A heat overflow may be defined in analogy to (8), and might imply an increasing temperature in the water of the district heating system or the storage of heat in a storage tank.

By reduction of the production level, cf. the previous subsection, it will be possible to avoid overflow in either heat or power production.

Now a key point in the CHP system is that overflow is not necessarily undesirable. This differs from the power–only system where the production level adjustment is always used to attain either an exact fulfillment of the load or, if this is not possible, to have unserved energy.

To understand why this is so, it should be noted that in general there is a trade-off between the following situations: "Unserved heat and power energy" versus "power (or heat) overflow but less unserved heat (or power) energy".

It is therefore necessary to define a strategy for production level adjustment, in the calculations in (5).

We shall in this paper assume that the heat-side determines the trade-off. The assumption may also be denoted as a heat priority criterion.

2.5 The Heat Priority Criterion

We now describe the heat priority criterion in more detail. It implies a hierarchical decision structure for production adjustment (dispatch), i.e. for choice of heat and power production. For any given unit the heat production is first determined, so that the remaining heat demand will be minimized, and so that there is no heat overflow. For the given heat production on the unit the power production is then determined. On a heat only unit there is no power production, but on a back-pressure unit the size of power production is implied by the size of the heat production. Therefore, only in the case of extraction and condensing units there is a freedom of choice of power production once the heat production is fixed. In general, the amount of the power production on the two units will be chosen in order to minimize power overflow as well as unserved power.

Considering the heat priority criterion, the main result from [5] may be summarized as follows,

1. There is no trade-off between the different heat criteria. In other words, there exist loading orders and dispatches such that the minimal values of EUE^{q^h} are attained simultaneously for all heat areas.

2. There is no trade-off between EOE^p and EUE^p. In other words, there exist loading orders and dispatches such that the minimal values of EOE^p and EUE^p are attained simultaneously.

3. The value EOE^p may be attained by performing convolutions where the units are loaded in sequence according to increasing c^m-values (extraction units are treated as back pressure units in the loading order and are only allowed to produce at the c^m- line; condensing units are not loaded).

4. The value EUE^p may be attained by performing convolutions where the units are loaded in the following order: first apply all non-extraction

units loaded in sequence according to decreasing c^m-values (this implies that all condensing units are loaded before any heat producing units); then apply all extraction units sorted according to increasing c^v-values (extraction units are only allowed to produce at the c^v- line).

5. $EOE^{q^h} = 0$, $h = 1, ..., d$.

6. EUE^{q^h}, $h = 1, ..., d$, may be attained from any of the calculations in the above items (3) and (4).

7. The two loading orders mentioned in items (3) and (4) need only be strict within each set of units connected to the same heat area. In other words, the convolutions and the calculation of EUE^{q^h} may be completed for one heat area at a time.

The above results 1–7 are consequences of the facts that the heat areas are completely separate with respect to heat, and the heat areas are only interrelated through the power production to a common power system. Moreover, by the choice of the heat priority criterion the loading orders and dispatches are determined primarily (in a hierarchical sense) by the heat side, and the implications for the power side are consequences of the handling of the heat side. A strict proof of the results were given in [5] for $d = 1$, the ideas of the proof may be extended to the present case of $d > 1$, but we shall not do so here.

3   Implementation and Simplifying Assumptions

The implementation of the method is relatively straightforward using a discretization of the probability space, introduced in Subsection 2.2.

Working with a discretized representation, the computational burden may be indicated as follows. Assume that the size of the grids is such that a total of D^{d+1} grid units cover the relevant space. Then the convolution of N units will require arithmetic operations approximately proportional do $D^{d+1}N$. Even for moderately sized values of d and D this may imply lengthy computations and large computer memory requirements.

Therefore in the following we suggest a simplifying assumption, without sacrificing the assumption of distinct heat areas.

Assume that the heat loads in the different heat areas are related such that the heat load in area h, $h = 2, ..., d$, may be written as a function $\phi^h : R \to R$ of the heat load in heat area 1, i.e., $q^h = \phi^h(q^1)$, $h = 2, ..., d$. In

particular, the relationship may be linear, such that $q^h = \alpha^h + \beta^h q^1$. This implies that the joint probability density function f_0 may be written as

$$f_0(q^1, q^2, ..., q^d, p) = \begin{cases} f_0(q^1, \phi^2(q^1), \phi^3(q^1), ..., \phi^d(q^1), p) & \text{if } q^h = \phi^h(q^1) \\ 0 & \text{otherwise} \end{cases}$$
(12)

where $h = 2, \ldots, d$. This assumption will be fulfilled for instance if the heat loads in all areas are perfectly correlated over time.

Under this assumption we can substitute the convolutions in $(d+1)$-dimensional space by a sequence of convolutions in 3-dimensional space as follows. First the subspace with variables (q^1, q^2, p) - i.e., the subspace representing heat areas 1 and 2 and power - is treated. In this, the units of heat area 2 are applied. When all these units have been applied, EUE^{q^2} may be calculated. Then the subspace with variables (q^1, q^3, p) is treated, the units of heat area 3 are applied and EUE^{q^3} is calculated. This continues with subspaces $(q^1, q^h, p), h = 4, \ldots, d$, until EUE^{q^d} has been found. Then the subspace with variables (q^1, p) is treated as a two dimensional case, and EUE^{q^1} is found.

The proof that this simplification is valid will be indicated in the following, which also describes in more detail the computational approach. For simplicity of exposition we assume that $d = 3$. Consider first the calculations for heat area 2. Define the auxiliary function $f_0^2 : R^3 \to R$ as

$$f_0^2(q^1, q^2, p) = \int_{-\infty}^{\infty} f_0(q^1, q^2, q^3, p) \, dq^3 = f_0(q^1, q^2, \phi^3(q^1), p)$$
(13)

By the assumption that $q^3 = \phi^3(q^1)$ it follows that inversely f_0 may be recovered from f_0^2 as

$$f_n(q^1, q^2, q^3, p) = \begin{cases} f_n^2(q^1, q^2, p) & \text{if } q^3 = \phi^3(q^1) \\ 0 & \text{otherwise} \end{cases}$$
(14)

where $n = 0$; see also (12).

Now the convolutions in (5) may be performed in relation to f_n^2. For unit n we get, cf. (5)

$$f_n^2(q^1, q^2, p) = (1 - r_n) f_{n-1}^2(q^1, q^2 + \mathbf{s}_n^q, p + \mathbf{s}_n^p) + r_n f_{n-1}^2(q^1, q^2, p)$$
(15)

Convolution on heat area 2 may continue this way. It may be verified that $f_n(q^1, q^2, q^3, p)$ may be recovered from $f_n^2(q^1, q^2, p)$ by the formula (14) for any n. Thus, no information is lost by using the 3-dimensional function f_n^2 rather than the (in this case with $d = 3$) 4-dimensional function f_n.

When we have completed heat area 2 we calculate, assuming that N_2 units have been loaded

$$EUE^{q^2} = \int_{-\infty}^{\infty} \int_{0}^{\infty} \int_{0}^{\infty} q^2 f_{N_2}^2(q^1, q^2, p) \, dq^1 dq^2 dp$$

$$= \int_{-\infty}^{\infty} \int_{0}^{\infty} \int_{0}^{\infty} \int_{0}^{\infty} q^2 f_{N_2}^2(q^1, q^2, q^3, p) \, dq^1 dq^2 dq^3 dp \quad (16)$$

The last equality holds because of (14). All subsequent convolutions will take place in relation to other heat areas (or with power–only units) and therefore all "movements" in probability space will be such that the q^2–values are unchanged. The value calculated is therefore equal to the value defined in (6). The formula (16) shows that EUE^{q^2} may be calculated by a simpler formula than in (6) and that it may be done immediately after completion of heat area 2, cf. also item (7) in Subsection 2.5. This is not surprising since the heat areas are only linked through the power side and are independent on the heat sides.

Now define $f_{N_2}^3 : R^3 \to R$ as

$$f_{N_2}^3(q^1, q^3, p) = \begin{cases} \int_0^{\infty} f_{N_2}^2(q^1, q^2, p) \, dq^2 & \text{if } q^3 = \phi^3(q^1) \\ 0 & \text{otherwise} \end{cases} \quad (17)$$

We now continue with heat area 3 as above, using $f_{N_2}^3$. After loading of all units in this heat area, and a total of say N_3 units, we calculate

$$EUE^{q^3} = \int_{-\infty}^{\infty} \int_{0}^{\infty} \int_{0}^{\infty} q^3 f_{N_3}^3(q^1, q^3, p) \, dq^1 dq^3 dp$$

$$= \int_{-\infty}^{\infty} \int_{0}^{\infty} \int_{0}^{\infty} \int_{0}^{\infty} q^3 f_{N_3}(q^1, q^2, q^3, p) \, dq^1 dq^2 dq^3 dp \quad (18)$$

The last equality follows from (17) and (16). It may be argued as before that this value EUE^{q^3} is the same as defined in (6). (If there were more that $d = 3$ heat areas, all remaining heat areas h, $h = 4, \ldots, d$, would be treated similarly as heat area 3, by repeated definition in line with (17) and calculations of EUE^{q^h} in line with (18).)

Finally we define $f_{N_3}^1 : R^2 \to R$ as

$$f_{N_3}^1(q^1, p) = \int_0^{\infty} f_{N_3}^3(q^1, q^2, p) \, dq^3 \quad (19)$$

We complete convolutions in heat area 1 according to (5) and calculate EUE^{q^1} according to (6) for $d = 1$.
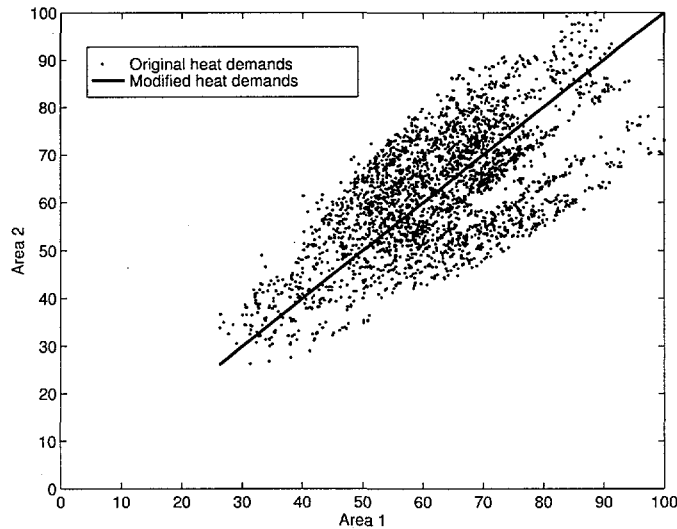
Figure 3: Heat demand in area 1 versus heat demand in area 2.

This is performed twice. First the set of convolutions has minimal power–to–heat relations and in this case it is now possible to calculate EOE^p, cf. item (3) in Subsection 2.5. Then the set of convolutions has maximal power–to–heat relations and it is now possible to calculate EUE^p, cf. item (4) in Subsection 2.5. The values EUE^{q^h} may be calculated from any one of these two sets of convolutions, cf. item (6) in Subsection 2.5.

With an implementation using discretization the computational burden of this is under the simplifying assumption reduced from being proportional to approximately $D^{d+1}N$ as mentioned above to being proportional to approximately D^3N. This is acceptable when applying a present day PC for calculations.

4 Case Study

We now describe the application of the above development to a general illustrative case. We assume two heat areas each one with a total yearly heat demand of 2066 W = 7438 TJ, divided into 8784 hours. The heat demands are connected as indicated in Figure 3. The yearly power demand is 4006 GWh.

The characteristics of the production units are described in Table 1. As seen, area 1 is equipped with a heat unit and a back pressure unit, whereas area 2 has a heat unit and an extraction power plant. Moreover, there is a condensing power plant.

Unit	Type	Area	FOR	Capacity		c^m	c^v
				Heat [MJ/s]	Power [MW]	[MW/MJ/s]	[MW/MJ/s]
HOB:1	Heat unit	1	0.1	600			
BUP:1	Back pressure unit	1	0.1	500	400	0.8	
HOB:2	Heat unit	2	0.1	600			
EXT:2	Extraction unit	2	0.1	500	500	0.8	0.1
COND	Condensing unit		0.1		600		

Table 1:   Data for the production units.

This system has been analyzed using three different techniques. In all three cases, a discretization with intervals of 25 MW on the power side and 25 MJ/s on the heat side(s) was used. The three techniques differ with respect to the approximations made.

In the first technique, the analysis is performed directly as described in Section 2, see in particular Subsection 2.5. This implies calculations with $d = 2$, i.e. three dimensional arrays are used in the representation of the discretizised values. The results are reported as 'Technique 1' in Table 2. Calculations 1 and 2 are referring to the criterions defined in times 3 and 4 in subsection 2.5. It is seen that the values of EOE^{q^1}, EOE^{q^2}, OPP^{q^1}, and OPP^{q^2} are all zero, as expected.

In the second technique, the two heat areas have been aggregated to one heat area. This is done by adding the heat demands hour by hour, and by assuming that all of the heat producing units, cf. Table 1, can produce to this common area. The LPDF, cf. Subsection 2.2, of the combined heat and power loads is shown in Figure 2, left. The calculations are performed as described in Section 2, with $d = 1$.

The results of the calculations are reported as 'Technique 2' in Table 2. Except of EOE^p and OPP^p, the values are smaller than those for 'Technique 1'. This is expected, as the aggregation of the two heat areas implies a greater (but artificial) flexibility, and therefore to more optimistic (i.e. smaller) values with respect to the indicators for the heat side (EUE^q, $LOLP^q$). As this will also permit more total power production, also EUE^p decreases. On the other hand, the increased heat production and the restrictions between heat and power production, cf. Figure 1, imply a larger value of EOE^p.

The third technique is the one described in Section 3. The assumption of completely correlated heat demands is clearly not fulfilled, cf. the dots in Figure 3. Therefore we hour by hour modify the heat demand during hour t

Technique	Calcu-lation	EUE [GWh]				EOE [GWh]			
		Heat			Power	Heat			Power
		Area 1	Area 2	Area 1+2		Area 1	Area 2	Area 1+2	
1	1	20.8	20.8	41.6		0.0	0.0	0.0	2.1
	2	20.8	20.8	41.6	29.0	0.0	0.0	0.0	
2	1			2.6				0.0	2.2
	2			2.6	20.1			0.0	
3	1	20.7	20.7	41.4		0.0	0.0	0.0	2.1
	2	20.7	20.7	41.4	28.9	0.0	0.0	0.0	

Technique	Calcu-lation	LOLP [°/oo]				OPP [°/oo]			
		Heat			Power	Heat			Power
		Area 1	Area 2	Area 1+2		Area 1	Area 2	Area 1+2	
1	1	10	10	21		0	0	0	2
	2	10	10	21	14	0	0	0	
2	1			2				0	3
	2			2	13			0	
1	1	10	10	20		0	0	0	2
	2	10	10	20	14	0	0	0	

Table 2: Results of the calculations
Technique 1: Two heat areas with (partly) uncorrelated heat demands.
Technique 2: One heat area with aggregated heat demand.
Technique 3: Two heat areas with fully correlated heat demands.
Case 1: Minimum power production.
Case 2: Maximum power production.

in each area j to the following value,

$$\sum_{i=1}^{d} q_t^i \cdot \frac{Q^j}{\sum_{i=1}^{d} Q^i} \tag{20}$$

Here q_t^i is the original heat demand in heat area i during hour t, and Q^i is the original total annual heat demand in heat area i. As seen, the formula assigns a new heat demand to heat area j during hour t which is proportional to the total annual heat demand in heat area j and proportional to the total heat demand. The heat demands in all heat areas will now be completely proportional, hour by hour, cf. the line in Figure 3.

The results of the calculations for the third technique are shown as 'Technique 3' in Table 2. The values are seen to be very close to those of 'Technique 1' in the same table.

The calculations for 'Technique 2' and 'Technique 3' in Table 2 may be seen as approximations to the correct values for 'Technique 1'. Here 'correct' is with respect to the definitions of Subsection 2.4, but disregarding discretization errors. In this perspective, the approximation introduced in Section 3, with results reported as 'Technique 3' in Table 2, are much better than the approximation resulting from aggregating the heat areas, reported as 'Technique 2'.

5 Conclusions

With large and even increasing shares of co–production of heat and power, it is of importance to be able to analyze system behavior when planning the expansion of CHP systems. This implies among other things evaluation of imbalances between demand and supply of heat and power.

Traditionally, for power–only systems this has been done by application of simulation tools such as the Baleriaux–Booth method, which permits evaluation of indicators of total system adequacy such as loss of load probability and expected unserved energy.

In the present paper we have extended this method to CHP systems with multiple heat areas. It is shown how it is computationally feasible to evaluate relevant system adequacy indicators. Specifically we introduce an assumption of completely correlated heat demands, which permits procedures with computation times that are linear in the number of units.

It is demonstrated with a simple illustrative case, that this technique is superior in terms of accuracy relative to the more straightforward procedure of aggregating all heat areas into one large area.

References

[1] H. Baleriaux, E. Jamouille, and Linard de Guertechin: "Simulation de l'exploitation d'un parc de machines thermiques de production d'électricité couplé à des stations de pompage." *Revue E (édition SRBE)*, vol. V, no. 7, pp. 225–245, 1967.

[2] R. R. Booth: "Power system simulation model based on probability analysis." *IEEE Trans. PAS-91*, , no. 1, pp. 62–69, 1972.

[3] C. Søndergren: *Planning Tools for Heat and Power Production.* Master's thesis, Institute for Mathematical Modelling, Technical University of Denmark, 1994.

[4] C. Søndergren and Hans F. Ravn: "A method to perform probabilistic production simulation involving combined heat and power units." *IEEE Trans. PWRS-11*, , no. 2, pp. 1031–1036, 1996.

[5] Helge V. Larsen, Halldór Pálsson, and Hans F. Ravn: "Probabilistic production simulation including CHP plants." Tech. Rep. R-968(EN), Risø National Laboratory, 1997.

Appendix F:
Probabilistic Production Simulation Including Combined Heat and Power Plants

Helge V. Larsen, Halldór Pálsson, Hans F. Ravn*

Abstract

Expansion planning of combined heat and power systems requires simulation tools for estimating key indicators for decision making. For power systems, so-called probability production simulation techniques have been used extensively. These techniques have been extended to include combined heat and power (CHP) systems with a single heat area and back-pressure type CHP units.

In this paper, existing simulation methods for CHP are extended to include extraction power plants. Furthermore, the case of multiple heat areas is addressed and three different simulation strategies are presented for such systems.

The results show that an assumption of perfectly correlated heat demands in all heat areas gives results that are very similar to a general case, whereas working with a system with all heat areas aggregated into one gives rather poor results.

It is demonstrated that it is possible to use the traditional concepts and methods for power-only analysis on a CHP system. Additional concepts are presented, depending on the heat criterion applied. It is concluded that probabilistic production simulation including CHP units can be performed with reasonable effort and accuracy.

1 Introduction

An important element in the planning of future heat and power production systems is the dimensioning of the system, that is, finding the appropriate

---

*Systems Analysis Department, Risø National Laboratory, DK–4000 Roskilde, Denmark.

types and capacities of production plants. The planning problem in this respect then consists of obtaining a balance between security of supply and a rarely used reserve capacity.

Traditionally, the dimensioning problem for power-only systems has been analyzed by using so-called probabilistic production simulation. In this method the power demand is represented by a probability distribution, and each power plant is represented by its capacity and forced outage rate, i.e. the probability of not being able to produce. This information is combined in a simulation, which gives results regarding the expected production of each power plant, the expected power demand that cannot be met because of failures in the plants and the loss of load probability. The method is often referred to as the Baleriaux-Booth method (see [1], [2]). Various refinements and implementations have been developed, see e.g. the reviews in [3] or [4]. Also, unconventional energy technology may be analyzed with these methods, see e.g. [5] for an evaluation of the capacity value of wind power.

However, due to the large extent of combined heat and power production (CHP) already existing, being planned or investigated in many countries, the production of heat to district heating or industrial CHP has to be considered as well. Therefore, work has been done to extend the classical method (see [6], [7], [8]).

Similar to the ideas in the classical method of probabilistic production simulation, the combined heat and power demand is here represented by a multidimensional probability distribution, where the dimensions are power demand and heat demand in each heat area. The CHP plants are represented by their power and heat capacities and forced outage rates.

The idea of using two-dimensional probability distributions has been applied independently within the analysis of power-only systems (see [9], [10], [11], [12], [13]). The specific application has been the analysis of two interconnected power systems.

While both interconnected power systems and CHP systems may be analyzed using two-dimensional probability distribution representations, it turns out that a CHP system has its unique features. For power-only systems there is a positive probability of unsatisfied power demands, due to forced outages. Similarly, for CHP systems there is a positive probability of unsatisfied power and heat demands. However, in addendum, an overflow power production may occur, assuming that the heat production is attempted to be satisfied. This is due to the problem of simultaneously satisfying both heat and power demands from the same plants.

In more general terms, in the CHP systems there is a trade-off between trying to satisfy power and heat demands and trying to avoid overproduction of power and heat. Therefore, in order to analyze such systems it is necessary

to develop concepts and methods that are specifically directed towards the systems' characteristics.

In the present work we extend the results in [7] on CHP systems to the situation frequently occurring where there are extraction-type CHP units and there is more than one district heating area.

While in theory this may be analyzed by a direct extension of the above mentioned method for CHP systems with single heat area, the computational difficulties in this are severe. This is due to the multidimensional analysis, which is demanding in terms of computation time and computer memory requirements. We therefore in this paper propose an implementation based on a simplifying assumption: that the heat demands in all heat areas are perfectly correlated.

We describe how to analyze this and we illustrate the results for a small system with two heat areas.

The paper is organized as follows: In Section 2 we introduce the basic concepts in the two-dimensional analysis of CHP systems. Section 3 defines the heat priority criterion, which is one out of several possible ways of balancing the different criteria. The main theoretical results for this criterion are presented. Section 4 describes implementation aspects and describes a simplifying assumption which permits attractive computation times even with several heat areas. Section 5 illustrates the method by application to a synthetic illustrative case.

2 Main Concepts

In this section we describe the main concepts that are necessary for the analysis. This includes the description of the system (units and demands), the convolutions, and the results in terms of expected unserved energies, expected overflow energies, loss of load probabilities and overflow production probability.

2.1 Description of the Units

The system considered is a combined heat and power (CHP) system. A CHP system consists of several units each producing power and/or heat.

The units in the system can be divided into two groups: units which have only one type of generation, either heat or power, and those which have a combined generation, both heat and power (CHP units). The former group consists of boiler units, which generate only heat, and condensing units, which generate only power. Within the group of CHP units we consider back
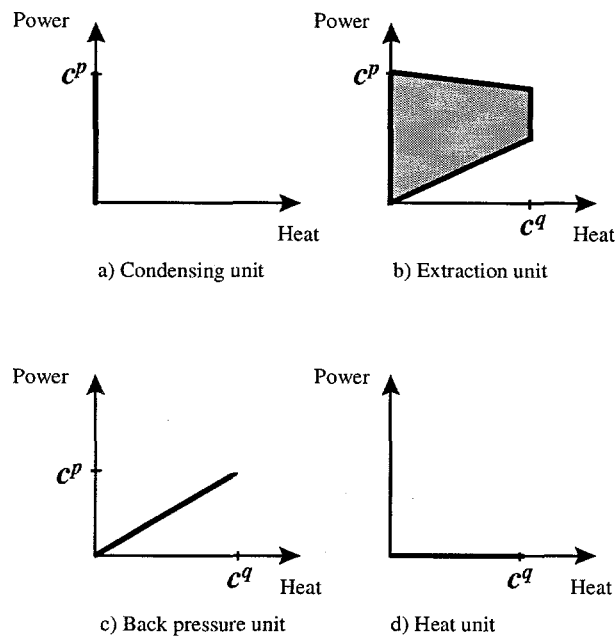
Figure 1: Working area for production units

pressure units and extraction units. Each heat-producing unit is connected to one out of d heating areas. In many analysis a heat area will be a district heating area, however a heat area might also represent an industrial CHP production plant.

Each unit is characterized by its working area, its forced outage rate (FOR) r, and its position in the loading order list of all units in the CHP system.

The relation between the possible heat and power generations for a unit is represented by the working area. The working areas of the four types of units are sketched in Figure 1. The shape of the working area defines the possible combinations of heat and power generation.

For a heat unit the working area is characterized by the capacity c^q [MJ/s] for heat, and for a condensing unit it is characterized by the capacity c^p [MW] for power. It is seen that a heat unit has zero power capacity, $c^p = 0$, and that a condensing unit has zero heat capacity, $c^q = 0$.

For back-pressure units, the back-pressure line is defined with a slope, $c^m = c^p/c^q$, where c^q and c^p are capacities for heat [MJ/s] and power [MW], respectively. Formally, we define $c^m = 0$ for heat units and $c^m = \infty$ for condensing units.

Extraction units permit some freedom in the choice of possible combinations of heat and power. This is in contrast to the back-pressure unit, where

the combinations are fixed at the back-pressure line.

The working area of the extraction unit is a polygon, defined by four lines. Two lines limit the heat production q to the interval $0 \leq q \leq c^q$. The back-pressure line with slope c^m defines the lower limit of power production corresponding to any given heat production. The line with slope $-c^v$ (observe that c^v is positive) defines the upper limit of power production corresponding to any given heat production. The combinations (q, p) of heat and power that are within the working area are therefore seen to satisfy:

$$0 \leq q \leq c^q \tag{1}$$

$$0 \leq p \leq c^p \tag{2}$$

$$c^m q \leq p \leq c^p - c^v q \tag{3}$$

As seen, the back-pressure and extraction units introduce a dependency between the production of heat and power. This dependency is fundamental to the method presented below since it introduces difficulties which are absent in the power-only systems. In fact, if the system contained only condensing units and heat units, then the power-only analysis could be readily extended to include the heat production as well.

Each of the units is assigned a forced outage rate, i.e. the probability of non-availability of the unit.

The N units are assigned to generate in the loading order. Traditionally the loading order, or priority list, reflects the economy of the units. The generation costs of the combined units are usually lower than the heat-only and power-only units, and therefore they might be placed first in the loading order. For the present analysis it will be found desirable to use other loading orders that better reflect the character of the problem (see Subsection 3).

In the sequel, lower indexes i will usually indicate the unit number, e.g., r_i , c_i^q, c_i^p and c_i^m.

2.2 Load probability density function

Based on, e.g. recorded data, the power load and d heat loads can be classified and represented as a function describing the relative frequency with which particular combinations of power and heat occurred during the period considered (typically one year), viz., the load probability density function (LPDF), $f_0 : R^{d+1} \to R$. For planning purposes the LPDF must be derived by forecasting. In practice, the data are typically represented as one-hour values over the 8760 hours of a year; multiplication of f_0 by $\tau = 8760$ hours then gives the number of hours that a particular combination of heat and power demands will occur during the year.
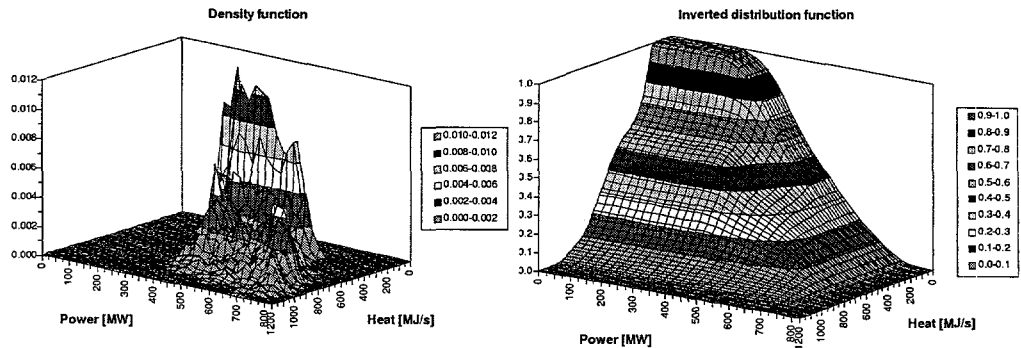
Figure 2: Density function and inverted distribution function, with $d = 1$

An example with $d = 1$, i.e. heat load in one heat area and one power load, is shown in Figure 2, left.

The occurrence depicted in Figure 2 will be considered as representing a two-dimensional stochastic variable. Thus, the graph in Figure 2, left, is interpreted as representing a joint probability density function of the two loads. Therefore, let the two loads, heat and power, be represented as random variables $X^q[MJ/s]$ and $X^p[MW]$, respectively. Thus, $f_0(x^q, x^p)$ represents their joint load probability density function LPDF; that is, $f_0(x^q, x^p)$ represents the probability that X^q takes the particular value x^q and X^p takes the particular value x^p.

Figure 2, right, shows the inverted distribution function. Observe that this function, according to the tradition of probabilistic power planning, is inverted relative to the statistical tradition. Thus, the inverted distribution function F_0, is defined as,

$$F_0(q, p) = \int_q^\infty \int_p^\infty f_0(x^q, x^p) \, dx^p dx^q \qquad (4)$$

These ideas may readily be extended for use in more than two dimensions, i.e. for $d > 1$.

2.3 Equivalent load probability density function

Now we analyze what happens when we attempt to satisfy the load by inserting the first unit in the priority list. Assume for a moment that the unit is not an extraction unit, and has capacity (c_1^q, c_1^p). The unit is associated with the district heating area h, where $1 \leq h \leq d$. Assuming furthermore that the unit produces at full capacity all the time (i.e., it has no outages and thus the forced outage rate is zero, i.e., $r_1 = 0$), we get the equivalent

load probability density function (ELPDF) for the remaining load, f_1 as ,

$$f_1(q^1, q^2, \ldots, q^h, \ldots, q^d, p) = f_0(q^1, q^2, \ldots, q^h + c_1^q, \ldots, q^d, p + c_1^p) \quad (5)$$

Thus, the equivalent load density function f_1 is obtained by figuratively "moving" all points representing probability mass in the direction of $(0, 0, \ldots, -c_1^q, \ldots, 0, -c_1^p)$ when inserting unit 1. This represents the load remaining to be served by the remaining $N-1$ units. This process is repeated for all N units.

Now, as the units have a FOR, $r_n > 0$ they are not available all the time but are available only with probability $(1 - r_n)$. Considering the equivalent load and the outages as independent stochastic variables, the recursive formula for the derivation of the ELPDF is obtained as the following convolution:

$$f_n(q^1, q^2, \ldots, q^h, \ldots, q^d, p) = (1 - r_n)f_{n-1}(q^1, q^2, \ldots, q^h + c_n^q, \ldots, q^d, p + c_n^p)$$
$$+ r_n f_{n-1}(q^1, q^2, \ldots, q^h, \ldots, q^d, p) \quad (6)$$

If all units considered are assumed to produce at capacity (c^q, c^p) then for some n, points with positive loads will move such that they may end up with either a negative equivalent power load or negative equivalent heat load (or both). Therefore, it might be desirable to reduce the generation of a unit to a level less than (c^q, c^p).

The selection of appropriate production levels is complicated. In particular it is not even clear what production at full capacity of an extraction unit should be interpreted to mean (cf. Figure 1). We must therefore state more explicitly what combination (q, p) of heat and power will be applied during the convolution of the unit. We shall describe this in more detail in Section 3.

2.4 Energy quantities

When all N units have been loaded, the expected unserved energies for heat in heat area h, EUE^{q^h} and for power, EUE^p are obtained as,

$$EUE^{q^h} = \tau \int_{-\infty}^{\infty} \int_{-\infty}^{\infty} \cdots \int_0^{\infty} \cdots \int_0^{\infty} q^h f_N(q^1, \ldots, q^d, p)\, dq^1 \ldots dq^h \ldots dq^d dp$$
$$(7)$$

$$EUE^p = \tau \int_0^{\infty} \int_{-\infty}^{\infty} \cdots \int_{-\infty}^{\infty} p f_N(q^1, \ldots, q^d, p)\, dq^1 \ldots dq^d dp \quad (8)$$

where τ is the time interval considered.

A distinctive feature of the CHP analysis is that relative to the power-only case, as treated in [1, 2], we have to introduce the concept of overflow energy. This is a direct consequence of the dependency between power and heat production described in Subsection 2.1.

The expected heat and power overflow energies, EOE^{q^h} and EOE^p can be determined in a way similar to the expected unserved energy. The expected power overflow EOE^q is calculated as the integral of all negative values of the equivalent power load, p, multiplied by the probability that it takes that value. The expected power overflow EOE^p (non-negative by convention) can therefore be calculated as,

$$EOE^p = -\tau \int_{-\infty}^{0} \int_{0}^{\infty} \cdots \int_{0}^{\infty} p f_N(q^1, \ldots, q^d, p) \, dq^1 \ldots dq^d dp \qquad (9)$$

The expected heat overflows EOE^{q^h} may be calculated similarly. Note that by definition of the heat priority criterion (to be presented in Section 3), EOE^{q^h} is zero in any heat area h, $h = 1, \ldots, d$. Therefore, in this case the lower limit of the integrals with respect to heat in Equations (7)–(9) may be taken as 0 (rather than $-\infty$).

The power overflow obtained is mathematically well defined through (9). Power overflow is simply represented by points $(q^1, \ldots, q^d, p)$ with $p < 0$, having $f_N(q^1, \ldots, q^d, p) > 0$, i.e., those points for which there is a positive probability that p is negative.

The physical and operational interpretation of power overflow can vary according to the circumstances. For instance, power overflow might imply that the surplus power is delivered as rotational energy (implying an increase in frequency) or it might imply that power is exported to neighboring systems. A heat overflow may be defined in analogy to (9), and might imply an increasing temperature in the water of the district heating system or the storage of heat in a storage tank.

By reducing the production level (cf. the previous subsection) it will be possible to avoid overflow in either heat or power production.

Now a key point in the CHP system is that overflow is not necessarily undesirable. This differs fundamentally from the power-only system where the production level adjustment is always used either to attain an exact fulfillment of the load or, if this is not possible, to have unserved energy.

To understand why this is so, it should be noted that in general there is a trade-off between the following situations: "Unserved heat and power energy" versus "power (or heat) overflow but less unserved heat (or power) energy".

It is therefore necessary to define a strategy for production level adjustment, in the calculations in (6).

We shall in this paper assume that the heat-side determines the trade-off. The assumption may also be denoted as a heat priority criterion.

Finally, observe that in addition to these energy quantities, the concept of loss of load probability (LOLP), known from the traditional power-only analysis, may be extended to the CHP analysis as follows:

$$LOLP^{q^h} = \int_{-\infty}^{\infty} \int_{-\infty}^{\infty} \cdots \int_{0}^{\infty} \cdots \int_{-\infty}^{\infty} f_N(q^1, \ldots, q^d, p) \, dq^1 \ldots dq^h \ldots dq^d dp$$
(10)

$$LOLP^p = \int_{0}^{\infty} \int_{-\infty}^{\infty} \cdots \int_{-\infty}^{\infty} f_N(q^1, \ldots, q^d, p) \, dq^1 \ldots dq^d dp$$
(11)

Similarly, a concept of overflow production probability (OPP) may be introduced. For the heat priority criterion $OPP^{q^h} = 0$, while

$$OPP^p = \int_{-\infty}^{0} \int_{-\infty}^{\infty} \cdots \int_{-\infty}^{\infty} f_N(q^1, \ldots, q^d, p) \, dq^1 \ldots dq^d dp$$
(12)

3 The Heat Priority Criterion

As pointed out above, a selection of production levels is necessary in order to calculate the terms EOE^p, EUE^p, etc. defined in the previous section.

This is in contrast to the power-only analysis. It seems that in general there is no natural way to calculate these terms without making assumptions on the relative priorities of the dimensions, or without in some other way balancing, e.g. unserved power against unserved heat in heat area h. In this section we develop the analysis for the case of the heat priority criterion.

This criterion implies a hierarchical decision structure for production adjustment (dispatch), i.e. for choice of heat and power production. For any given unit the heat production is first determined so that the remaining heat demand will be minimized; as a result there is no heat overflow. For the given heat production on the unit the power production is then determined. On a heat-only unit there is no power production, but on a back-pressure unit the size of power production is determined by the size of the heat production. Therefore, only in the case of extraction and condensing units is there a freedom of choice of power production once the heat production is fixed. In general, the amount of the power production on the two units will be chosen in order to minimize power overflow as well as unserved power. Also the loading order influences the production of the individual unit, even if there are no extraction units [7].
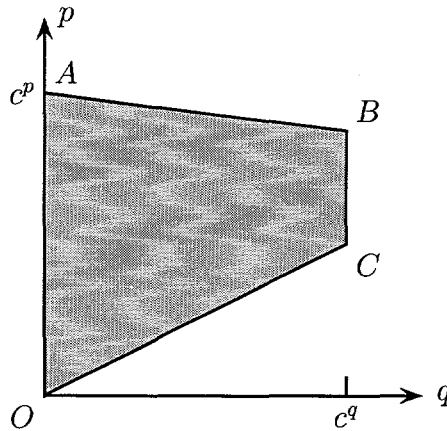
Figure 3: Loading of an Extraction Unit

3.1 Loading points

Consider partial loading of the units, which may be necessary in order to avoid overflow. For condensing units, back-pressure units and heat units there is a one-to-one relationship between heat and power production. Letting the capacity of such units be defined by (c^q, c^p), a reduced production level may be indicated by (s^q, s^p). If, e.g. the unit is a back-pressure one producing at 80% of full capacity, then $(s^q, s^p) = (0.8c^q, 0.8c^p)$. Similarly, a condensing unit producing at 80% of full capacity has $(s^q, s^p) = (0.8c^q, 0.8c^p) = (0.0, 0.8c^p)$.

Now consider extraction units. These are more complicated because there is freedom of choice of production combinations of p and q. We may therefore consider the following main types of loading of an extraction unit,

- As a fully loaded back-pressure unit, point C in Figure 3.

- As a partially loaded back-pressure unit, a point on the line OC in Figure 3.

- Maximum q load and, relative to this, also maximum p load, point B in Figure 3.

- Partially loaded on the c^v–line, i.e., a point on the line AB in Figure 3.

As indicated it suffices to consider points on either the c^m–line or on the c^v–line. Any relevant loading point will be specified by (s^q, s^p) as for the other types of units.

3.2 Loading orders

We consider two specific loading orders for any given outage pattern.

1. Treat all extraction units as back-pressure units. Then apply all units sorted according to increasing c^m-values.

2. First apply all non-extraction units sorted according to decreasing c^m-values. Then apply all extraction units sorted according to increasing c^v-values.

In both cases the dispatch is adjusted according to the heat priority criterion. As before, heat units are formally defined with $c^m = 0$, while condensing units are defined with $c^m = \infty$.

In loading order "1", this implies that as long as no q-overflow is generated the units are used with full capacities (extraction units are treated as back-pressure units, i.e., point C in Figure 3 is used). Then capacity is reduced so that no q-overflow is generated (extraction units produce at a point on the line OC in Figure 3), or units do not produce at all. Loading order "1" may be characterized as minimum p-production to any given q-production.

In loading order "2", condensing units are applied first, at full capacities (p-overflow need not be avoided). Then back-pressure units are applied, followed by heat units, where both types are applied with suitable adjustments of production according to the heat priority criterion. And finally, extraction units are loaded as follows: As long as no q-overflow is generated, they are loaded to point B in Figure 3. If the point B in Figure 3 will produce q-overflow, then production is reduced to a point on the line AB so that no q-overflow is attained and (possibly) no unserved q-energy remains. Observe that extraction units must be applied even if no unserved q-energy exists (in which case they are loaded to point A). Loading order "2" may be characterized as maximum p-production to any given q-production.

Observe that loading order "2" may be described as taking all the units in sequence according to decreasing slope of the "upper" limit of the working areas, this being c_i^m for non-extraction units and $-c_i^v$ for extraction units. Recall that the c^v-value for a given unit i is defined as the negative of the slope, i.e., c_i^v is positive.

Figure 4 illustrates the two loading orders and possible loading points for six different units. We call the resulting end points (q^1, p^1) and (q^2, p^2).

3.3 Results for the heat priority criterion

We are now in a position to see how the quantities EOE, EUE, $LOLP$ and OPP may be derived for the heat priority criterion. They may be derived by performing two convolutions: The first one, "1", characterized as minimum p-production for given q-production, is used to determine EUE^p, EUE^q,
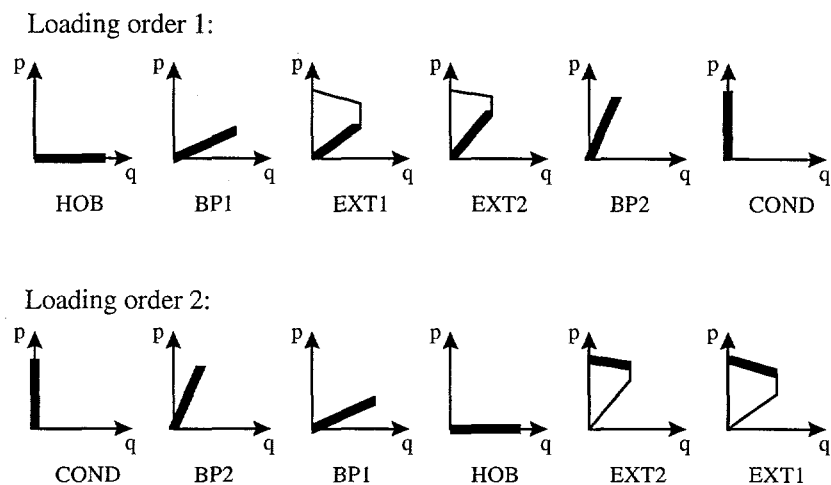
Loading order 1:

Loading order 2:

Figure 4: The two loading orders and possible loading points

$LOLP^p$ and $LOLP^q$. Observe that by definition of the heat priority criterion $EOE^q = 0$ and $OPP^q = 0$.

Now we extend the above results in two ways as follows: A convenient property of the heat priority criterion is that it yields well-defined minimum values of EUE^q, EOE^p, EUE^p, $LOLP^q$, OPP^p and $LOLP^p$ (recall that $EOE^q = 0$ and $OPP^q = 0$). This in particular means that there is no trade-off between these values.

Observe that slight savings in computation may be obtained because in the convolution "1" the condensing units need not be applied in order to calculate EOE^p, EUE^q, OPP^p and $LOLP^q$. Further, in the convolution "2" the condensing units may be placed anywhere in the loading order. Thus, by placing them last only that part of the probability space with $p > 0$ need be considered because the purpose of the convolution "2" is the calculation of EUE^p, EUE^q, $LOLP^p$ and $LOLP^q$. And finally, EUE^q and $LOLP^q$ may be calculated from any one of the convolutions.

The application of this is illustrated in Figure 5 for a case with $d = 1$. The plants of the CHP system used are described in Table 1.

Figure 5 shows the two frequency functions after convolution with minimum power production relative to heat production (convolution "1") and maximum power production relative to heat production (convolution "2"). In convolution "1" the units are applied in the loading order HOB, BP1, BP2, EXT and COND, while in convolution "2" the loading order is COND,
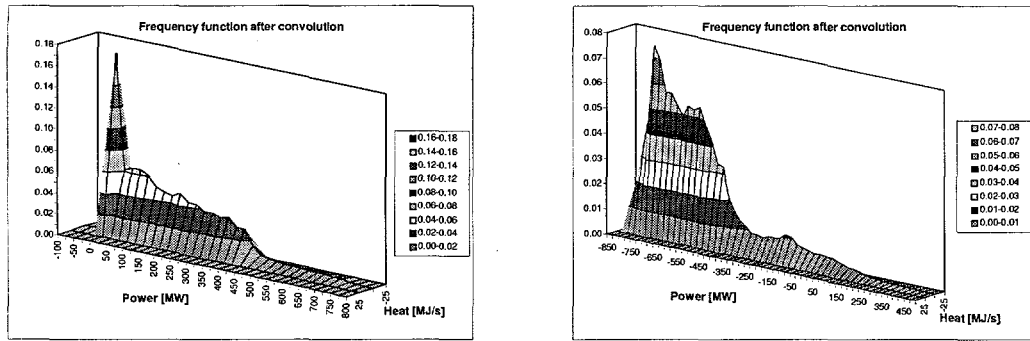
Figure 5: Frequency functions after convolution. Left: Minimum power production relative to heat production. Right: Maximum power production relative to heat production

BP2, BP1, HOB and EXT.

Figure 6 shows the corresponding marginal frequency functions for heat and power.

Observe that the two marginal frequency functions for heat (top graphs) are identical. The two bottom graphs in Figure 6, indicating the overflow power production and the unserved power demand, are enlargements of the left and right parts of the middle graphs in Figure 6.

By taking the two bottom graphs of Figure 6 together, as shown in Figure 7, we get a marginal frequency function for the unbalances between power demand and production, i.e. the power overflow and the unserved power demand. Most of the power demand is satisfied exactly. This gives a large probability value at $p = 0$ (not shown in the figure).

Considering the heat priority criterion, the main results may be summarized as follows:

1. There is no trade-off between the different heat criteria. In other words, there exist loading orders and dispatches such that the minimal values of EUE^{q^h} and $LOLP^{q^h}$ are attained simultaneously for all heat areas.

2. There is no trade-off between EOE^p and EUE^p nor between OPP^q and $LOLP^p$. In other words, there exist loading orders and dispatches such that the minimal values of EOE^p, EUE^p, OPP^p and $LOLP^p$ are attained simultaneously.

3. The values EOE^p and OPP^p may be attained by performing convolutions where the units are loaded in sequence according to increasing c^m-values (extraction units are treated as back-pressure units in the
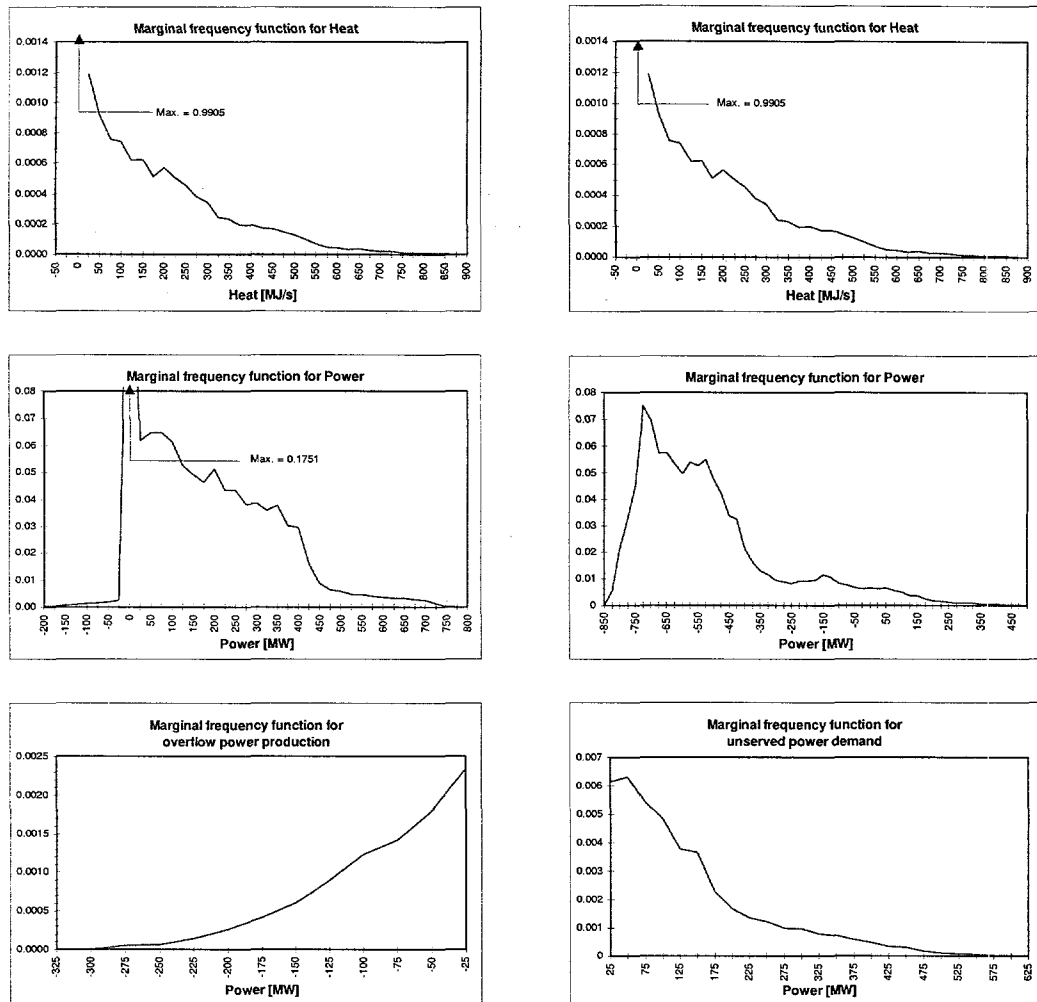
Figure 6: Marginal frequency functions after convolution. Left: Minimum power production relative to heat production. Right: Maximum power production relative to heat production
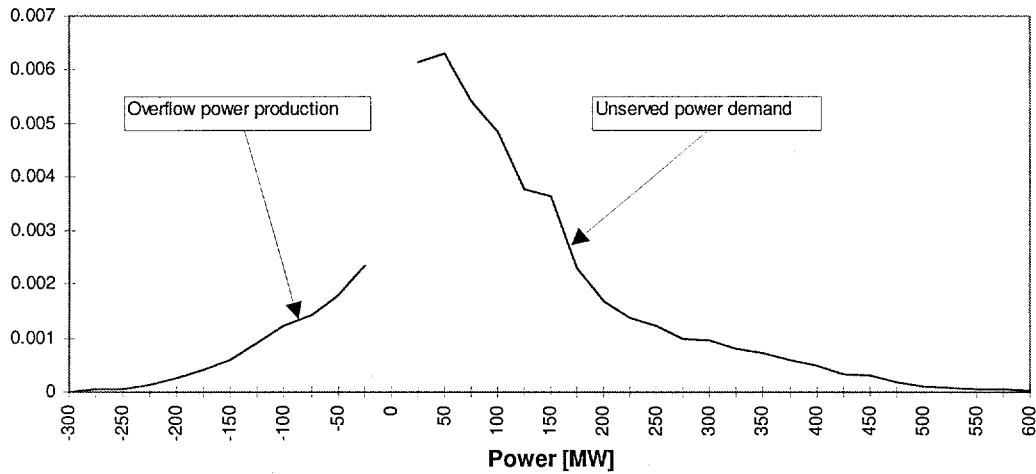
Figure 7: Marginal frequency function for the unbalances between power demand and production

loading order and are only allowed to produce at the c^m–line; condensing units are not loaded).

4. The values EUE^p and $LOLP^p$ may be attained by performing convolutions where the units are loaded in the following order: First apply all non-extraction units loaded in sequence according to decreasing c^m–values (this implies that all condensing units are loaded before any heat producing units). Then apply all extraction units sorted according to increasing c^v–values (extraction units are only allowed to produce at the c^v–line).

5. $EOE^{q^h} = 0$ and $OPP^{q^h} = 0$, $h = 1, ..., d$.

6. EUE^{q^h} and $LOLP^{q^h}$, $h = 1, ..., d$, may be attained from any of the calculations in the above items (3) and (4).

7. The two loading orders mentioned in items (3) and (4) need only be strict within each set of units connected to the same heat area. In other words, the convolutions and the calculations of EUE^{q^h} and $LOLP^{q^h}$ may be completed for one heat area at a time.

The above results, items (1)–(7), are consequences of the fact that the heat areas are completely separated with respect to heat, and that the heat areas are interrelated only through the power production to a common power system. Moreover, by the choice of the heat priority criterion the loading orders and dispatches are determined primarily (in a hierarchical sense) by

the heat side, and the implications for the power side are consequences of the handling of the heat side. A strict proof of the results was given in [8] for $d = 1$, the ideas of the proof may readily be extended to the present case of $d > 1$. The main ideas of the proof may be sketched as follows:

Consider as an example the calculation of EUE^p for $d = 1$. The calculation of this value may be imagined as being performed in three steps. (i) Calculate the minimum unserved power for any demand value (q, p) and for any outage pattern, observing the heat priority criterion. Here, an outage pattern is one specific combination of outages of the units. (ii) Multiply each such value by the probability of occurrence of this particular (q, p) and by the probability of occurrence of this particular outage pattern. (iii) Sum up all such values.

Finding a minimum value may be formulated as a linear programming (LP) problem, cf. e.g. [14]. Application of the loading order "1", may then be seen to provide the optimal solution. Similarly, loading order "2" represents a solution to a LP problem that minimizes EOE^p.

These two observations and the one that the working areas for all units are convex ([14]) imply that the values found may in fact be interpreted as the desired quantities EUE^p and EOE^p. The remaining items are also consequences of LP reformulations in relation to the heat priority criterion.

4   Implementation and Simplifying Assumptions

The implementation of the method is relatively straightforward using a discretization of the probability space, introduced in Subsection 2.2.

For specificity, assume that a grid with $25\,[MJ/s] \times 25\,[MW]$ squares is used. This is interpreted to mean that all probability mass is located at points $(25i, 25j)$, where i and j are integers. The probability mass in a specific point $(x_{i^*}^q, x_{j^*}^p) = (25i^*, 25j^*)$ is assumed to represent all the probability mass distributed over the square with x^q–co-ordinate satisfying $25i^* - 12.5 \leq x^q < 25i^* + 12.5$ and the x^p–co-ordinate satisfying $25j^* - 12.5 \leq x^p < 25j^* + 12.5$. Similar ideas may be used in higher dimensions.

The advantage of the discretization procedure is that it is relatively straightforward to conceive and implement. The disadvantage is that some errors are introduced, and errors will most probably be introduced due to inconsistencies between the grid-sizes and the magnitudes c_i^q, c_i^p and c^p/c^q of the individual units. In one-dimensional analysis this may be avoided by applying grid-sizes that are consistent with the capacities (see e.g. [3]). But with two or more dimensions this is most unlikely to be avoidable. Thus ad hoc approximation and interpolation must be developed.

Working with a discretized representation, the computational burden may be indicated as follows: Assume that the size of the grids is such that a total of D^{d+1} grid units cover the relevant space. Then the convolution of N units will require arithmetic operations approximately proportional to $D^{d+1}N$. Even for moderately sized values of d and D this may result in lengthy computations and large computer memory requirements.

Therefore, in the following we suggest a simplifying assumption without sacrificing the assumption of distinct heat areas.

Assume that the heat loads in the different heat areas are related such that the heat load in area h, $h = 2, ..., d$, may be written as a function $\phi^h : R \to R$ of the heat load in heat area 1, i.e., $q^h = \phi^h(q^1)$, $h = 2, ..., d$. In particular, the relationship may be linear, such that $q^h = \alpha^h + \beta^h q^1$. This enables the joint probability density function f_0 to be written as

$$f_0(q^1, q^2, ..., q^d, p) = \begin{cases} f_0(q^1, \phi^2(q^1), \phi^3(q^1), ..., \phi^d(q^1), p) & \text{if } q^h = \phi^h(q^1) \\ 0 & \text{otherwise} \end{cases}$$

(13)

for $h = 2, ..., d$. This assumption will be fulfilled, for instance, if the heat loads in all areas are perfectly correlated over time.

Under this assumption we can substitute the convolutions in $(d + 1)$ dimensional space by a sequence of convolutions in 3–dimensional space as follows: First the subspace with variables (q^1, q^2, p) - i.e., the subspace representing heat areas 1 and 2 and power - is treated. In this, the units of heat area 2 are applied. When all these units have been applied, EUE^{q^2} and $LOLP^{q^2}$ may be calculated. Then the subspace with variables (q^1, q^3, p) is treated, the units of heat area 3 are applied and EUE^{q^3} and $LOLP^{q^3}$ are calculated. This continues with subspaces (q^1, q^h, p), $h = 4, ..., d$, until EUE^{q^d} and $LOLP^{q^d}$ have been found. Then the subspace with variables (q^1, p) is treated as a two-dimensional case, and EUE^{q^1} and $LOLP^{q^1}$ are found.

This is performed twice. First the set of convolutions has minimal power-to-heat relations and in this case it is now possible to calculate EOE^p and OPP^p, cf. item (3) in Subsection 3.3. Then the set of convolutions has maximal power-to-heat relations and it is now possible to calculate EUE^p and $LOLP^p$ (cf. item (4) in Subsection 3.3). The values EUE^{q^h} and $LOLP^{q^h}$ may be calculated from any one of these two sets of convolutions (cf. item (6) in Subsection 3.3).

With an implementation using discretization the computational burden of this is under the simplifying assumption reduced from being proportional to approximately $D^{d+1}N$ as mentioned above to being proportional to approximately $D^3 N$. This is acceptable when applying a modern PC for calculations.
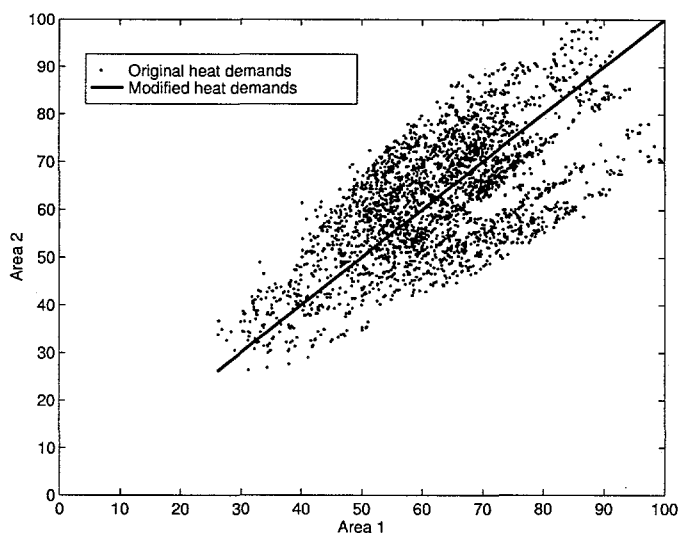
Figure 8: Heat demand in area 1 versus heat demand in area 2.

Unit	Type	Area	FOR	Capacity		c^m	c^v
				Heat [MJ/s]	Power [MW]	$[\frac{MW}{MJ/s}]$	$[\frac{MW}{MJ/s}]$
HOB:1	Heat unit	1	0.1	600			
BUP:	Back pressure unit	1	0.1	500	400	0.8	
HOB:2	Heat unit	2	0.1	600			
EXT:	Extraction unit	2	0.1	500	500	0.8	0.1
COND	Condensing unit		0.1		600		

Table 1:   Data for the production units.

5   Case Study

We now describe the application of the above development to a synthetic illustrative case. We assume two heat areas each one with a total yearly heat demand of 2066 GWh = 7438 TJ, distributed over 8784 hours. The heat demands are correlated as indicated by the dots in Figure 8. The yearly power demand is 4006 GWh.

The characteristics of the production units are described in Table 1. As seen, area 1 is equipped with a heat unit and a back-pressure unit, whereas area 2 has a heat unit and an extraction power plant. Moreover, there is a condensing power plant.

This system has been analyzed using three different techniques. In all three cases, a discretization with intervals of 25 MW on the power side and 25 MJ/s on each heat side was used. The three techniques differ with respect to the approximations made.

Tech.	Loading order	EUE [GWh]				EOE [GWh]			
		Heat Area			Power	Heat Area			Power
		1	2	1+2		1	2	1+2	
1	1	20.8	20.8	41.6		0.0	0.0	0.0	2.1
	2	20.8	20.8	41.6	29.0	0.0	0.0	0.0	
2	1			2.6				0.0	2.2
	2			2.6	20.1			0.0	
3	1	20.7	20.7	41.4		0.0	0.0	0.0	2.1
	2	20.7	20.7	41.4	28.9	0.0	0.0	0.0	

Tech.	Loading order	$LOLP$ [°/oo]				OPP [°/oo]			
		Heat Area			Power	Heat Area			Power
		1	2	1+2		1	2	1+2	
1	1	10	10	21		0	0	0	2
	2	10	10	21	14	0	0	0	
2	1			2				0	3
	2			2	13			0	
3	1	10	10	20		0	0	0	2
	2	10	10	20	14	0	0	0	

Table 2: Results of the calculations

Technique 1: Two heat areas with (partly) uncorrelated heat demands.

Technique 2: One heat area with aggregated heat demand.

Technique 3: Two heat areas with fully correlated heat demands.

In the first technique, the analysis is performed directly as described in Section 3. This implies calculations with $d = 2$, i.e. three-dimensional arrays are used in the representation of the discretizised values. The results are reported as 'Technique 1' in Table 2. Loading orders 1 and 2 refer to the loading orders defined in items (3) and (4) in Subsection 3.3. It is seen that the values of EOE^{q^1}, EOE^{q^2}, OPP^{q^1} and OPP^{q^2} are all zero, as expected for the heat priority criterion. It is further seen that there are positive values for EUE^{q^1}, EUE^{q^2} and EUE^q, and also for $LOLP^{q^1}$, $LOLP^{q^2}$ and $LOLP^p$. This is a consequence of having positive forced outage rates on the units. However, it is also seen that EOE^p and OPP^p are positive, and this is a unique feature of the CHP system, never experienced in the power-only system.

In the second technique, the two heat areas have been aggregated to a single heat area. This is done by adding the heat demands hour by hour, and by assuming that all of the heat-producing units (cf. Table 1) can produce heat to this common area. The LPDF (cf. Subsection 2.2) of the combined heat and power loads is shown in Figure 2, left. The calculations are performed as described in Section 3, with $d = 1$.

The results of the calculations are reported as 'Technique 2' in Table 2. Except for EOE^p and OPP^p, the values are smaller than those for 'Technique

1'. This is expected, as the aggregation of the two heat areas implies a greater (but artificial) flexibility, leading therefore to more optimistic (i.e. smaller) values with respect to the indicators for the heat side (EUE^q, $LOLP^q$). As this will also permit more total power production, also EUE^p decreases. On the other hand, the increased heat production and restrictions between heat and power production (cf. Figure 1) imply a larger value of EOE^p.

The third technique is the one described in Section 4. The assumption of completely correlated heat demands is clearly unfulfilled (cf. the dots in Figure 8). Therefore we modify the heat demand hourly during hour t in each area j to the following value:

$$\sum_{i=1}^{d} q_t^i \cdot \frac{Q^j}{\sum_{i=1}^{d} Q^i} \tag{14}$$

Here q_t^i is the original heat demand in heat area i during hour t, and Q^i is the original total annual heat demand in heat area i. As seen, the formula assigns a new heat demand to heat area j during hour t which is proportional to the total annual heat demand in heat area j and proportional to the total heat demand. The heat demands in all heat areas will now be completely proportional, hour by hour, and are represented by the line in Figure 8.

The results of the calculations for the third technique are shown as 'Technique 3' in Table 2. The values are seen to be very close to those of 'Technique 1' in the same table.

The calculations for 'Technique 2' and 'Technique 3' in Table 2 may be seen as approximations to the correct values for 'Technique 1'. Here 'correct' means with respect to the definitions of Subsection 2.4, but disregarding discretization errors. In this perspective, the approximation introduced in Section 4, with results reported as 'Technique 3' in Table 2, are seen to be much better than the approximation resulting from aggregating the heat areas, reported as 'Technique 2'.

6   Conclusions

With large and even increasing shares of co-production of heat and power, it is important to be able to analyze system behavior when planning the expansion of CHP systems. This implies among other things evaluation of imbalances between demand and supply of heat and power.

Traditionally, for power-only systems this has been done by applying simulation tools such as the Baleriaux-Booth method, which permits the evaluation of indicators of total system adequacy such as loss of load probability and expected unserved energy.

In the present paper we have extended this method to CHP systems with multiple heat areas, containing the main CHP–type production units of back-pressure and condensing types.

The indicators used are direct generalizations of similar uses from the power-only analysis, in particular loss of energy and loss of load concepts, extended to cover the heat sides. However, it has also been shown that new concepts, particular to the CHP systems, must be considered, viz. expected overflow energy and overflow production probability for the power side. This is a direct consequence of the technically determined linkage between the heat and power production of the individual units. Therefore there is in the CHP system a trade-off between the different indicators.

We have performed the analysis under the assumption that the heat side has priority, i.e., that the heat demand should be covered with the highest priority. This permits the development of specific formulae for the various indicator, which have been given.

Based on this, it has been shown how the values may actually be calculated, and a simple synthetic case has illustrated the various concepts. Further, accuracy of calculation have been discussed.

In conclusion we see that it has been possible to apply, with suitable extension, the traditional concepts and methods for power-only systems analysis to the CHP domain. The new concepts have natural interpretation, and under the assumption of the heat priority criterion applied here, their values are unique and they may be computed with reasonable effort and accuracy.

References

[1] H. Baleriaux, E. Jamouille, and Linard de Guertechin: "Simulation de l'exploitation d'un parc de machines thermiques de production d'électricité couplé à des stations de pompage." *Revue E (édition SRBE)*, Vol. V, No. 7, pp. 225–245, 1967.

[2] R. R. Booth: "Power system simulation model based on probability analysis." *IEEE Trans. PAS-91*, No. 1, pp. 62–69, 1972.

[3] M. Lin, A. Breipol, and F. Lee: "Comparisons of probabilistic production cost simulation methods." *IEEE Trans. PWRS-4*, No. 4, pp. 1326–1333,, 1989.

[4] M. Caramanis, J. Stremel, W. Fleck, and S. Daniel: "Probabilistic production costing. An investigation of alternative algorithms." *Electrical Power and Energy Systems*, Vol. 5, No. 2, pp. 75–86, 1983.

[5] A. J. M. Van Wijk, N. Halberg, and W. C. Turkenburg: "Capacity credit of wind power in the netherlands." *Electric Power Systems Research*, Vol. 23, pp. 189–200, 1992.

[6] C. Søndergren: *Planning Tools for Heat and Power Production.* Master's thesis, Institute for Mathematical Modelling, Technical University of Denmark, 1994.

[7] C. Søndergren and H. F. Ravn: "A method to perform probabilistic production simulation involving combined heat and power units." *IEEE Trans. PWRS-11*, No. 2, pp. 1031–1036, 1996.

[8] H. V. Larsen, H. Pálsson, and H. F. Ravn: "Probabilistic production simulation including CHP plants." Tech. Rep. R-968(EN), Risø National Laboratory, 1997.

[9] Q. Ahsan, K. F. Schenk, and R. B. Misra: "Expected energy production cost of two interconnected systems with correlated demands." *IEEE Trans. PAS-102*, No. 7, pp. 2155–2164, 1983.

[10] L. R. Noyes: "Two-Area probabilistic production costing by the method of Bi-Variant cumulants." *IEEE Trans. PAS-102*, No. 2, pp. 433–443,, 1983.

[11] N. S. Rau, C. Necsulescu, K. F. Schenk, and R. B. Misra: "Reliability of interconnected power systems with correlated demands." *IEEE Trans PAS-101*, No. 9, pp. 3421–3430,, 1982.

[12] N. S. Rau, C. Necsulescu, K. F. Schenk, and R. B. Misra: "A method to evaluate economic results in interconnected systems." *IEEE Trans. PAS-102*, No. 2, pp. 472–482, 1983.

[13] K. F. Schenk and Q. Ahsan: "Impact of load management and joint ownership of generation of two interconnected systems utilizing the Bi-Variant Gram-Charlier expansion." *Electrical Power and Energy Systems*, Vol. 7, pp. 101–108, 1985.

[14] David G. Luenberger: *Linear and Nonlinear Programming*. Addison-Wesley, 1984.

Bibliographic Data Sheet   Risø–R–1185(EN)

Title and author(s)

Methods for Planning and Operating Decentralized Combined Heat and Power
Plants

Halldór Pálsson

ISBN	ISSN
87–550–2709–1	0106–2840

Dept. or group	Date
Systems Analysis Department	February 2000

Groups own reg. number(s)	Project/contract No.

Pages	Tables	Illustrations	References
199	5	59	58

Abstract (Max. 2000 char.)

In recent years, the number of decentralized combined heat and power (DCHP)
plants, which are typically located in small communities, has grown rapidly. These
relatively small plants are based on Danish energy resources, mainly natural gas,
and constitute an increasing part of the total energy production in Denmark.
The topic of this thesis is the analysis of DCHP plants, with the purpose to opti-
mize the operation of such plants. This involves the modeling of district heating
systems, which are frequently connected to DCHP plants, as well as the use of
heat storage for balancing between heat and power production. Furthermore, the
accumulated effect from increasing number of DCHP plants on the total power
production is considered.
Methods for calculating dynamic temperature response in district heating (DH)
pipes have been reviewed and analyzed numerically. Furthermore, it has been
shown that a tree-structured DH network consisting of about one thousand pipes
can be reduced to a simple chain structure of ten equivalent pipes without loosing
much accuracy when temperature dynamics are calculated.
A computationally efficient optimization method based on stochastic dynamic
programming has been designed to find an optimum start-stop strategy for a
DCHP plant with a heat storage. The method focuses on how to utilize heat
storage in connection with CHP production.
A model for the total power production in Eastern Denmark has been applied
to the accumulated DCHP production. Probability production simulations have
been extended from the traditional power-only analysis to include one or several
heat supply areas.

Descriptors INIS/EDB